



Technische Universität München
Lehrstuhl für Chemie Biogener Rohstoffe

Biotechnological production of dicarboxylic acids as building blocks for bio-based polymers

Irina Funk

Vollständiger Abdruck der von der promotionsführenden Einrichtung Campus Straubing für Biotechnologie und Nachhaltigkeit der Technischen Universität München zur Erlangung des akademischen Grades eines

Doktors der Naturwissenschaften (Dr. rer. nat)

genehmigten Dissertation.

Vorsitzender: Prof. Dr. Cordt Zollfrank
Prüfer der Dissertation: 1. Prof. Dr. Volker Sieber
2. Prof. Dr. Bastian Blombach

Die Dissertation wurde am 08.02.2019 bei der Technischen Universität München eingereicht und von der promotionsführenden Einrichtung Campus Straubing für Biotechnologie und Nachhaltigkeit am 28.10.2019 angenommen.

Acknowledgements

First, I would like to express my sincere thanks to Prof. Dr. Volker Sieber, head of the Chair of Chemistry of Biogenic Resources, TU Munich, Campus Straubing for Biotechnology and Sustainability for giving me the opportunity to work on such an interesting topic and for the constant support throughout the duration of this work.

Next, I would like to thank my supervisor, Dr.-Ing. Jochen Schmid for his guidance, scientific inquisitiveness and helpful advice during my thesis. Additionally, I am thankful to my colleagues Dr. Broder Rühmann and Petra Lommes for the help and support on the analytical studies, to Dr. Nina Rimmel for interesting and supportive work collaboration, to Dr. Timo Huber and Paul Stockman for assistance in NMR analysis, Anja Schmidt, Irmgard Urban, Melanie Speck, Alfiya Wohn and Manuel Döring for their technical assistance and constant help in the lab. Also, I would like to acknowledge Sumanth Ranganathan as the second reader of this thesis for valuable comments.

List of publications

Irina Funk, Nina Rimmel, Christoph Schorsch, Volker Sieber and Jochen Schmid (2017)

Production of dodecanedioic acid via biotransformation of low cost plant-oil derivatives using *Candida tropicalis*. Journal of Industrial Microbiology and Biotechnology, Vol 44.

DOI:10.1007/s10295-017-1972-6 (2017)

Irina Funk, Volker Sieber and Jochen Schmid (2017)

Effects of glucose concentration on 1,18-*cis*-octadec-9-enedioic acid biotransformation efficiency and lipid body formation in *Candida tropicalis*. Scientific Reports, Vol. 7.

DOI:10.1038/s41598-017-14173-7 (2017)

Contents

| | |
|---|-----------|
| Summary | 1 |
| 1 Introduction | 3 |
| 1.1 Bioeconomy and green chemistry | 3 |
| 1.2 Biomass for production of biomaterials | 5 |
| 1.3 Bifunctional monomers as building blocks for polymers | 6 |
| 1.4 Fatty acids as precursors for dicarboxylic acids | 8 |
| 1.5 Microbial production of dicarboxylic acids | 9 |
| 1.5.1 Bioprocess engineering towards enhanced DCAs production..... | 12 |
| 1.5.2 Characterizing DCA production at the cellular level..... | 14 |
| 1.6 Biotechnological DCA conversion towards industrial production..... | 16 |
| 1.6.1 Industrial use and production of dodecanedioic acid | 16 |
| 1.6.2 1,18- <i>cis</i> -octadec-9-enedioic acid on the way to industrial production | 18 |
| 1.7 Aim of the thesis..... | 20 |
| 2 Materials and Methods | 21 |
| 2.1 Materials | 21 |
| 2.1.1 Chemicals..... | 21 |
| 2.1.2 Enzymes | 21 |
| 2.1.3 Kits and Standards | 21 |
| 2.1.4 Equipment..... | 22 |
| 2.1.5 Software | 23 |
| 2.1.6 Microorganisms..... | 23 |
| 2.1.7 Oligonucleotides..... | 23 |
| 2.1.8 Media | 25 |
| 2.1.9 Buffers and solutions | 25 |
| 2.1.9.1 Preparation of RNase free buffers | 26 |
| 2.1.9.2 Whole-cell biotransformation buffers | 26 |
| 2.1.9.3 Thin-layer chromatography buffers | 26 |
| 2.1.9.4 Standards applied for the GC/FID analysis..... | 26 |
| 2.1.9.5 Agarose gel electrophoresis buffers | 27 |
| 2.1.9.6 Denaturing agarose gel electrophoresis buffers..... | 27 |
| 2.1.9.7 Buffers applied for disruption of the yeast cell | 27 |
| 2.1.9.8 Total RNA extraction buffers | 27 |
| 2.1.9.9 gDNA extraction buffers | 27 |
| 2.2 Methods..... | 28 |
| 2.2.1 Microbiological methods | 28 |
| 2.2.1.1 Cell cultivation..... | 28 |
| 2.2.1.2 Cell growth determination | 28 |
| 2.2.1.3 Determination of colony-forming units (CFU)..... | 28 |

| | | |
|-----------|--|-----------|
| 2.2.1.4 | Microscopy..... | 28 |
| 2.2.1.5 | Yeast cell wall disruption | 28 |
| 2.2.1.6 | Total lipid extraction and lipid saponification..... | 29 |
| 2.2.2 | Molecular biology methods | 30 |
| 2.2.2.1 | Isolation of genomic DNA (gDNA) | 30 |
| 2.2.2.2 | RNA extraction | 30 |
| 2.2.2.3 | Determination of DNA/RNA concentration..... | 31 |
| 2.2.2.4 | Polymerase chain reaction (PCR) for DNA amplification..... | 31 |
| 2.2.2.5 | Quantitative PCR (qPCR)..... | 31 |
| 2.2.2.5.1 | Determination of qPCR specificity..... | 33 |
| 2.2.2.5.2 | Determination of qPCR efficiency..... | 33 |
| 2.2.2.5.3 | Selection of reference genes and normalization procedure..... | 34 |
| 2.2.2.6 | Agarose gel-electrophoresis and ethidium bromide-staining..... | 35 |
| 2.2.2.6.1 | DNA separation..... | 35 |
| 2.2.2.6.2 | Denaturing agarose gel-electrophoresis for RNA separation..... | 35 |
| 2.2.2.6.3 | Ethidium bromide-staining..... | 35 |
| 2.2.2.7 | DNA Sequencing | 36 |
| 2.2.2.8 | Reverse transcription..... | 36 |
| 2.2.3 | Analytical methods..... | 37 |
| 2.2.3.1 | Gas chromatography coupled with flame ionisation detector (GC/FID) | 37 |
| 2.2.3.2 | Gas chromatography coupled with mass spectroscopy (GC/MS)..... | 38 |
| 2.2.3.3 | High-performance liquid chromatography (HPLC)..... | 38 |
| 2.2.3.4 | Thin layer chromatography (TLC)..... | 39 |
| 2.2.3.5 | Glucose assay | 39 |
| 2.2.3.6 | Nuclear magnetic resonance (NMR)..... | 39 |
| 2.2.3.7 | Melting point determination..... | 40 |
| 2.2.4 | Biotransformation of fatty acids..... | 40 |
| 2.2.4.1 | Pre-culture in shake flask | 41 |
| 2.2.4.2 | Cultivation of pre-culture in 2 L bioreactor | 41 |
| 2.2.4.3 | Whole-cell biotransformation in DASGIP system..... | 42 |
| 2.2.4.4 | Whole-cell biotransformation in a shake flask..... | 47 |
| 2.2.4.5 | Whole-cell biotransformation in 2 L bioreactor | 47 |
| 2.2.5 | Downstream processing of <i>cis</i> -ODA | 47 |
| 2.2.6 | Equations..... | 48 |
| 3 | Results | 49 |
| 3.1 | Biotransformation of dodecanoic acid methyl ester | 49 |
| 3.1.1 | Introduction to dodecanedioic acid production process | 49 |
| 3.1.2 | Optimization of the DDA production process..... | 49 |
| 3.1.2.1 | Application of pH shift for enhanced DAME biotransformation..... | 49 |
| 3.1.2.2 | Effect of temperature on the biotransformation efficiency..... | 51 |

| | | |
|-----------|--|------------|
| 3.1.2.3 | Determination of an optimal substrate feed rate | 53 |
| 3.1.3 | Development of RT-qPCR method for gene expression | 58 |
| 3.1.3.1 | Establishment of an appropriate RNA extraction method..... | 58 |
| 3.1.3.1.1 | Enzymatic cell wall digestion | 59 |
| 3.1.3.1.2 | gDNA degradation | 60 |
| 3.1.3.1.3 | RNA Integrity..... | 61 |
| 3.1.3.2 | Validation of qPCR assay..... | 62 |
| 3.1.3.2.1 | Establishment of qPCR specificity and efficiency..... | 62 |
| 3.1.3.2.2 | Selection of reference genes for normalization | 65 |
| 3.1.4 | Monitoring of gene expression during DDA production process | 66 |
| 3.2 | Characterization and optimization of the pre-culture | 70 |
| 3.2.1 | Cell growth on agar plates..... | 70 |
| 3.2.2 | Optimization of liquid pre-culture | 71 |
| 3.3 | Biotransformation of oleic acid..... | 73 |
| 3.3.1 | Establishment of suitable GC/FID method | 73 |
| 3.3.2 | <i>cis</i> -ODA production: from shake flask towards bioreactor scale | 75 |
| 3.3.2.1 | Oleic acid biotransformation in the shake flask..... | 75 |
| 3.3.2.2 | Conversion of oleic acid in the parallel bioreactor system | 76 |
| 3.3.2.3 | Biotransformation of oleic acid in 2 L bioreactor scale..... | 78 |
| 3.3.3 | Optimization of <i>cis</i> -ODA production in parallel bioreactor system | 80 |
| 3.3.3.1 | Biomass production in the growth phase..... | 80 |
| 3.3.3.2 | Design of the pH shift strategy..... | 81 |
| 3.3.3.3 | Product yield in dependency of glucose feed | 84 |
| 3.3.3.3.1 | Incorporation of oleic acid into the lipid bodies..... | 85 |
| 3.3.3.3.2 | Effect of glucose on the transcriptional level..... | 88 |
| 3.3.3.3.3 | Production of DDA in dependency of glucose feed | 89 |
| 3.3.3.4 | <i>cis</i> -ODA production in correlation to substrate feed | 91 |
| 3.3.4 | Recovery and purification of <i>cis</i> -ODA | 93 |
| 4 | Discussion..... | 95 |
| 4.1 | Enhanced biomass production supporting biotransformation..... | 95 |
| 4.2 | DCA productivity in dependency on the pH..... | 97 |
| 4.3 | Effect of temperature on DCA production | 99 |
| 4.4 | Feed strategies in biotransformation phase | 100 |
| 4.4.1 | Effects of the glucose concentration on the product yield | 100 |
| 4.4.1.1 | LBs formation in dependency on substrate | 103 |
| 4.4.2 | Substrate feed | 106 |
| 4.5 | Monitoring biotransformation at transcriptional level | 108 |
| 4.6 | Purification of <i>cis</i> -ODA | 110 |
| 4.7 | Comparison of DDA and <i>cis</i> -ODA production processes | 111 |
| 5 | Outlook..... | 114 |

| | | |
|----------|---|------------|
| 6 | References | 116 |
| 7 | Attachments | 125 |
| 7.1 | List of tables..... | 125 |
| 7.2 | List of figures..... | 127 |
| 7.3 | Abbreviations..... | 129 |
| 7.4 | 5.8 rRNA analysis of <i>C. tropicalis</i> ATCC 20962..... | 132 |
| 7.5 | Analysis of hydrolyzed lipids..... | 134 |
| 7.6 | Nuclear magnetic resonance (NMR) spectroscopy of <i>cis</i> -ODA [107]..... | 135 |

Summary

Industrial biotechnology offers an attractive alternative for chemical bulk production by utilizing biogenic resources, thereby enabling efficient and sustainable production processes. In the last decades, the industry has been focusing on the biotechnological production of bifunctional monomers as building blocks for bio-based polymers. An increased attention in this area was aroused by dicarboxylic acids (DCAs) representing versatile building blocks for polymers. Even though, several DCAs of various chain lengths are available on the market, a biotechnological production of the medium- and long-chain DCAs represents a substantial gap.

The present work focuses on the development and optimization of production process for bio-based DCAs of varying chain lengths. The DCAs production relies on the biotransformation of fatty acids by a genetically modified *Candida tropicalis* strain as a whole-cell biocatalyst. Using benchtop parallel bioreactor system, a biotransformation platform for DCAs production was established enabling fast and reliable process development. To enhance insights at the cellular level of biotransformation, the transcriptional profile of selected genes of the first and rate-limiting conversion step in the reaction pathway was studied. Application of this system enabled appropriate process development of valuable precursors of bio-based polymers: dodecanedioic acid (DDA) and 1,18-*cis*-octadec-9-enedioic acid (*cis*-ODA). The substrates used for biotransformation, dodecanoic acid methyl ester (DAME) and oleic acid, respectively, were found to influence the process differently, thereby needing individual process modifications. DAME being a toxic substrate, required the application of an accurate feed strategy, accompanied by slow pH shift, which was essential for enhanced DDA production. Although, the transcriptional analysis revealed a negative impact of the pH shift on the expression level of *CPR*, the gene encoding the crucial enzyme of the bioconversion pathway, a slow pH increase was found to be essential for high DAME conversion rates. The transcriptional level of corresponding *CYPs* did not seem to be affected by the applied operational conditions. Oleic acid conversion on the other hand, was enabled by fast pH shift that increased substrate solubility and thus, *cis*-ODA

productivity. Reduction of the pH shift led to a distinct increase of *CPR* expression level yielding high volumetric productivity. However, the most critical parameter of the *cis*-ODA production process was the glucose feed rate. It was observed that elevated levels of glucose triggered the storage of oleic acid in lipid bodies and resulted in drastically lowered product yields.

By using the optimal conditions, a final titer of 65.9 ± 3.1 g/L with volumetric productivity of 0.35 ± 0.02 g/(L·h) was obtained for DDA. Similarly, optimized production of *cis*-ODA resulted in a final concentration of 49.6 ± 3.4 g/L with volumetric productivity of 0.58 ± 0.04 g/(L·h).

1 Introduction

1.1 Bioeconomy and green chemistry

Plastics are important and irreplaceable products in today's world owing to their unique properties such as durability and strength, and its broad range of applications. They are used extensively in various industry fields such as packaging, transport, automotive, and agriculture. Ever since the first polymeric material, rubber [1], was discovered, the scientific community focused its attention towards the production and modification of polymers, the basic components of plastics. In the year 1839, Charles Goodyear successfully developed the vulcanization technology imparting great elasticity to natural rubber [1]. This is considered as the first breakthrough in the area of polymer processing technology. Soon, the first fully synthetic polymer, Bakelite, was introduced to the market and produced at an industrial scale [2].

Since then, the production of plastics has gained extensive importance due to its wide range of properties along with low manufacturing costs. In the year 2015, the annual production of plastics worldwide accounted to 322 million tons [3]. Rapid increase in the demand of plastic materials during the recent years has led to enormous waste generation. Every year, over 35 million tons of waste originating from various plastic materials is produced and only 7% of them are recycled [4]. Deposited in the landfills or dispersed in the oceans, plastics accumulate as whole or in the form of microplastic in the environment. Due to lack of natural biological processes being able to degrade synthetic polymers, global pollution by plastics grew enormously in the past years [2]. Therefore, the substitute of synthetic polymers by bio-based and biodegradable polymers is an attractive alternative, which should contribute to sustainable society reducing environmental print.

Commonly, biopolymers are defined as natural polymers derived from plants and microbes, whereas bio-based polymers are chemically synthesized from biological building blocks. Compared to conventional polymers derived from non-renewable and exhaustible petroleum feedstock, the production of bio-based polymers implements biomass as the starting biological material. Along with the practice of waste prevention,

the utilization of biomass as a renewable feedstock, represents the basic principle of green chemistry [5]. The concept of green chemistry was defined by Anastas and Warner in 1998 and contains the guidelines for clean and safe production of chemicals [5]. The introduction of this concept represented a first step towards reduction of the enormous dependency of the chemical industry on fossil fuels. However, the term green chemistry does not comprise an economic element [5]. To compete with current petroleum-based economic models, an alternative, sustainable, and eco-friendly bioeconomy has been introduced [5-7].

The term bioeconomy was first introduced by scientists acknowledging the potential of biological sciences and biotechnology to support industrial production processes. Promoted by the European Commission, bioeconomy became an important European policy supporting appropriate technologies to enable reduction of greenhouse gases release and to promote the transition from fossil fuels to alternative sources [7, 8]. As defined in *Cologne Paper* of 2007, the main concept of bioeconomy reflects the perspective of biotechnology and its role in substituting the petroleum-based feedstock by bio-based, renewable resources [7, 9]. After Europe, the idea and concept of bioeconomy spread all over the world. In 2017, the German Economic Council published strategies and policies related to bioeconomy of 49 countries [10].

The transition to a bio-based economy should primarily decrease the dependency on fossil resources. The so-called “peak oil” is considered to be one of the driving forces of this concept [7]. In general, “peak oil” describes the production pattern of crude oil: reaching the maximum, at the peak of which, the production is expected to drop, thereby resulting in the continuously increasing crude oil prices, which is expected soon. [11]. Thus, the fundamental technology of bioeconomy is directed towards introducing new possibilities to substitute petroleum-based refineries. Based on this approach, the next step would be the emphasis of biomass utilization as a sustainable and renewable feedstock to the existing non-renewable resource-based production [5-7].

1.2 Biomass for production of biomaterials

The term biomass summarizes all non-fossil resources recently derived from living organisms, such as plants, microorganisms, and animals or organic waste streams. Biomass can be classified according to its origin, its production sector, and also according to its major components [7]. The biomass produced on agricultural land and forests represent an important sector accounting to a global production of around 11.4 billion tons as described in the year 2011 [12]. Nonetheless, the primary task of agricultural biomass, also called first-generation biomass, is to ensure food supply. The potential conflict between the food industry and application of biomass to produce energy or bulk chemicals became the main issue of the first-generation biorefinery principles.

On the other hand, the utilization of second-generation feedstocks containing lignocellulosic biomass and inedible oils and fats, represents a great alternative and sustainable resource. The availability of second-generation biomass can be implemented, for example, by cultivating non-edible and fast-growing crops. However, the focus of biomass conversion is the valorization of waste biomass, which enables economical and sustainable exploitation of water and energy resources [5, 7]. Since, waste streams of agriculture or food industry is inevitable, the effective utilization of these residues represents a valuable source of biomass for chemical or energy production. Using biomass as feedstock along with biotechnological tools found multiple industrial applications for the production of bulk chemicals, polymers and active pharma ingredients, but is still underrepresented in the worldwide chemical production [5, 13].

The market for bio-based polymers seems to be one of the most promising and growing sector of biomaterials and is estimated to account for 32.5% of all biochemicals to be produced by the year 2020 [13]. In the year 2012, around 0.3 million tons of bioplastics was manufactured in Europe alone, which represents 0.5% of the total plastic production [13]. As the bioplastic sector is expected to grow in the years to come, the potential production could reach up to 0.9 million tons by the year 2020 and up to 50 million tons by 2050, considering the potential substitution of 85% of petroleum-based products [13].

1.3 Bifunctional monomers as building blocks for polymers

The production of bio-based polymers relies on the implementation of renewable resources as starting material. Some of these polymers can be produced directly by plants or microorganisms and are generally biodegradable. Probably, one of the most prominent examples of biodegradable biopolymers is the class of polyhydroxyalkanoates (PHAs), a biogenic polyester, which accumulates naturally in microbial cultures grown on renewable feedstock [14, 15]. On the other hand, bio-based polymers are obtained from bio-derived monomers, which are then processed using standard chemical polymerization conditions. The monomers used for polymer manufacturing by polycondensation require two terminal functional groups and are aptly named bifunctional monomers. These monomers with terminal hydroxyl, amino, and carboxyl functionalities are widely used to produce polyesters and polyamides, thereby accounting to the largest fraction of polymers [16]. The variety of the functional groups in combination with the wide range of backbones, provided by renewable feedstocks, facilitates the production of tailored polymers by choosing the appropriate monomer.

Biomass is generally considered a great platform to produce bifunctional monomers, since it involves various valuable precursors, such as sugars, polysaccharides, lignocellulose, proteins, terpenes and triacylglycerols [5]. In the figure 1-1, some of the precursors and corresponding bifunctional monomers and their application in the polymer industry are elucidated.

Lignocellulose, the most abundant part of biomass, is the major by-product of the agricultural and pulp industry and is used as a feedstock for the production of several monomers. Chemical or enzymatic hydrolysis of lignocellulose leads to the release of C5 and C6 sugars serving as precursors for bifunctional monomers. For example, 1,3-propanediol, a monomer produced from glucose, is used for manufacturing polyesters such as polytrimethylene terephthalate, which finds its application in the fiber, clothing, solvent, and coating industries [17]. 1,3-propanediol represents one of the first bio-based chemicals manufactured by engineering the metabolic pathway of an *Escherichia coli* strain. Lactic acid is another prominent example of the first-generation of bio-based chemicals. It is produced by the utilization of glucose as fermentation

substrate and is used to produce polylactic acid (PLA), a thermoplastic and biodegradable material, with a global production of around 370,000 tons in 2011 [17].

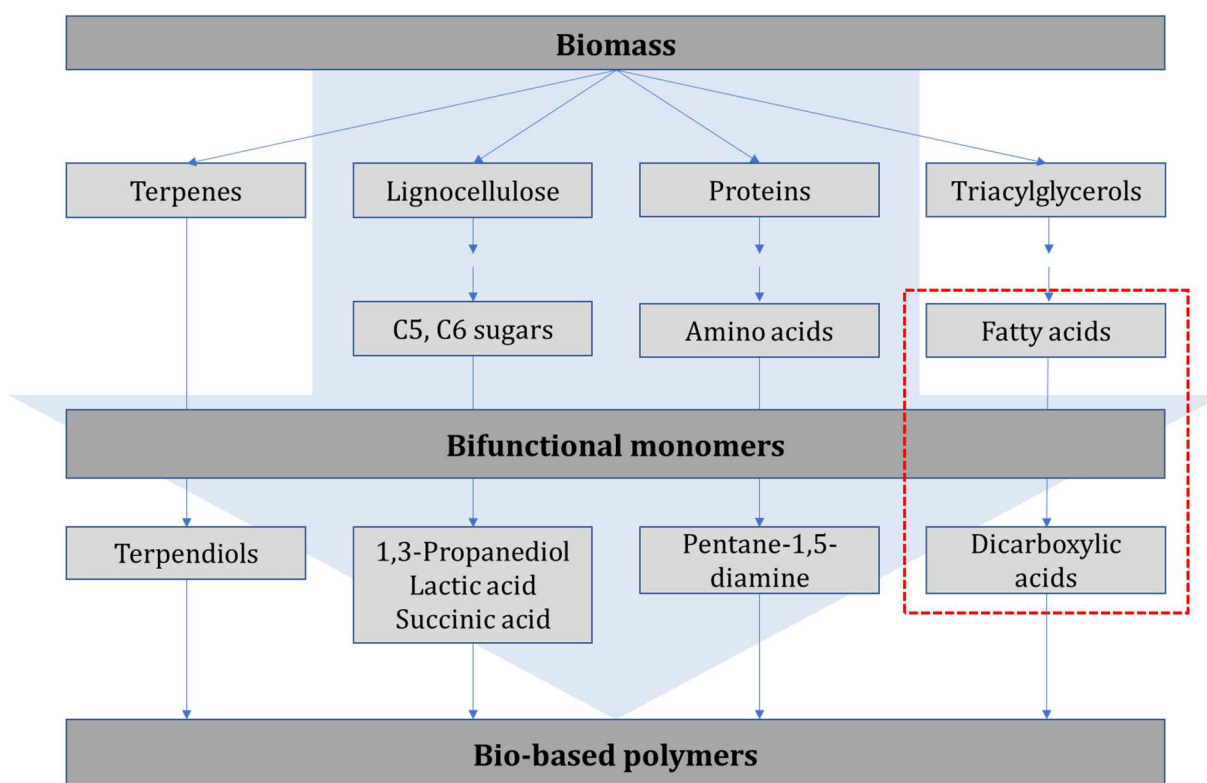


Figure 1-1: Overview over the possibilities of bio-based polymer production from biomass

Biomass comprises of various precursors, such as lignocellulose, proteins, terpenes and triacylglycerols. And thus, represents a valuable starting material for the production of bifunctional monomers, building blocks for bio-based polymers.

Besides lignocellulose, biomass consists of a reasonable amount of proteins. Hydrolysis of the proteins results in release of amino acids, which on further modifications produce value added chemicals. For example, L-lysine, is a non-essential amino acid, that serves as an important precursor for the production of cadaverine (pentane-1,5-diamine), a short-chain diamine applied for production of polyamides and polyurethane [18]. Terpenes, as valuable components produced by conifers, represent rather new, but quite promising substrates for manufacturing bio-based polymers. Recently, the biotechnological production of bifunctional terpendiols for the putative application in the field of polyesters has been reported [19].

Additionally, triacylglycerols (TAGs), as components of fats and oils, are also obtained from biomass. The hydrolysis or transesterification of the TAGs leads to the release of glycerol and fatty acids and their methyl and ethyl esters, respectively. Due to a great variety of fatty acids and their derivatives with respect to chain length, and degree of saturation, they represent an interesting starting material to produce tailor-made bio-based polymers suitable for industrial and medical applications.

1.4 Fatty acids as precursors for dicarboxylic acids

Dicarboxylic acids (DCAs) are aliphatic diacids of varying chain length, comprising of two terminal carboxylic acid functional groups, which makes them suitable for the production of polymers by condensation polymerization. Polyamides represent one of the most important polymer classes produced from diacids, and nylon-6,6 is the most prominent representative of this class. The production of nylon-6,6 was established in early 1930s by DuPont (USA) and involved the polycondensation of diamine and adipic acid, a short-chain dicarboxylic acid [20]. At that time, adipic acid was obtained by chemical synthesis from petroleum-based benzene. As inspired by green chemistry and bioeconomical aspects, the production of adipic acid was modified towards a sustainable route. In 2009, Rennovia Inc. (USA) presented a glucose-based production of adipic acid and have occupied a good position in today's market [21]. Verdezyne (USA) uses a slightly different technology to obtain bio-based adipic acid by selective ω -functionalization of fatty acids from vegetable oils and fats [22].

Fatty acids, as one of the most abundant materials in nature, possess already one functional group and are therefore attractive precursors for diacids. Production of α, ω -DCAs can be achieved by self-metathesis of monounsaturated fatty acids catalyzed by a second-generation Grubbs catalysts [23, 24]. However, on using chemical syntheses, only a limited product portfolio is available. In addition, self-metathesis of fatty acids results in the formation of by-products and leads to poor product yields [25, 26]. Enzymatic conversion, on the other hand, allows selective functionalization of the fatty acids under mild reaction conditions compared to current chemical methods. Therefore, the development of biotechnological production methods of α, ω -DCAs based on the

renewable feedstocks opens a new perspective of process design to use novel substrates for bio-based polymer manufacturing and thus, supporting the concept of bioeconomy.

1.5 Microbial production of dicarboxylic acids

Oleaginous yeasts, like *Candida tropicalis* and *Yarrowia lipolytica*, are known for their ability to utilize alkanes and fatty acids very efficiently as a carbon source. The metabolic pathway involves the import of aliphatic substrates, followed by a β -oxidation or an ω -oxidation (Figure 1-2). For β -oxidation alkanes and fatty acids are transported to the peroxisomes, whereas ω -oxidation is performed in the endoplasmic reticulum (ER) [27]. β -oxidation represents the main degradation pathway and involves several enzymatic steps, finally resulting in acetyl-CoA, which can directly enter the citric-acid cycle to provide the cells with energy (Figure 1-2).

As an alternative pathway for the hydrophobic substrate degradation, ω -oxidation describes the production of dicarboxylic acids, which can also be metabolized via the β -oxidation pathway [28]. The first and rate-limiting step of ω -oxidation is catalyzed by a ω -hydroxylase complex, comprised of a cytochrome P450 monooxygenase (CYP) and an associated NADPH reductase (CPR) (Figure 1-2). The resulting ω -hydroxyl molecule is further converted to the corresponding aldehyde by a fatty alcohol oxidase (FAO) or an alcohol dehydrogenase (ADH). Finally, the aldehyde group is oxidized to a carboxyl group by a fatty aldehyde dehydrogenase (FAlDH) [27, 28]. The industrial production of dicarboxylic acids via biotransformation uses this unique ω -oxidation pathway to enable highly selective functionalization of fatty acids and alkanes towards selected dicarboxylic acids of higher value.

Microbial production of dicarboxylic acids has been an important research focus for a long time. In early 1970s, Japanese researchers, Shiio and Uchio published an extensive study on the production of dicarboxylic acids from *n*-alkanes [29, 30]. The authors evaluated several *Candida* strains for the ability of DCA production from alkanes of various chain lengths in the range of C9 - C18. However, the degradation of the product chain-length was observed, which prevented successful production [29]. Further studies performed using mutant *Candida* strain, which was unable to assimilate alkanes,

reported conversion of alkanes to the corresponding DCAs of the same chain length. Even though, several investigations on the optimal conditions for the targeted conversion were performed, only low product titers could be achieved, such as 8.20 g/L for C12 and 6.46 g/L for C18 after 72h [30].

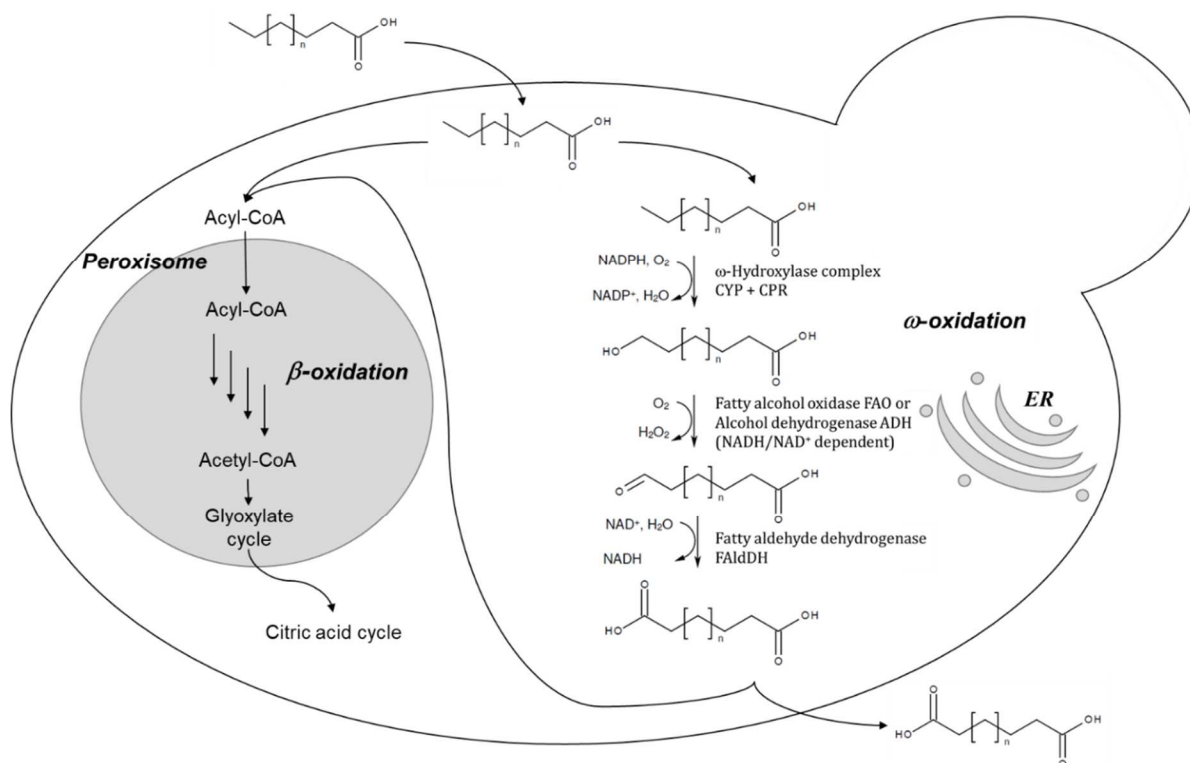


Figure 1-2: Fatty acid degradation pathway in *Candida tropicalis*

The pathway involves the uptake of aliphatic substrates, followed by a β -oxidation or an ω -oxidation. For subsequent β -oxidation fatty acids are activated to form acyl-CoA and to enter the peroxisome. Acyl-CoA is further catalyzed to generate acetyl-CoA, which is further converted into succinate and can enter the citric acid cycle. Also succinate represents a precursor for amino acid or carbohydrate synthesis [31]. In contrast, ω -oxidation occurs in the endoplasmic reticulum (ER). The first step is the oxidation of the terminal methyl group catalyzed by a ω -hydroxylase complex. Afterwards, the fatty alcohol is converted by a fatty alcohol oxidase or an alcohol dehydrogenase into its corresponding aldehyde. Finally, the aldehyde group is oxidized to a carboxyl group. The dicarboxylic acids produced can be degraded via β -oxidation or can be excreted into the surrounding environment [27].

Application of alkanes as precursors for dicarboxylic acids opened the possibility to design novel products, that were not possible by conventional chemical syntheses. And soon, the production of DCAs via biotransformation became prevalent. In the year 1982,

a German research group showed the possibility to use other substrates such as diols and hydroxy acids to produce the corresponding DCAs of a defined chain length [32, 33]. Furthermore, they identified a process strategy to use fatty acids for DCA production of corresponding chain length [34]. As the major component of various natural oils and fats, fatty acids are highly promising precursors for a green and sustainable DCA synthesis. These research group successfully applied oleic and elaidic acid for the production of corresponding 1,18-*cis*-octadec-9-enedioic acid (*cis*-ODA) [35] and 1,18-*trans*-octadec-9-enedioic acid (*trans*-ODA) [36]. These results demonstrate the unique possibility of biotechnological production of unsaturated DCAs from corresponding fatty acids with respect to the preservation of the double bond configuration. However, the product yields for *cis*-ODA remained in the range of 5 g/L, mainly due to product degradation by the yeast cells themselves [35].

Later, Fabritius *et al.* used di-unsaturated fatty acids to enable the production of long-chain DCAs and hydroxyl fatty acids, which can serve as precursors for bio-based polymer production. Besides pure substrates, such as linoleic [37] or ricinolic acid [38], they also successfully used sunflower and rapeseed oil for production of DCAs and hydroxyl fatty acids [38, 39]. Nevertheless, low production rates due to degradation of the DCAs via β -oxidation were observed.

Degradation of DCAs remained the main issue during the biotransformation by *C. tropicalis* resulting in low yields. A breakthrough in this area was achieved by Canadian researches in the year 1992 [40]. By using genetic engineering, the researchers enabled inactivation of the β -oxidation pathway by silencing the *POX* genes, encoding the acyl-CoA oxidase, the first enzyme of the β -oxidation pathway. The engineered strain showed a higher product yield and a conversion efficiency of 100%. Moreover, this approach demonstrated the possibility for further enhancing the production rates by overexpressing cytochrome P450 monooxygenase and the corresponding reductase. Using *C. tropicalis* strain AR40, with a blocked β -oxidation containing multiple copies of *CYP* and two additional copies of *CPR*, they achieved high product titers for several DCAs [40]. The broad spectrum of predominantly long-chain substrates was applied for the

biotransformation by the genetically modified strain AR40 yielding final DCAs concentrations of more than 100 g/L (Table 1-1).

1.5.1 Bioprocess engineering towards enhanced DCAs production

The bio-oxidation of fatty acids represents a highly complex pathway involving several enzymatic conversion steps and various co-factors (Figure 1-1). Therefore, *C. tropicalis* has been applied as a whole-cell biocatalyst for the biotransformation of fatty acids to corresponding DCAs based on its enzymatic machinery. The application of microorganisms for the conversion of substrates can come along with several drawbacks, such as unwanted side-pathways and therefore occurrence of by-products. *C. tropicalis* not only possesses the desired ability of fatty acid oxidation to DCAs, but also provides enzymes, which enable disadvantageous degradation of fatty acids and DCAs. As described in the previous part (1.5), the undesired β -oxidation pathway could be eliminated resulting in increased production rates of DCAs [40]. Thus, the yeast strain incapable of utilizing fatty acids as carbon source became of interest for the industrial production of DCAs.

Generally, the DCA production process in *C. tropicalis* can be divided into two phases: a growth phase, which provides appropriate number of biocatalysts, and a biotransformation phase, as the actual DCAs production step. Working with the living microorganisms and using them as whole-cell biocatalysts require specific attention on growth conditions and process parameters. Since, the *C. tropicalis* strain used is incapable of assimilating fatty acids as a carbon source, an additional C-source must be supplied. Several C-sources have been used for the production of DCAs by various *Candida* strains: glycerol [38, 39, 41, 42], sorbitol [30], glucose [32, 40, 43-46] and sucrose [47-49]. However, the application of glucose as easy utilizable carbon source remains favorable owing to its availability and purity. Due to the possible occurrence of the Crabtree effect, induced by even low glucose concentrations below 0.15 g/L as described for *Saccharomyces cerevisiae* [50, 51], the growth phase should be designed carefully to achieve appropriate biomass concentrations. Usually, the growth phase is performed in batch mode with a medium containing high glucose concentrations of around 30 g/L [40, 43-45]. Besides possible negative effects of ethanol on cell viability

and on the targeted bioconversion, channeling of glucose into the fermentation pathway results in reduced biomass production. Thus, to avoid the Crabtree effect, the growth phase can be performed in a fed-batch mode. As shown by Zibek *et al.*, altering the operation mode to fed-batch resulted in around 40 g/L of biomass, which is four times higher compared to the batch process [43].

Nevertheless, glucose represents a critical parameter not only for the growth phase, but also the biotransformation phase can be negatively affected by high glucose concentrations. Glucose can be easily metabolized via glycolysis and represents, therefore, a preferable energy source for most microorganisms. Thus, application of glucose at high concentrations could lead to inhibition or suppression of ω -oxidation pathway as the alternative pathway for degradation of the aliphatic C-sources. Glucose was already reported to have a negative effect on the ω -oxidation pathway due to catabolite repression [41, 52, 53] and inhibitory effects on the induction of the alkane and DCA-producing enzymes [26, 44]. Therefore, an accurate design of glucose feed during the biotransformation phase is essential for the efficient production of DCAs.

Besides the issues provoked by glucose, the inhomogeneity caused by using highly hydrophobic substrates also represents an enormous limitation of the biotransformation phase. To enhance the solubility of the substrates and to subsequently increase its availability for the conversion process, application of organic solvents to create a second phase can be effective. Green *et al.* demonstrated a three-fold increase of dodecanedioic acid (DDA) production from lauric acid using pristane, a chemically stable organic solvent [44]. But, running such a process is not economically efficient due to the application of expensive solvents in combination with low product yields of 8.4 g/L. Nevertheless, using hydrophobic solid substrates, such as lauric acid, necessarily requires implementation of a second organic phase. Thus, instead of solid components their derivatives like alkanes, methyl esters or hydroxy fatty acids can be used. Another method to increase the solubility of the aliphatic substances was proposed by Liu *et al.* [47]. As an end-product of the ω -oxidation, DCAs can inhibit the pathway by competitive binding to the monooxygenase complex. The authors described that by increasing the pH of the medium towards slight basic conditions, the DCA can be excreted

from the cell into the surrounding medium, thereby enhancing DCA production. Using this strategy, Liu *et al.* demonstrated the biotransformation of *n*-dodecane and *n*-tetradecane to their corresponding dicarboxylic acids with a productivity of 166 g/L and 138 g/L, respectively [47]. Thus, raising the pH towards basic conditions, called pH shift, enables enhanced DCA production making this strategy interesting for industrial production and was applied by several researchers during the studies on DCA production via yeast catalyzed biotransformation [37-40, 43, 45, 48, 54].

1.5.2 Characterizing DCA production at the cellular level

Classical bioprocess engineering and genetic engineering can be applied for the optimization of production processes. The successful application of both approaches requires an understanding of the conversion process at the cellular level, gaining insights regarding the enzymatic reactions.

As described above, due to possible competitive binding of DCA to the monooxygenase complex, DCA could inhibit the ω -oxidation pathway. Therefore, the intracellular DCA concentration should be kept as low as possible. The application of a pH shift during the biotransformation was shown to favor DCA excretion out of the yeast cells resulting in enhanced DCA production [47]. Sagehashi *et al.* focused on enhanced DCA excretion by using a genetic engineering approach. Researches targeted the ABC transporter, responsible for the efflux of hydrophobic compounds, in the DCA producing strain *C. maltose* [55]. The overexpression of genes encoding ABC transporter showed promising results and potential application for enhanced DCA production.

In general, uptake and transport of fatty acids and alkanes in yeast cells represents an underexplored research area, and the exact mechanism is just poorly understood. The transport of free fatty acids can occur by a simple diffusion across the membrane [26, 56, 57] or by specific transport proteins [31, 57-59]. Protein-facilitated uptake of fatty acids in *S. cerevisiae* is probably the best described transport mechanism among eukaryotic organisms. Interestingly, the transport of free fatty acids is coupled with their activation to corresponding acyl-CoAs mediated by the transporter, ScFat1p, and fatty acyl-CoA synthetases, ScFaa1p and ScFaa4p [58-61]. However, the lipid metabolism and the

transport mechanisms differ greatly amongst yeast species [58]. The oleaginous yeast *Y. lipolytica* is described to take fatty acids up by a still unknown mechanism using single or multiple transporters and then activate them by an acyl-CoA synthetase, YlFaa1p [58, 59]. Unfortunately, no such detailed studies on the fatty acid uptake by *C. tropicalis* have been described until now. Thus, understanding fatty acid transport mechanism in *C. tropicalis* will open the opportunity to improve and facilitate fatty acid uptake allowing an increased DCA production.

Nevertheless, the facilitated uptake of fatty acids alone would lead to their accumulation within the cell and thus provoke toxic effects. Therefore, increased fatty acid transport should be followed by improved conversion to DCAs. The oxidation of fatty acids and alkanes represents a very complex enzymatic cascade involving several enzymes and co-factors (Figure 1-2). The first and rate-limiting step of the conversion process is catalyzed by ω -hydroxylase complex comprising of CYP monooxygenase and associated NADPH reductase [27, 28]. Several studies have focused on this first conversion step and were able to identify enzymes of CYP52A family to be important for DCA production. Seghezzi *et al.* characterized the alkane-inducible gene, encoding *CYP52A2*, derived from *C. tropicalis*. The induction of *CYP52A2* by tetradecane was verified by the hybridization of total RNA with specifically designed probes [62]. Nonetheless, recent technological advances in the field of transcriptomics promise more accurate gene profiling and detailed insight into the cellular processes on the transcriptional level. So, application of microarrays, which allows parallel quantification of large number of mRNA, gained high popularity in the past [63]. On the other hand, for investigation of limited number of genes in various samples quantitative competitive reverse transcription PCR (QC RT-PCR) [64] and reverse transcription quantitative PCR (RT-qPCR) represent methods of choice [65]. Thus, applying a QC RT-PCR, Craft *et al.* identified several CYP52A family enzymes of *C. tropicalis* that were important for the fatty acid and alkane conversion. Two allelic variants *CYP52A13/14* and *CYP52A17/18* revealed to be strongly induced by fatty acids among other genes [64]. The gene encoding for CPR, which enables electron transfer from co-factors to cytochrome P450, was also found to be induced by fatty acids. Another research group working with separate expressed *CYP52A13* and *CYP52A17* in

insect cells supported this finding as well [66]. Both enzymes exposed to fatty acids exhibited comparable activity pattern, but CYP52A17 showed higher activity for the short and saturated fatty acids, whereas CYP52A13 displayed only poor activity on saturated fatty acids [66]. Besides fatty acids, other substrates are capable to induce *CYP52* as well. So, Jiao *et al.* demonstrated the induction of P450 by H₂O₂, as applied for enhanced oxygen supply during the DCA production process [67]. Thus, knowledge of the substrate uptake mechanism, the bioconversion pathway, the exact excretion route of the product, and possible side reactions in combination with directed genetic engineering supported by bioprocess engineering will facilitate the process optimization leading to high product yields.

1.6 Biotechnological DCA conversion towards industrial production

The biotransformation of fatty acids and alkanes has been studied intensively over the past few years. Whereas, development of a DCA production process suitable for industrial application was the main focus of these studies. With the help of bioprocess or genetic engineering as well as combined approaches, an impressive increase of the product yields was seen. Starting with concentrations below 10 g/L the product yield was drastically increased and accounts nowadays over 100 g/L depending on the substrate (Table 1-1). Table 1-1 summarizes studies using *Candida* as a whole-cell biocatalyst for DCA production applying corresponding fatty acids or *n*-alkanes of various chain lengths. The most desirable products were medium- and long-chain DCAs, since the chemical synthesis of these compounds comes along with numerous by-products and low product yields, leading to high downstream processing costs [25, 26]. Especially, the production of dodecanedioic acid and 1,18-*cis*-octadec-9-enedioic acid, as universal building blocks for various bio-based polymers, has gained great attention.

1.6.1 Industrial use and production of dodecanedioic acid

As a medium-chain DCA, dodecanedioic acid (DDA) represents a versatile precursor and a basic compound of polyamide 6,12 (PA612), also called nylon-6,12. Nylon is manufactured by polycondensation of the reacting monomers, DCAs and diamines, linked by peptide bonds [68]. Nylon-6,12 is used in various technical applications, due to

its superior behavior concerning water adsorption and chemical resistance [69]. Thus, the industrial production process of DDA has been in the focus of several companies such as Degussa AG (now part of Evonik Industries AG, Germany) [70, 71], Verdezyne (USA) [72] and DuPont (USA) [73, 74]. In 1986, Degussa AG proposed a DDA manufacturing process based on the pyrolysis of ricinoleic acid with subsequent oxidation of undecylenic acid to DDA [70]. Later Evonik switched to a completely biotechnological production of DDA from fatty acids [71]. Nowadays, Evonik Industries AG distributes a biobased polyamide 6,12 derived from ω -aminododecanoic acid under the commercial name of VESTAMID® [75, 76]. Meanwhile, DuPont seems to produce polyamide 6,12, known commercially as Zytel®, by use of intermediates based on conventional chemical synthesis [77]. Recently, Verdezyne (USA) announced the sale and distribution of biobased dodecanedioic acid derived from plant-oil based feedstock, BIOLON™DDDA [72, 78]. Also, Cathay Industrial Biotech, Ltd. (China) produces DDA by converting vegetable oils using biotechnological approaches [79].

Nevertheless, the biotechnological production of DDA remains attractive for the scientific community as the production process represents a highly complex biotransformation with a broad spectrum for optimization. Studies of DDA production have been focused predominantly on the application of petroleum-derived *n*-dodecane as the substrate (Table 1-1) and high product yields have been reported [41, 47, 48]. Obviously, bio-based production of DDA from renewable resources is still underrepresented. A conversion process based on the utilization of dodecanoic acid (DA), derived from palm and coconut oil [80], was described by Green *et al.* [44]. Due to poor water solubility and cellular toxicity of DA [44, 81], the process seems to be less efficient [44]. However, toxicity and solubility issues can be minimized by using fatty acids derivatives, such as methyl esters [81, 82], which have been described earlier by Picataggio *et al.* for the successful conversion to the corresponding long-chain DCAs [40]. From an industrial point of view, fatty acids methyl esters offer several advantages, such as lower energy consumption during chemical synthesis from natural oils and therefore require, less expensive equipment [83]. Thus, fatty acid methyl esters show high potential for various applications in oleochemical industry.

1.6.2 1,18-*cis*-octadec-9-enedioic acid on the way to industrial production

1,18-*cis*-octadec-9-enedioic acid (*cis*-ODA) is an unsaturated long-chain DCA and thus serves as highly useful precursor for bio-based cross-linked polymers with subsequent modification of the double bond, such as epoxidation [25, 26]. Even though unsaturated DCAs represent interesting bifunctional monomers, production of C18 dioic acids on the industrial scale remains moderate. In 2003, Cognis group (Germany) introduced C18 dibasic acids as Emerox 118[®] (saturated C18) and Emerox 118U[®] (partially unsaturated C18) derived from vegetable oils to the market [84, 85]. Since the acquisition of Cognis group by BASF in the year 2010 [86], no information for the products is available. In 2013, Elevance Renewable Sciences (USA) started the distribution of saturated octadecanedioic diacid under the brand name of Inherent[®] C18 Diacid obtained by metathesis technology [87]. Also, Cathay Industrial Biotech, Ltd. (China) offers custom manufacturing of the C18 dibasic acids [84].

Nonetheless, in recent years, oleic acid has been in the research focus for the production of *cis*-ODA (Table 1-1). Since oleic acid occurs at high concentrations in several natural oils, e.g. sunflower and rapeseed oil [38, 43], it represents an important renewable feedstock for the production of DCAs. Moreover, in comparison to the majority of other fatty acids, oleic acid is not toxic to microbial cells [81, 82], and thus, can be effectively applied for whole-cell biotransformation. To increase attractiveness of the process for industrial application, cheap and non-purified oils containing oleic acid can be applied directly for the biotransformation. As shown by Fabritius *et al.*, *cis*-ODA can be produced from sunflower and rapeseed oils, which contain 85% and 63% oleic acid, respectively [38]. However, the volumetric productivity in this case reached a maximum of 0.07 g/(L·h). Simultaneous application of rapeseed oil and a lipase leading to the release of oleic acid resulted in comparably high volumetric productivity of 0.27 g/(L·h) [43]. The production route using biogenic oils for biotransformation via *C. tropicalis* has an enormous potential, but the process must be improved to enable an efficient industrial production.

Table 1-1: Overview of studies on biotransformation of fatty acids, alkanes and their derivatives as substrates to the corresponding DCAs

| Chain length | Substrate | Strain | Duration [h] | DCA concentration [g/L] | Volumetric productivity [g/(L·h)] | Product yield [%] | Scale | Year | Reference |
|--------------|-----------------------|---------------------------------|--------------|-------------------------|-----------------------------------|-------------------|-----------|------|-----------|
| C12 | <i>n</i> -Dodecane | <i>C. cloacae</i> M-1 | 72 | 8.2 | 0.11 | - | 500 mL SF | 1972 | [30] |
| | <i>n</i> -Dodecane | <i>C. tropicalis</i> S 76 | 36 | 2.1 | 0.06 | 22 | 300 mL SF | 1982 | [32] |
| | <i>n</i> -Dodecane | <i>C. tropicalis</i> CGMCC 356 | 120 | 166 | 1.38 | - | 5 L BR | 2004 | [47] |
| | <i>n</i> -Dodecane | <i>C. tropicalis</i> ATCC 20962 | 34 | 17 | 0.50 | 49 | 2.5 L BR | 2016 | [41] |
| | <i>n</i> -Dodecane | <i>C. viswanathii</i> ipe-1 | 115 | 181.6 | 1.58 | 70 | 7.5 L BR | 2017 | [48] |
| | Dodecanoic acid | <i>C. cloacae</i> FERM P736 | 96 | 5 | 0.05 | 50 | 2 L BR | 2000 | [44] |
| C13 | <i>n</i> -Tridecane | <i>C. tropicalis</i> AR40 | 170 | 140 | 0.82 | - | 15 L BR | 1992 | [40] |
| | <i>n</i> -Tridecane | <i>C. tropicalis</i> CGMCC 356 | 120 | 152 | 1.27 | - | 5 L BR | 2004 | [47] |
| C14 | Methylmyristate | <i>C. tropicalis</i> AR40 | 170 | 180 | 1.06 | - | 15 L BR | 1992 | [40] |
| | <i>n</i> -Tetradecene | <i>C. tropicalis</i> CGMCC 356 | 120 | 138 | 1.15 | - | 5 L BR | 2004 | [47] |
| C16 | Methylpalmitate | <i>C. tropicalis</i> AR40 | 170 | 110 | 0.65 | - | 15 L BR | 1992 | [40] |
| C18 | <i>n</i> -Octadecane | <i>C. cloacae</i> M-1 | 72 | 6.46 | 0.09 | - | 500 mL SF | 1972 | [30] |
| | Methylstearate | <i>C. tropicalis</i> AR40 | 118 | 75 | 0.64 | - | 5 L BR | 1992 | [40] |
| | Oleic acid | <i>C. tropicalis</i> S76 | 96 | 5 | 0.05 | - | 300 mL SF | 1989 | [35] |
| | Oleic acid | <i>C. tropicalis</i> AR40 | 147 | 220 | 1.50 | - | 15 L BR | 1992 | [40] |
| | Oleic acid | <i>C. tropicalis</i> DSM 3152 | 86.5 | 21.5 | 0.25 | - | 1 L BR | 1996 | [39] |
| | Oleic acid | <i>C. tropicalis</i> M25 | 192 | 8.1 | 0.04 | - | 1 L BR | 1996 | [39] |
| | Oleic acid | <i>C. tropicalis</i> ATCC 20962 | 225 | 100 | 0.44 | - | BR | 2009 | [43] |
| | Oleic acid | <i>C. tropicalis</i> ATCC 20962 | 72 | 31 | 0.43 | - | 3 L BR | 2010 | [45] |
| C22 | Erucic acid | <i>C. tropicalis</i> ATCC 20962 | 48 | 12,5 | 0.26 | - | 3 L BR | 2010 | [45] |

SF: shake flask, BR: bioreactor

1.7 Aim of the thesis

Sustainable and efficient production of dicarboxylic acids still represents a challenging process due to its complexity and severity. Despite industrial manufacturing of few dicarboxylic acids, the number of bio-based products remains very poor. To enable reliable process development for biotechnological production of various dicarboxylic acids, this thesis aimed at designing an appropriate lab-scale biotransformation platform.

The biotransformation process of fatty acids and their derivatives using a whole-cell biocatalyst possess several limitations. Inhomogeneity issues and low cell viability addressed to unfavorable properties of the fatty acids require individual process solutions. To optimize and characterize the process in more detail a biotransformation platform on the basis of a benchtop parallel bioreactor system (8x1L) was applied. Owing to precise process control and automation by parallel processing, the biotransformation platform assures efficient and reliable process development. In addition to on-line measurements, the characterization of the process was supported by transcriptional analysis to demonstrate the DCAs production at the cellular level. To reveal a wide range of possible products for the biotransformation platform, a process for production of medium- as well as of long-chain dicarboxylic acids was developed. As a medium-chain dicarboxylic acid, DDA represents a valuable precursor for the polyamide 6,12. Until now, the studies on the biotechnological production of DDA described the application of the fossil-based component, *n*-dodecane. To support the idea of bioeconomy and to achieve more sustainable production of dodecanedioic acid, dodecanoic acid methyl ester, which can be easily obtained from coconut and palm kernel oil, was used in this work as a substrate. Additionally, the production process of *cis*-ODA, being the most desired representative of the long-chain unsaturated dicarboxylic acids, was aimed applying biotransformation of oleic acid.

2 Materials and Methods

2.1 Materials

2.1.1 Chemicals

Following chemicals were used as analytical standards or applied for biotransformation.

| | | |
|--|---------------------------------------|------------------------|
| Substrates for biotransformation (technical grade) | dodecanoic acid methyl ester, ~98% | Sigma Aldrich, USA |
| | oleic acid, 94.7% | Alfa Aesar, Germany |
| Analytical standards | dodecanoic acid methyl ester, ≥ 99.5% | Sigma Aldrich, USA |
| | dodecanoic acid, ≥ 99.5%, | Sigma Aldrich, USA |
| | dodecanedioic acid, ≥ 98% | Sigma Aldrich, USA |
| | oleic acid, ≥ 99% | Sigma Aldrich, USA |
| | <i>cis</i> -ODA, 94% | This work |

All other chemicals were obtained at highest possible purity from different suppliers.

2.1.2 Enzymes

| | |
|--------------------------------------|------------------------------------|
| NEB-Taq DNA Polymerase | New England Biolabs (Ipswich, USA) |
| Phusion High-Fidelity DNA Polymerase | New England Biolabs (Ipswich, USA) |
| LongLife™ Zymolyase® | G-Biosciences (St. Luis, USA) |

2.1.3 Kits and Standards

| | |
|------------------------------------|---|
| Aurum™ Total RNA Mini Kit | Bio-Rad (Hercules, USA) |
| iScript™ cDNA Synthesis Kit | Bio-Rad (Hercules, USA) |
| SsoAdvanced™ Universal SYBR® Green | Bio-Rad (Hercules, USA) |
| RapidOut DNA Removal Kit | Thermo Fisher Scientific (Waltham, USA) |
| 2-Log DNA Ladder | New England Biolabs (Ipswich, USA) |
| PageRuler unstained Protein Ladder | Fermentas (St. Leon-Rot, USA) |

2.1.4 Equipment

Chromatography systems

High-performance liquid chromatography

| | |
|-----------------------------------|---------------------------------|
| HPLC system | Dionex® Sunnyvale, CA, USA |
| Refractive index detector, RI 101 | Shodex (Tokyo, Japan) |
| PDA detector | Dionex® (Sunnyvale, CA, USA) |
| Rezex ROA-H ⁺ column | Phenomenex® (Torrance, CA, USA) |

Gas chromatography

| | |
|--|--|
| Trace GC Ultra | Thermo Fischer Scientific (Waltham, USA) |
| TriPlus Autosampler | Thermo Fischer Scientific (Waltham, USA) |
| BPX5 capillary column 30 m, Ø 0.25 mm, 0.25 µm film thickness | SGE Analytical Science (Australia) |
| Rxi®-5Sil MS column 30 m, Ø 0.25 mm, 0.25 µm film thickness | Restek, (USA) |

Bioreactors

DASGIP parallel bioreactor bench-top system Eppendorf (Jülich, Germany)

| |
|---|
| DASGIP® GA4 Exhaust analyzing module |
| DASGIP® Bioblock |
| DASGIP® Bioblock stirrer vessels (8 × 1 L, 2x Rushton-type impeller, L-sparger) |
| DASGIP® MX4/4 Gas mixing module |
| DASGIP® MP8 Multi pump module |
| DASGIP® PH4PO4RD4 Monitoring module |
| DASGIP® TC4SC4 Temperature and agitation control module |

2 L System

| | |
|--------------------------------|--------------------------------------|
| 2 L Bioreactor, Biostat® Bplus | Sartorius Stedim, Göttingen, Germany |
|--------------------------------|--------------------------------------|

Others

CFX96 Touch™ Real-Time PCR Detection System Bio-Rad (Hercules, USA)

Motic Microscope BA310 Hongkong, China

| | |
|----------------------------|---|
| Melting point meter MPM-H2 | Schorpp Gerätetechnik (Überlingen, Germany) |
|----------------------------|---|

2.1.5 Software

| | |
|---------------------|--|
| ImageJ | ImageJ 1.51d software |
| Motic Images | Plus 2.0 software |
| Chromeleon | Dionex, Dreieich |
| DASGIP Control 4.5 | DASGIP Information and Process Technology GmbH |
| Clone Manager 8 | Scientific & Educational Software (USA) |
| Xcalibur | Thermo Fisher Scientific (USA) |
| Bio-Rad CFX Manager | Bio-Rad CFX Manager 3.1(Hercules, USA) |
| BLAST | Basic Local Alignment Search Tool, National Center for Biotechnology Information (http://blast.ncbi.nlm.nih.gov) |

2.1.6 Microorganisms

All experiments in this work were performed using the *Candida tropicalis* ATCC 20962 yeast strain (Genotype: *pox5:ura3A pox5:ura3A pox4A:ura3A pox4B:URA3A*) with a blocked β -oxidation pathway, which was purchased from the American Type Culture Collection (ATCC).

2.1.7 Oligonucleotides

The following oligonucleotides were designed using Clone Manager software (Sci-Ed, Version 8) and synthesized by biomers.net GmbH (Ulm, Germany). The oligonucleotides were dissolved in ddH₂O to a concentration of 100 pmol/ μ L and stored at -20°C. The sequences of all primer pairs used for gene expression studies, the amplicon size as well as the gene accession number of the corresponding target genes are summarized in Table 2-1. In general, allelic variants of the cytochromes P450 features less than 3% variation at the amino acid level [64], therefore the primer for genes *CYP52A13/14* and *CYP52A17/18* were designed for the detection of both alleles respectively.

Table 2-1: Sequences of primer pairs used for RT-qPCR and accession numbers of target genes

| Gene | Direction | Gene Sequence 5'-3' | Amplicon size [bp] | Accession number |
|------------------|-----------|------------------------|--------------------|------------------|
| <i>ACT1</i> | forward | TGCTTTGGCTCCATCTTC | 147 | EER33201.1 |
| | reverse | GGACCAGATTCGTCGTATTC | | |
| <i>GAPDH</i> | forward | GGTAGAACTGCTTCTGGTAAC | 101 | EER30670.1 |
| | reverse | GACATACCAGTCAATTTACCG | | |
| <i>CYP52A13*</i> | forward | GGTTTGAGCCAGAGACAAAG | 97 | AY230499.1 |
| <i>CYP52A14*</i> | reverse | GCTTCTGTCAAGGCAAACCTG | | AY230500.1 |
| <i>CYP52A17*</i> | forward | TGATGCTGCTGAGTTCAGAC | 83 | AY230504.1 |
| <i>CYP52A18*</i> | reverse | CACCGTTGAATGGCAAGTAAG | | AY230505.1 |
| <i>CPR</i> | forward | TGCCAGTAGAATGGCTAGAG | 103 | AY705446.1 |
| | reverse | CCAGGACTTGACCAATTCAG | | |
| <i>PGK1</i> | forward | AACTGGATGGGTTTGGACTG | 100 | XM002548594.1 |
| | reverse | AAACACCTGGTGGACCGTTC | | |
| <i>ATPase</i> | forward | CTTTGGGTGTTGCCAGAAAG | 94 | XM002551378.1 |
| | reverse | GTGGCAGCAGTATCATCTCTTG | | |

* Primers are designed for amplification of both alleles

Primer pair applied for 5.8 S analysis:

5.8SR TCGATGAAGAACGCAGCG
 LR7 TACTACCACCAAGATCT

2.1.8 Media

If not stated otherwise, all media and media components were autoclaved at 121°C for 20 min. The given concentrations represent the final concentrations for the complete medium, i.e. with carbon source.

| Medium | Final concentration |
|-------------------|--|
| YPD liquid medium | 10 g/L yeast extract, 20 g/L peptone, 20 g/L glucose |
| YPD agar | 10 g/L yeast extract, 20 g/L peptone, 20 g/L glucose, 15 g/L agar-agar |
| OPT-1 medium [88] | 8 g/L (NH ₄) ₂ SO ₄ , 1 g/L K ₂ HPO ₄ , 2 g/L KH ₂ PO ₄ , 4.5 g/L yeast extract, 0.1 g/L NaCl, 0.1 g/L CaCl ₂ , pH 5.8 30 g/L glucose, 4 mM MgSO ₄ and 1 mL/L trace elements solution |

Medium components were prepared separately and autoclaved, except of trace element solution, which was filtered using sterile 0.2 µm PTFE filter.

| Medium component | Final concentration |
|-------------------------|---|
| Glucose solution | 500 g/L |
| Magnesium sulfate | 1 M |
| Trace elements solution | 0.4 g/L MnSO ₄ ·H ₂ O, 0.4 g/L ZnSO ₄ ·7H ₂ O, 0.1 g/L KI, 0.5 g/L H ₃ BO ₃ , 0.6 g/L FeCl ₃ ·6H ₂ O and 0.04 g/L CuSO ₄ ·5H ₂ O |

2.1.9 Buffers and solutions

Buffers and solutions were autoclaved at 121°C for 20 min or filtered using sterile 0.2 µm PTFE filter if needed. If not stated otherwise, pH adjustment was performed by 10 M NaOH or 37% HCl.

2.1.9.1 Preparation of RNase free buffers

All buffers prepared for RNA related work were treated with diethyl pyrocarbonate (DEPC), which inhibits RNases as well as DNases by modification of histidine residues to N-carbethoxyhistidine [89]. If not stated otherwise, buffers containing 0.1% (v/v) DEPC were incubated at 37°C for 1 h and then autoclaved as usual.

2.1.9.2 Whole-cell biotransformation buffers

Feed A: 500 g/L glucose

Feed B: 6 N NaOH

Feed C: 10% Antifoam B[®] Silicon emulsion (v/v), Sigma Aldrich

Feed D: DAME, ~98% or oleic acid, technical grade, 94.7%

2.1.9.3 Thin-layer chromatography buffers

Two different methods were applied for the detection of free fatty acids and the lipids.

Analysis of fatty acids:

| | |
|--------------------|--|
| Mobile phase | 1% (v/v) acetic acid in ethyl acetate |
| Detection solution | 7.5 g/L KMnO ₄ , 50 g/L K ₂ CO ₃ , 0.15% (w/v) NaOH in ddH ₂ O |
| Standards, 50mM | DAME, DDA, DA, OA, <i>cis</i> -ODA, <i>trans</i> -ODA in MTBE |

Analysis of lipids:

| | |
|--------------------|---|
| Mobile phase | <i>n</i> -Hexane:diethyl ether:acetic acid (80:20:2 v/v) |
| Detection solution | 48 g/L phosphomolybdic acid in ethanol |
| Standards, 4mg/μL | dioleoyl-sn-glycero-3-phosphocholine, ergosterol, triolein and cholesteryl oleate in chloroform |

2.1.9.4 Standards applied for the GC/FID analysis

50 mM solutions of DAME, DDA, DA, OA, *cis*-ODA, *trans*-ODA were always freshly prepared in methyl-tert-butyl ether (MTBE).

2.1.9.5 Agarose gel electrophoresis buffers

| | Final concentration |
|-------------------------------|--|
| 50x TAE-Buffer | 2 M Tris, 50 mM EDTA, 17.5% (v/v) acetic acid |
| Agarose gel | 2.0% (w/v) agarose in 1x TAE-buffer Storage at 60°C |
| Ethidium bromide-dye solution | 0.01 mg/mL ethidium bromide in 1x TAE-Buffer |
| 5x DNA-loading dye | 0.075 mM Tris, 0.05 mM EDTA, 50% (v/v) glycerin, 0.025% (w/v) bromophenol blue, 0.025% (w/v) xylene cyanol, pH 7.6 |

2.1.9.6 Denaturing agarose gel electrophoresis buffers

Denaturing agarose gel electrophoresis was performed to assure the integrity of isolated RNA; therefore, all buffers were treated using DEPC as described in 2.1.9.1.

| | Final concentration |
|-------------------------------|---|
| 10x MOPS-Buffer | 200 mM MOPS, 20 mM sodium acetate, 10 mM EDTA, pH 7.0 |
| Denaturing agarose gel | 1.0% (w/v) agarose, 16% (v/v) 37% formaldehyde in 1x MOPS-buffer |
| Ethidium bromide-dye solution | 0.01 mg/mL ethidium bromide in 1x MOPS-buffer |
| 5x RNA-loading dye | 30% (v/v) formamide, 7.2% (v/v) 37% formaldehyde, 0.05 mM EDTA, 50% (v/v) glycerin, 0.025% (w/v) bromophenol blue in 1x MOPS-buffer |

2.1.9.7 Buffers applied for disruption of the yeast cell

Enzyme dilution (RNase free): 1 M sorbitol, 100 mM EDTA, 1% (v/v)
 β -mercaptoethanol, pH 7.4

2.1.9.8 Total RNA extraction buffers

DNase I buffer, RNase free: 10 mM Tris buffer, pH 7.0

2.1.9.9 gDNA extraction buffers

Harju buffer: 2% (w/v) TritonX-100, 1% (w/v) SDS, 100 mM NaCl, 10 mM Tris, pH 8.0,
1 mM EDTA, 1x TE (10 mM Tris; 1 mM EDTA, pH 8.0)

2.2 Methods

2.2.1 Microbiological methods

2.2.1.1 Cell cultivation

Yeast cells from glycerol stocks were seeded on YPD-agar plates and cultivated for 48 h at 30°C. For cultivation in liquid medium, a single *C. tropicalis* colony was transferred into 15 mL YPD liquid medium in an Erlenmeyer flask and cultivated for 12 h at 30°C by 150 rpm shaking conditions.

For durable storage of the cells, glycerol stocks were prepared by mixing 1 mL sterile 100% glycerol with 1 mL of cell culture from the exponential growth phase and stored at -80°C.

2.2.1.2 Cell growth determination

The cell growth was determined by measuring optical density at 600nm, OD₆₀₀ (Thermofischer Scientific, Multiscan Spectrum). For determining the cell dry weight (CDW), 1 mL fermentation broth was centrifuged (21,000×g, 5 min, RT), the supernatant was discarded, and the pellet was completely dried (24 h) at 65°C and weighed thereafter.

2.2.1.3 Determination of colony-forming units (CFU)

Colony forming units were determined by seeding serial dilutions of cell culture (10⁻¹-10⁻¹⁰) on YPD agar plates. After incubation at 30°C for 24 h, the colonies were counted, and the CFU/mL was calculated.

2.2.1.4 Microscopy

Microscopic images were obtained using a Motic Microscope BA310 and Motic Images Plus 2.0 software. ImageJ 1.51d software and an object measuring plate (Mikroskop Technik Rathenow, Germany) were used for image analysis.

2.2.1.5 Yeast cell wall disruption

An enzymatic lysis of yeast cell wall was performed for subsequent RNA extraction. 1 mL of cell culture at OD₆₀₀ of ~3 was centrifuged (21,000×g, 1 min, RT), and the cell pellet was

resuspended in 100 μL of enzyme dilution buffer (2.1.9.7). 15 U of Zymolyase or 50 U of Lyticase (contained in Aurum™ Total RNA Mini Kit (Bio-Rad, USA)) were added, followed by incubation at 37°C for 15 min. Protoplasted cells were harvested by a centrifugation step (2,400 $\times g$, 5 min, RT) and used further for the RNA extraction. To monitor protoplast formation absorption at 600nm was measured.

2.2.1.6 Total lipid extraction and lipid saponification

Total lipid was extracted from yeast using a chloroform : methanol : water mixture as described earlier [90]. Briefly, approximately 0.1 g cell pellet as obtained by centrifugation (21,000 $\times g$, 5 min, RT) was dissolved in 1.5 mL methanol : chloroform (2:1, v/v) and vortexed for 6 min with glass beads ($\varnothing=1$ mm). Then, 500 μL chloroform was added and the mixture was vortexed for another 1.5 min. This step was then repeated after adding 500 μL ddH₂O. After phase separation, the lower chloroform phase containing extracted lipids was recovered and the chloroform evaporated. Prior to saponification (Figure 2-1), lipids were solubilised in 1 M KOH (in 70% ethanol) and heated in a water bath at 70°C–75°C for 1 h [91]. The lipid mixture was acidified with sulfuric acid, and released fatty acids were extracted using *n*-hexane and analysed by GC/FID. The glycerol remaining in the aqueous phase was analysed using HPLC.

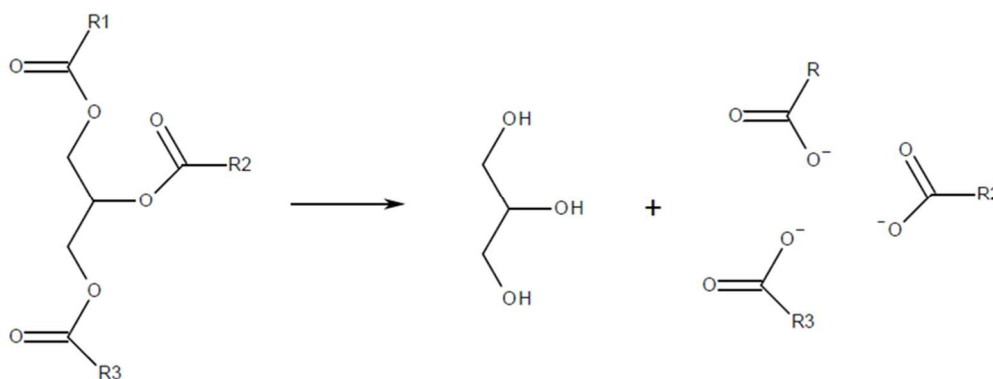


Figure 2-1: General saponification procedure

2.2.2 Molecular biology methods

2.2.2.1 Isolation of genomic DNA (gDNA)

The cells of the 5 mL overnight culture were harvested at 21,000×*g*, 5 min, RT and resuspended in 200 μL Harju buffer (2.1.9.9). For cell lysis, the cell suspension was exposed 2 min to liquid nitrogen and heated directly afterwards for 1 min at 95°C; this cycle was repeated two times. Then, cells were vortexed for 30 s, 200 μL of chloroform was added and cell broth vortexed again for 2 min. To enable phase separation the cell suspension was centrifuged at 21,000×*g*, 3 min, RT. The upper phase was then combined with 400 μL of ice-cold ethanol (100%) and mixed gently. After incubation at -20°C for 5 min the gDNA was recovered by a centrifugation step (21,000×*g*, 3 min, RT). gDNA contained in the pellet was washed with 500 μL of 70% ethanol. After centrifugation at 21,000×*g*, 5 min, RT the pellet was resuspended in 400 μL of TE buffer (2.1.9.9). 15 μL of RNase was added and the solution was incubated for 5 min at 37°C. Finally, after addition of 10 μL of ammonium acetate and 1 mL of ice-cold ethanol (100%) the suspension was gently mixed and centrifuged at 21,000×*g*, 2 min, 4°C. Pellet containing pure gDNA was dried at RT for 15 min and dissolved in 40 μL ddH₂O. The obtained gDNA was stored at -20°C.

2.2.2.2 RNA extraction

Protoplasted cells obtained after yeast cell wall disruption (2.2.1.5) were used for the RNA extraction, which was performed using Aurum™ Total RNA Mini Kit (Bio-Rad, USA) according to the manufacturer's manual with the following modification: prolongation of DNase treatment to 30 min. After elution of RNA an additional DNA degradation step before reverse transcription was performed using a RapidOut DNA Removal Kit (Thermo Fisher Scientific, USA) according to the manufacturer's instructions. Then, isolated RNA was directly transcribed to cDNA (2.2.2.8) and stored at -80°C until further utilization.

2.2.2.3 Determination of DNA/RNA concentration

The concentration and purity of the gDNA and RNA was determined by measuring its absorbance at 230, 260, and 280 nm with a NanoPhotometer P330 (Implen GmbH, Germany). The DNA was considered to be pure when the ratio of absorbance at 260 nm to 280 nm was around 1.8. In case of RNA the ratio was targeted towards 2.0.

2.2.2.4 Polymerase chain reaction (PCR) for DNA amplification

The polymerase chain reactions were performed using Phusion™ High-Fidelity DNA Polymerase (Thermo Fisher Scientific) in a volume of 50 µL. For the reaction the following components were used at a final concentration: 1-2 ng/µL of template DNA, 500 pM of each primer (forward and reverse), 200 µM of dNTPs (dATP, dGTP, dCTP, dTTP), 1 U of DNA Polymerase and 1x Phusion HF-Reaction buffer. The following Table 2-2 shows the typical PCR protocol.

Table 2-2: PCR conditions for DNA amplification

| Cycle Step | Temperature | Duration | Number of cycles |
|----------------------|-------------|----------|------------------|
| Initial Denaturation | 98°C | 5 min | 1 |
| Denaturation | 98°C | 30 s | 30 |
| Annealing | 54°C | 30 s | |
| Extension | 72°C | 1 m | |
| Final Extension | 72°C | 10 min | 1 |
| | 16°C | hold | - |

2.2.2.5 Quantitative PCR (qPCR)

Real-time qPCR assays were carried out using SsoAdvanced™ Universal SYBR® Green (Bio-Rad, USA) according to the manufacturer's manual. The master mix was prepared for each designed primer pair (Table 2-1) by adding all required components: SYBR Green Mix, primer pairs at an appropriate concentration and nuclease-free H₂O if needed. The optimal primer concentration as well as annealing temperature (T_a) were identified as described in 2.2.2.5.1. 8 µL of prepared master mix were pipetted in white multiplates (Bio-Rad, USA) and 2 µL of a template or of an appropriate control were added (Table 2-3).

Table 2-3: Templates and controls applied for qPCR

| Template | Name | Description |
|--------------------------------|-----------------------------------|--|
| cDNA | Sample | - |
| Nuclease-free H ₂ O | NTC (no template control) | Included in every run for each primer pair to test buffers and solutions for gDNA contamination and to assess for primer-dimers |
| Isolated RNA | NRT (no reverse transcription) | RNA samples, that were not reverse transcribed, used to assure the absence of gDNA contamination. Each sample that has been used for cDNA synthesis was analyzed |
| cDNA | IRC (inter-run calibrator) | Used to minimize technical variability between samples and was included in every run for each primer pair |

The plates were sealed, vortexed and shortly centrifuge prior to measuring the plate according to the conditions described in Table 2-4 using the CFX96 Touch™ Real-Time PCR Detection System (Bio-Rad, USA). To verify that each primer pair resulted in a single amplicon, the melting curve analysis at the end of qPCR protocol for each PCR product was applied as described in 2.2.2.5.1.

All samples and controls were measured in triplicates. During the measurements an inter-run calibrator was used to minimize technical variability between samples.

Table 2-4: qPCR conditions

| Cycle Step | Temperature | Duration | Number of cycles |
|------------------------|--------------------|---------------------------|-------------------------|
| Initial Denaturation | 95°C | 30 s | 1 |
| Denaturation | 95°C | 15 s | 40 |
| Annealing + Extension | T _a | 15 s | |
| Final Extension | 95°C | 10 s | 1 |
| Melting curve analysis | 65-95°C | 0.5°C increment every 5 s | - |

T_a was identified as described in 2.2.2.5.1.

qPCR assay was validated for each primer pair. The validation included determination and optimization of the reaction specificity (2.2.2.5.1) and efficiency (2.2.2.5.2) to assure a successful and accurate qPCR assay as recommended [92, 93].

2.2.2.5.1 Determination of qPCR specificity

To prevent nonspecific annealing and primer-dimer formation during a PCR reaction an optimal primer concentration, as well as, annealing temperature was identified. The optimal conditions were approved by determining quantification cycle (C_q value). The C_q represents the cycle at which the fluorescence signal from the template exceeds the background fluorescence. Thus, lower C_q value indicates higher template concentration in the sample. The data analysis was performed using CFX Manager Software (Bio-Rad, USA).

For determination of the optimal primer concentration, primers in the range of 50 nM to 600 nM were tested applying T_a at 61°C as recommended by manufacturer. Then, using optimal primer concentration, the temperature gradient in the range of 58-65°C, around the melting temperature (T_m), was applied in order to investigate the optimal T_a.

The conformation of the primer specificity was enabled by analysis of the qPCR amplification product, which comprised of melting curve analysis and agarose gel analysis. The melting curve analysis, as performed at the end of the qPCR protocol, displays change in the fluorescence intensity resulted by dissociation of the dsDNA bound with SYBR[®] Green with increasing temperature [94]. Thus, the dissociation of the qPCR amplification product is directly related to the length and G/C content of the sequence and results in specific melting temperature for each qPCR product. Only the primer pairs resulted in one sharp peak were selected for the qPCR assay. In addition, at least one sample per primer pair was used to run 1% (w/v) agarose gel to verify the expected size of the amplicon as described in 2.2.2.6.2.

2.2.2.5.2 Determination of qPCR efficiency

The efficiency of the qPCR reaction was determined for each primer pair at the optimal conditions as described in 2.2.2.5.1. Therefore, standardized 5-fold dilution series of the template cDNA with a broad dynamic range was carried out, covering at least eight dilutions. The qPCR assay was performed as described in 2.2.2.5. PCR efficiency, [%], was calculated according to the following equation:

$$E = (10^{\frac{1}{slope}} - 1) \cdot 100 \quad (1)$$

Acceptable range for the qPCR efficiency is 90-110% [65]. Usually, reaction efficiency lower than 90% indicates non-optimal reagent concentrations or suboptimal reaction conditions. Meanwhile, nonspecific amplification or formation of primer dimers leads to qPCR efficiency higher than 110% [93, 94].

2.2.2.5.3 Selection of reference genes and normalization procedure

The normalization of qPCR data with the references genes enables comparison of the mRNA levels across different samples. Usually housekeeping genes serve as appropriate reference genes, since they show stable expression during the entire cell cycle. The following housekeeping genes were tested:

- ***GAPDH*** encoding glyceraldehyde-3-phosphate dehydrogenase, a classical glycolytic protein, which catalyzes the reaction of glyceraldehyde-3-phosphate to 1,3-bisphosphoglycerate [95].
- ***ACT1*** encoding β -actin, the most abundant and highly conserved intracellular protein of eukaryotic cells, involved in a variety of cell functions that include cell divisions and cytokinesis, maintenance of cell junctions and cell shape, and organelle transport [96].
- ***PMA1*** encoding H⁺-ATPase, electrogenic proton pump involved in crucial cell functions such as nutrient uptake, osmotic balance and ion homeostasis [97].
- ***PGK1*** encoding phosphoglycerate kinase, also involved in glycolysis catalyzes the reversible transfer of a phosphate group from 1,3-bisphosphoglycerate to ADP producing 3-phosphoglycerate and ATP [98].

Data and stability of the different reference genes were analyzed using Bio-Rad CFX Manager (Bio-Rad, USA), following the instructions of geNorm. Accordingly, the expression stability (M), indicating pairwise variation, and the coefficient of variation (CV), describing the expression stability of the particular gene, of the respective reference genes were calculated by Bio-Rad CFX Manager. Two genes showing the lowest M and CV values were used for normalization [65].

2.2.2.6 Agarose gel-electrophoresis and ethidium bromide-staining

2.2.2.6.1 DNA separation

The DNA separation and detection were performed by gel electrophoresis in 1% or 2% (w/v) agarose gel depending on the purpose. Agarose was prepared in 1x volume of TAE buffer and boiled until it liquefied. Following which, the tray containing a sample comb was filled with the prepared agarose and cooled until hardening. After the gel was solidified, the gel carrier was inserted into a tank filled with TAE buffer, a running buffer, and the sample comb was removed. The samples were mixed with 5x volume of DNA loading dye and injected into the pockets. Depending on the length of the separated fragments 1000 bp or 100 bp markers were used. The gel was run at 120 V for about 25 min. Ethidium bromide staining was performed as described in 2.2.2.6.3.

2.2.2.6.2 Denaturing agarose gel-electrophoresis for RNA separation

Denaturing agarose gel electrophoresis was performed to assure the integrity of isolated RNA (2.2.2.2). As a single stranded molecule, RNA is able to form a secondary structure. To avoid this, formaldehyde was applied, which is able to form a Schiff base with RNA preventing the base pairing of RNA [93]. A 1% agarose gel was prepared in 1xMOPS buffer and was run without the samples at 60 V for 20 min. The samples were mixed with 5xRNA Loading dye, subsequently exposed to 70°C for 5 min and then directly cooled on ice for 2 min. In this manner, the prepared samples and a 1kb marker were injected into the pockets. The gel was run at 60 V for about 1.5 h. Due to low ionic strength of the MOPS buffer, a pH gradient along the length of the gel may occur leading to a hydrolysis of agarose gel. To reduce this occurrence, the MOPS buffer was recirculated by pipetting from one side of tank to another after approximately 30 min of the run. Ethidium bromide staining was performed as described in 2.2.2.6.3

2.2.2.6.3 Ethidium bromide-staining

The gels were stained in 0.1% (v/v) ethidium bromide solution for 10 min and then discolored in TAE buffer for another 10 min. The gel was then analyzed in a dark hood from Biostep GmbH INTAS, Gel iX Imager under UV light and pictures of the gel were made.

2.2.2.7 DNA Sequencing

The sequencing was performed by the company GATC Biotech, Konstanz, Germany. The analysis and comparison of the DNA sequence was carried out using Clone Manager Suite 8.

2.2.2.8 Reverse transcription

Reverse transcription was performed with 160 ng of isolated RNA (2.2.2.2) in a final volume of 20 μ L, using an iScript cDNA synthesis kit (Bio-Rad, USA) containing Moloney Murine Leukemia Virus (MMLV)-derived reverse transcriptase with a RNase H activity and set of primers: oligo (dT) and random hexamer primer. Successfully transcribed cDNA samples were stored at -20°C until further utilization.

2.2.3 Analytical methods

2.2.3.1 Gas chromatography coupled with flame ionisation detector (GC/FID)

The samples from the cultivation broth were prepared for the GC/FID as followed. First, samples were acidified using 2 N HCl and extracted with two volumes of MTBE on a rocking shaker for 2 h. Then samples were filtered using a 0.2 μ m PTFE filter. Further, the filtered organic phase was diluted to appropriate concentrations within the calibration range. Then the samples were mixed with N-methyl-N-(trimethylsilyl) trifluoroacetamide (MSTFA) in the ratio of 4:1(v/v) respectively and measured using appropriate GC/FID method (Table 2-5).

Table 2-5: GC/FID parameters applied for different methods

| | C12 | C18:1 |
|------------------------------------|----------------------|----------------------|
| Column | BPX5 | Rxi®-5Sil MS |
| Carrier gas | He | He |
| Gas flow | 1 mL/min | 0.5 mL/min |
| Start temperature | 180 | 90 |
| Gradient ramp I | 8°C/min until 245°C | 50°C/min until 210°C |
| Gradient ramp II | 30°C/min until 300°C | 10°C/min until 220°C |
| Gradient ramp III | - | 15°C/min until 280°C |
| Gradient ramp IV | - | 60°C/min until 330°C |
| Injector | | |
| Type | SSL (Split/Spitless) | |
| Basic temperature | 340°C | |
| Split flow | 1 mL/min | |
| Injection volume | 0.5 μ L | |
| FID-Detector | | |
| Basic temperature | 320°C | 340°C |
| H ₂ flow rate | 35 mL/min | |
| Synthetic air flow rate | 350 mL/min | |
| Make up gas flow (N ₂) | 30 mL/min | |

Depending on the chain length of the fatty acids, two different GC/FID methods were applied. DAME, DA and DDA were detected using the C12 method. For detection of oleic acid and *cis*-ODA the C18:1 method was applied. GC/FID was performed using equipment

described in 2.1.4. For quantification of the samples standard curves were prepared. The calibration range of the C12 fatty acid and its derivatives was 0.25 mM-15 mM and for oleic acid and *cis*-ODA 0.25 mM-10 mM. Standards were prepared by the same procedure as the samples

2.2.3.2 Gas chromatography coupled with mass spectroscopy (GC/MS)

Derivatized samples as prepared for GC/FID measurements (2.2.3.1) were diluted using MTBE to reach a concentration range of 10 µM-50 µM and measured applying conditions described in following Table 2-6.

Table 2-6: Conditions applied for GC/MS

| | |
|-------------------|--|
| Column | Rxi®-5Sil MS |
| Carrier gas | He |
| Gas flow | 0.5 mL/min |
| Start temperature | 90 |
| Gradient ramp I | 50°C/min until 210°C |
| Gradient ramp II | 10°C/min until 220°C |
| Gradient ramp III | 15°C/min until 280°C |
| Gradient ramp IV | 60°C/min until 330°C |
| Injector | |
| Type | PTV Programmed Temperature Vaporising |
| Basic temperature | 340°C |
| Split flow | 10 mL/min |
| Injection volume | 0.5 µL |
| MS | |
| Scan Mode | Full scan |
| Mass range | 50-650 |
| Ions | positive |
| Ions source | 250°C |

2.2.3.3 High-performance liquid chromatography (HPLC)

Ethanol and glycerol were released after the saponification of lipids (2.2.1.6) in aqueous phase, and were quantified by HPLC. Samples were analysed using HPLC equipment as

described in 2.1.4. The mobile phase (sulfuric acid, 2.5 mM) flow was set to 0.5 mL/min at an oven temperature of 70°C. For quantification of samples standard curves with the calibration range of 0.5-50 mM were prepared.

2.2.3.4 Thin layer chromatography (TLC)

Thin layer chromatography was applied for the qualitative analysis of the fatty acids and dicarboxylic acids during the biotransformation. Since, the sample preparation and measurement of the CG/FID is time consuming, TLC was applied for the quick analysis during the biotransformation to detect substrates and products. Therefore, the cell broth samples were centrifuged (21,000×g, 5 min, RT) and 3 µl of supernatant was spotted on a TLC plate (TLC Silica gel 60 F254, Merck) and separated using *n*-hexane : diethyl ether : acetic acid (80:20:2 v/v) as the mobile phase. Spots were visualised using phosphomolybdic acid dissolved in ethanol (48 g/L). To verify the composition of extracted lipids, the following standards were used: dioleoyl-sn-glycero-3-phosphocholine, ergosterol, triolein and cholesteryl oleate.

2.2.3.5 Glucose assay

A photometric enzyme assay was applied to quantify glucose concentration during the biotransformation of fatty acids. The cell broth was centrifuged at 21,000×g, 5 min, RT and supernatant used for subsequent analysis. The supernatant samples were mixed in a volume ratio of 1:1 with assay mixture solution (40 mM potassium phosphate, pH 6.0, 1.5 mM 2,2-azino-bis-(3-ethylbenzthiazoline)-6-sulfonic acid, 0.4 U glucose oxidase and 0.02 U horseradish peroxidase) and incubated at 30°C for 30 min with shaking at 400 rpm. The resulting extinction at 418 nm was measured and subtracted from absorption at 480 nm to eliminate background signals.

2.2.3.6 Nuclear magnetic resonance (NMR)

NMR-measurements were carried out at 25°C using standard pulse programs on JNM-ECA 400 MHz spectrometer (JEOL, USA). Chemical shifts are given as δ -values in ppm and reported as follows: value (multiplicity, coupling constant(s) were applicable, number of protons). Coupling constants (J-values) are given in Hertz (Hz). The DEPT135 technique was used to assign CH₂-signales. NMR spectra assignation was supported by

comparison with literature values for similar compounds. Only clearly identifiable peaks were assigned. For the characterization of observed signal multiplicities, the following abbreviations were applied: s (singlet), d (doublet), dd (double doublet), dt (double triplet), t (triplet), q (quartet), quint (quintet) and m (multiplet).



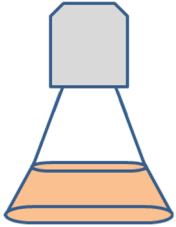
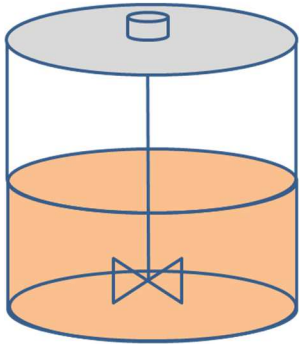
2.2.3.7 Melting point determination

Prior to determining the melting point of *cis*-ODA and *trans*-ODA, samples were dried overnight in a vacuum desiccator. Dry samples were placed inside a glass capillary and measured using melting point meter MPM-H2 (Schorpp Gerätetechnik, Germany).

2.2.4 Biotransformation of fatty acids

Biotransformation of the fatty acids and their derivatives was performed in a benchtop parallel bioreactor system comprising of eight bioreactors with maximal working volume of 1 L (2.1.4). The pre-culture for the bioreactor system was prepared first in a shake flask (2.2.4.1) followed by a pre-culture in a 2 L bioreactor (2.2.4.2) as summarized in the following Table 2-7.

Table 2-7: Pre-culture preparation: from agar plate to a 2 L bioreactor

| | Agar plate | Pre-culture I | Pre-culture II | Pre-culture III |
|-------------------------------------|---|---|--|---|
| |  |  |  |  |
| Volume [mL] | - | 25 | 150 | 2000 |
| Duration [h] | 48-72 | 10-12 | 10-12 | 12 |
| Achived OD₆₀₀ [-] | - | 8-10 | 8-10 | 24 |

2.2.4.1 Pre-culture in shake flask

Yeast cells from glycerol stocks were seeded on YPD-agar plates and cultivated for 48 h at 30°C. For cultivation in liquid medium, a single *C. tropicalis* colony was transferred into 15 mL YPD liquid medium and cultivated for 12 h at 30°C by 150 rpm shaking conditions. Then, a 1L shake flask containing 150 mL OPT-1 medium was inoculated at OD₆₀₀ of around 0.5 and further cultivated for 12 h at 30°C by 150 rpm shaking conditions.

2.2.4.2 Cultivation of pre-culture in 2 L bioreactor

In order to inoculate the DASGIP parallel bioreactor system, the pre-culture was prepared in a 2 L bioreactor (Biostat® Bplus, Sartorius Stedim). The working volume was set to 1 L comprising of 900 mL OPT-1 medium and 100 mL pre-culture conducted in a shake flask as described in 2.2.4.1.

The 2 L bioreactor was equipped with all the necessary accessories as summarized in Table 2-8. Prior to sterilisation, the pH probe was calibrated applying a two-point calibration at pH 7 and pH 4. Then, the bioreactor containing 900 mL OPT-1 media (without supplements) was sterilised in an autoclave at 121°C for 30 min. OPT-1 was completed by adding glucose, trace elements and magnesium sulphate after sterilisation (refer to 2.1.8). The bioreactor was connected to a control unit and the pO₂ probe was polarised for at least 6 h.

Table 2-8: 2 L bioreactor set up

| | Description |
|-----------------------------|--|
| Bioreactor | 2 L glass double-wall |
| Working volume | 0.6-2 L |
| Stirrer | 2x4 blade impeller |
| Aeration type | Ring sparger |
| pH probe | 405-DPAS-SCK8S, Mettler Toledo |
| pO₂ probe | inPro 6820, Mettler Toledo |
| Temperature probe | Pt100 |
| Exhaust gas analysis | CO ₂ and O ₂ , BlueSens, Germany |
| Others | Antifoam probe, sampling tube, baffles, exhaust cooler |

Table 2-9: Operational conditions of pre-culture in 2 L bioreactor

| | Batch | Fed-Batch |
|------------------------|--|--|
| Working volume | 1 L | |
| Inoculation | 10% (v/v) | |
| Medium | OPT-1 | |
| pH | 5.8 Regulation by 2N NaOH and 7% H ₃ PO ₄ | |
| pO₂ | No regulation | |
| Temperature | 30°C | |
| Aeration | 0.24 L/min | |
| Agitation | 600 rpm | |
| Foam regulation | Antifoam probe, regulation by 10% (v/v) Antifoam B | |
| Glucose Feed | - | 30 g/L at final concentration after 8h cultivation |
| Duration | 24 h | 12 h |

Before inoculating 2 L bioreactor, the pO₂ probe was also calibrated. Therefore, the parameters were set to desired operational conditions as described in Table 2-9. Additionally, 5 mL of antifoam was initially supplied before the calibration. After the parameters reached stable values, the pO₂ probe was calibrated applying one-point calibration at 100%. The cultivation was initiated by inoculating with 100 mL of the cell culture prepared in a shake flask (2.2.4.1). Initially, cell culture in 2 L bioreactor was performed in a batch mode for 24 h (Table 2-9). During process optimization a fed-batch mode was applied by supplying additional glucose at final concentration of 30 g/L after 8 h of cultivation (for details refer to 3.2.2). Total duration of the cultivation in fed-batch mode was reduced to 12 h (Table 2-9).

2.2.4.3 Whole-cell biotransformation in DASGIP system

The whole-cell biotransformation process was performed in DASGIP parallel bioreactor system (Eppendorf, Germany). The bioreactor system was equipped as summarized in Table 2-10 and prepared for sterilisation. Prior to sterilisation, the pH probe was calibrated applying two-point calibration at pH 7 and pH 4. Then, bioreactors containing 270 mL OPT-1 medium (without supplements) were sterilised in an autoclave at 121°C

for 20 min. OPT-1 was completed by adding glucose, trace elements and magnesium sulphate after sterilisation (refer to 2.1.8).

Table 2-10: Set up of DASGIP parallel bioreactor system

| | Description |
|-----------------------------|---|
| Bioreactors | Glass vessels DASGIP, Eppendorf |
| Quantity | 8 |
| Working volume | 0.2-1 L |
| Stirrer | Rushton-type impeller |
| Aeration type | L-sparger |
| pH probe | 405-DPAS-SCK8S, Mettler Toledo |
| pO₂ probe | inPro 6820, Mettler Toledo |
| Temperature probe | Pt100 |
| Exhaust gas analysis | DASGIP GA4 |
| Others | Antifoam probe, sampling tube, exhaust cooler |

To enable the correct supply of various supplements during the biotransformation, pumps with appropriate tubings were calibrated using the corresponding supplements (Table 2-11). Afterwards, tubings were cleaned with 80% ethanol, followed by 6 M NaOH and finally, flushed with sterile water and connected to the bioreactors. Prior to inoculation, the pO₂ probes were calibrated. The parameters were set to initial operational conditions as described in Table 2-12 and the agitation speed was kept at 1.200 rpm for calibration. Also, 3 mL of antifoam was initially supplied before the calibration. After the parameters reached stable values, the pO₂ probe was calibrated applying one-point calibration at 100%.

Table 2-11: Assignment of the pumps and corresponding supplements (DASGIP)

| | Supplement |
|---------------|--------------------------------------|
| Pump A | 500 g/L Glucose |
| Pump B | 6 M NaOH |
| Pump C | 10% (v/v) Antifoam B |
| Pump D | Substrate feed DAME or oleic acid |

Table 2-12: General parameters and their regulation during the biotransformation process

| | Parameters |
|------------------------|---|
| Starting volume | 300 mL |
| Inoculation | 10% (v/v) |
| Medium | OPT-1 |
| pO₂ | 15% Regulation by varying agitation speed from 600 to 1200 rpm |
| pH | Starting pH of 5.8 Regulation by 6 M NaOH |
| Temperature | 30°C |
| Aeration | 6 sL/h |
| Agitation | 600 - 1200 rpm |
| Duration | 24 h |

The cultivation was initiated by inoculation with 30 mL of the cell culture prepared in 2 L bioreactor (2.2.4.2). Directly at the beginning of the cultivation, 0.5 mL of the corresponding substrate (DAME or oleic acid) was supplied into the bioreactors. During the entire process, the foam formation was visually controlled, and antifoam was added, if needed to avoid constant anti-foam addition.

In general, the DCA production process can be divided into two phases: growth and biotransformation phase. During the optimization process both phases were optimized and adapted for the corresponding substrate. In the following, all applied variants are summarized.

Initially growth phase was performed in a batch mode at a constant pH of 5.8 (Table 2-13, A) and used prior to DAME biotransformation. Application of oleic acid as a substrate required an optimization of the growth phase. In order to achieve a high cell density of biomass, the final glucose concentration in the reactor was adjusted to 30 g/L after 8 h of the cultivation (Table 2-13, B). Later, the pH shift was transferred towards the growth phase (Table 2-13, C). Starting at 8 h of cultivation, the pH was increased from 5.8 to 8.0 within 6 h (0.55 steps every 2 h). This variant was finally used as the standard procedure prior to biotransformation of oleic acid.

Table 2-13: Operational parameters of various variants of growth phase

| | A | B | C |
|---------------------|--|---|--|
| | - | Extended growth | Extended growth pH Shift |
| Mode | Batch | Fed-Batch | Fed-Batch |
| pH | 5.8 | 5.8 | 5.8 until 8 h from 8 h: pH shift from 5.8 to 8.0 |
| Glucose Feed | - | 30 g/L at final concentration after 8 h cultivation | |
| Duration | 16 h | 16 h | 14 h |
| Application | Standard procedure applied prior to DAME biotransformation | Intermediate step towards variant C | Standard procedure applied prior to oleic acid biotransformation |

Independent of the performed growth phase, the biotransformation phase was initiated as soon as start of glucose and substrate feeds. Performance of the pH shift depended on the substrate used; thus, defining the selected growth phase as well (Table 2-13). Therefore, distinct types of growth phase were combined with various performances of the pH shift. The combinations are assigned to the same alphabetic character. As an example, growth phase A (Table 2-13) was always followed by a pH shift A (Table 2-14).

DAME biotransformation

As a standard, DAME biotransformation was carried out after the growth phase as described in Table 2-13, A. The biotransformation phase was initiated by starting a constant glucose feed rate of 1 g/h, a prolonged pH shift (variant A, refer also to Figure 3-1) and DAME feed as summarized in Table 2-14. Glucose feed rate is given in g/h and is independent of the bioreactor volume. Whereas DAME feed is related to the current volume in bioreactor and is given in g/(L·h).

Oleic acid biotransformation

Biotransformation of oleic acid was initiated by feeding oleic acid at a constant feed rate of 1 g/(L·h). Glucose feed was varied between 0.4 and 1.0 g/h depending on the experiment. The biotransformation of oleic acid was performed using various pH shift

strategies: prolonged pH shift (A), reduced pH shift (B) or reduced pH shift in the growth phase(C) as summarized in Table 2-14.

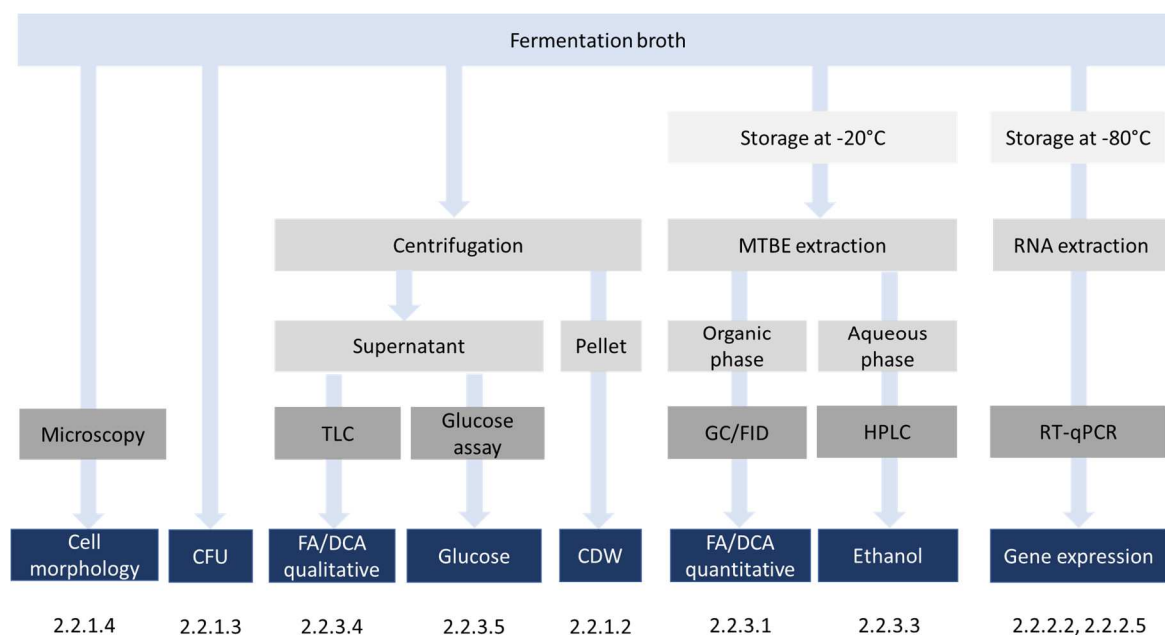
Table 2-14: Operational parameters of the biotransformation of DAME and oleic acid

| | | DAME | Oleic acid |
|----------------|---|--|-------------|
| Glucose feed | | 1 g/h | 0.4 - 1 g/h |
| pH shift | A | From 16 h to 45 h: shift from 5.8 to 7.7 with 0.13 steps over 2 h From 45 h: shift from 7.7 to 8.0 with 0.1 steps over 8 h | |
| | B | From 16 h to 22 h: shift from 5.8 to 8.0 with 0.55 steps over 2 h | |
| | C | From 8 h to 14 h: shift from 5.8 to 8.0 with 0.55 steps over 2 h | |
| Substrate Feed | | From 16 h to 45 h: constant at 0.5 g/(L·h) After 45h increasing until 0.9 g/(L·h) or 1.2 g/(L·h), when constant at 0.9 g/(L·h) or 1.2 g/(L·h) | 1 g/(L·h) |

Sampling

During the biotransformation process samples were taken to monitor various parameters, such as formation of the product or cell growth. The following scheme summarizes the sampling procedure, storage conditions and refers to the corresponding measuring method (Figure 2-2).

Figure 2-2: Schematic overview over the sampling procedure during the DCA production



2.2.4.4 Whole-cell biotransformation in a shake flask

Yeast cells from the glycerol stocks were streaked on YPD-agar plates and cultivated for 48 h at 30°C. For cultivation in liquid medium, a single *C. tropicalis* colony was transferred into 15 mL YPD liquid medium and cultivated for 12 h at 30°C with 150 rpm shaking. Then, 150 mL OPT-1 medium was inoculated at OD₆₀₀ of around 0.5, substrate (oleic acid or DAME) were added at a final concentration of 16 mM and further cultivated for 12 h at 30°C by 150 rpm shaking conditions. The biotransformation was monitored by GC/FID (2.2.3.1).

2.2.4.5 Whole-cell biotransformation in 2 L bioreactor

Whole-cell biotransformation in 2 L bioreactor was performed after the initial growth phase as described in 2.2.4.2. At the end of the growth phase after 8 h and 12 h the cell culture was supplied with additional glucose at a final concentration of 30 g/L. The biotransformation was initiated by supplying oleic acid at a final concentration of 18 g/L after 22 h of cell growth. pH shift from 5.8 to 8.0 was performed manually by increasing 0.15 steps each hour. The biotransformation was monitored by GC/FID (2.2.3.1).

2.2.5 Downstream processing of *cis*-ODA

A hot-filtration recrystallization method was used to purify *cis*-ODA. First, cell broth obtained after biotransformation was centrifuged (15,000×*g*, 30 min, RT). Prior to extraction, the supernatant was acidified with 2 N HCl and filtered. The solid fraction obtained was dissolved in a 6:1 mixture of hexane and ethyl acetate (v/v), followed by heating up to 90°C for 40–60 min until boiling. The mixture was then filtered immediately to remove insoluble impurities and then cooled to 4°C for 12 h. The obtained crystals were filtered using a pre-cooled 6:1 mixture of hexane and ethyl acetate (v/v). The obtained solid was further dried using a vacuum desiccator (12–24 h). In this way, obtained *cis*-ODA with a purity of 94% (confirmed by GC/FID) was used as the analytical standard for GC/FID.

2.2.6 Equations

$$\text{Specific growth rate [h}^{-1}\text{]} \quad \mu_{max} = \frac{\ln X - \ln X_0}{t - t_0} \quad (2)$$

$$\text{Doubling time [h]} \quad t_D = \frac{\ln 2}{\mu_{max}} \quad (3)$$

$$\text{Biomass yield coefficient [g}_{\text{biomass}}/\text{g}_{\text{glucose}}\text{]} \quad Y_{X/C} = \frac{X}{C} \quad (4)$$

$$\text{Substrate conversion [\%]} \quad X_S = \frac{S_0 - S}{S_0} \cdot 100\% \quad (5)$$

$$\text{Product yield [\%]} \quad Y_P = \frac{P - P_0}{S_0} \cdot 100\% \quad (6)$$

$$\text{Space time yield [g}/(\text{L}\cdot\text{h)}\text{]} \quad STY = \frac{P}{V \cdot t} \quad (7)$$

$$\text{Specific productivity [mg}_{\text{product}}/(\text{g}_{\text{biomass}}\cdot\text{h)}\text{]} \quad S_p = \frac{P}{X_B \cdot t} \quad (8)$$

$$\text{Reaction yield [g}_{\text{product}}/\text{g}_{\text{substrate}}\text{]} \quad q_p = \frac{P}{S} \quad (9)$$

Where,

- X biomass (OD₆₀₀) at the end of the growth phase, [-]
- X₀ biomass (OD₆₀₀) at the start of the growth phase, [-]
- (t-t₀) growth phase duration, [h]
- C glucose amount at the start of the growth phase, [g]
- S₀ amount of substrate at the start of the process, [g]
- S amount of substrate at the end of the process, [g]
- P amount of product at the end of the process, [g]
- P₀ amount of product at the start of the process, [g]
- t process time, [h]
- V working volume at the end of the process, [L]
- X_B cell biomass at the end of the process, [g]

3 Results

3.1 Biotransformation of dodecanoic acid methyl ester

3.1.1 Introduction to dodecanedioic acid production process

A fundamental concept of the DDA production process comprising of a growth and biotransformation phase was developed earlier using a β -oxidation deficient *C. tropicalis* ATCC 20962 strain [99]. Shortly, intense cell flotation as a result of pseudo-mycelium formation during the growth phase was minimized by the application of mechanical foam breakers and an adapted aeration strategy. This combination enabled an efficient and reproducible biomass production and characterization. DAME, a highly hydrophobic and toxic substrate, was identified as the main limitation of the subsequent biotransformation phase. High DAME feed rates in the range of 1-8 g/(L·h) were found to induce the accumulation of DAME and DA, a hydrolyzed product of the methyl ester. The accumulation of toxic substrates affected cell viability and consequently led to a drastic decrease of productivity. Reduction of the DAME feed rate to 0.5 g/(L·h) seemed to support cell viability. However, owing to strong hydrophobicity of the substrate, inhomogeneity resulted during the production process hindered efficient biotransformation. The following study proceeds from this point and was addressed towards the optimization of various bottlenecks and issues identified.

3.1.2 Optimization of the DDA production process

3.1.2.1 Application of pH shift for enhanced DAME biotransformation

Using DAME as a highly hydrophobic substrate usually resulted in the formation of a second organic phase hindering efficient biotransformation and prevented the reliability and reproducibility of analytical measurements. Thus, to increase the substrate as well as product solubility, a pH shift towards slightly basic conditions as described by Liu *et al.* [47] was adapted for the DDA production process. Starting simultaneously with the beginning of the biotransformation phase, the pH was increased stepwise from 5.8 to 7.7 from 17 h to 45 h, followed by a reduced rate of increase up to pH 8.0 within the next 45 h as summarized in Figure 3-1.

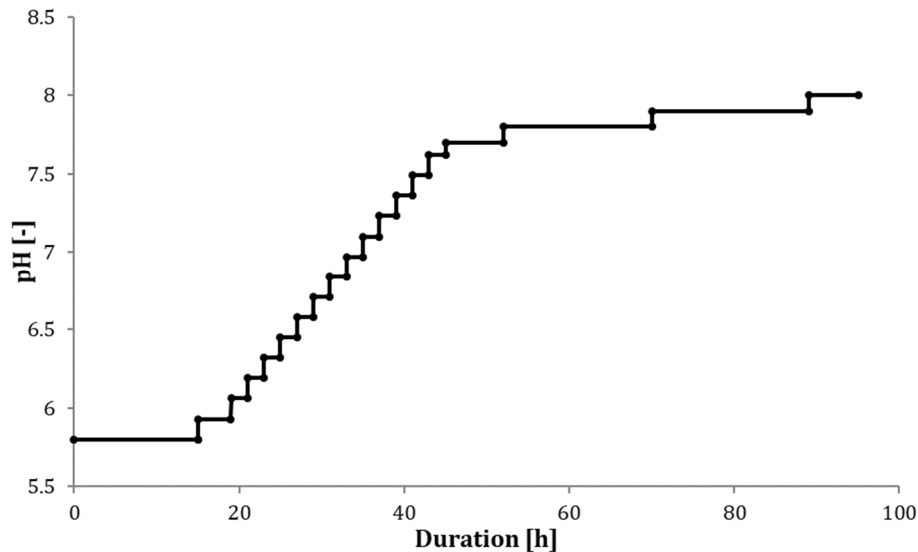


Figure 3-1: pH shift in the biotransformation phase applied for DDA production

Starting at 17 h the pH was gradually increased from 5.8 to 7.7 until 45 h, followed by a reduced rate of increase up to pH 8.0 within the next 45 h.

Application of the pH shift initiated simultaneously with the DAME feed, resulted obviously in enhanced DAME and DDA solubility, since a second phase was not observed. However, the pH shift was found to negatively influence the cell growth. As summarized in the following Table 3-1, application of the pH shift led to reduced cell biomass production compared to the approach at a constant pH of 5.8. Interestingly, biotransformation of DAME seemed to not be affected by reduced cell biomass and nearly the same DDA concentration for both variants was achieved. Obviously, besides lowering the visible inhomogeneity of the biotransformation broth, the pH shift led also to a 2.3-fold increase of specific productivity in comparison to the biotransformation at constant pH, and therefore was applied for all upcoming experiments on DDA production.

Table 3-1: Overview of process parameters at constant pH in comparison to pH shift during the biotransformation

| | Cell biomass [g/L] | Final DDA concentration [g/L] | Specific productivity [mg_{DDA}/(g_{biomass}·h)] |
|----------------------------|-------------------------------|--|---|
| Constant pH at 5.8* | 51.1 ± 1.3 | 23.9 ± 1.6 | 5.0 ± 0.2 |
| pH shift** | 20.0 ± 1.4 | 21.2 ± 0.8 | 11.4 ± 1.1 |

The experiment was performed using DASGIP 8x1L parallel bioreactor system as described in methods applying constant DAME feed of 0.5 g/(L·h). The data represent the mean ± standard deviation at the end of the production process (94 h). Sample size: * n = 2, ** n = 3

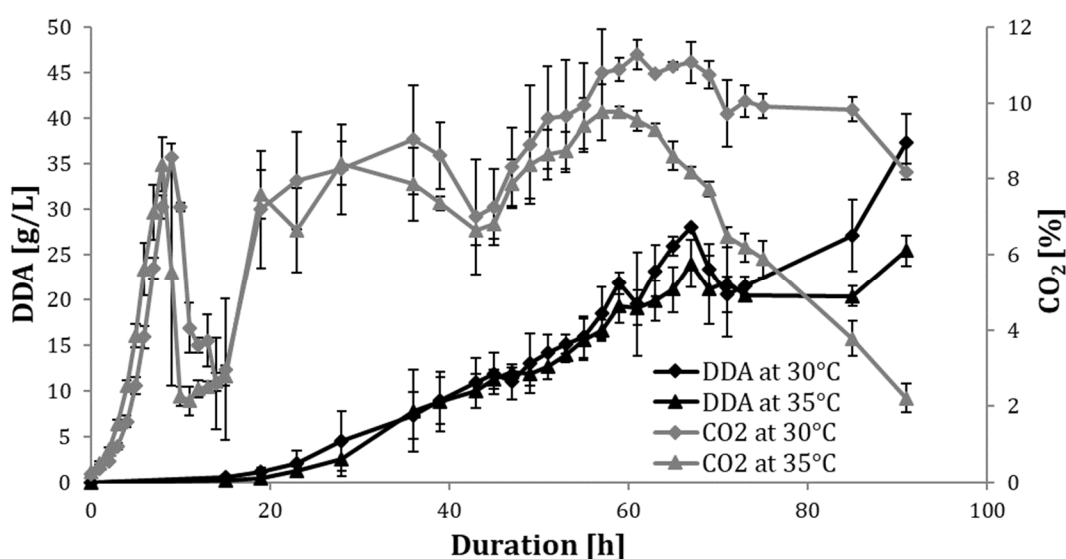
3.1.2.2 Effect of temperature on the biotransformation efficiency

As a part of the optimization procedure, the impact of temperature on cell growth, especially on DDA productivity was studied. DDA production including pH shift was carried out at two different temperatures: 30°C and 35°C. Monitoring CO₂ formation in the exhaust flow and biomass production led to the conclusion that the temperature does not have any distinct influence on the cell growth and viability during the growth phase. Shortly after the inoculation, the yeast cells at both temperatures showed enhanced growth as indicated by the drastic increase of CO₂ in exhaust flow (Figure 3-2). The subsequent decrease of CO₂ after 8 h in both variants suggests a depletion of the carbon source resulting in a distinct CO₂ peak. During the first 20 h of the biotransformation phase cells of the 30°C and 35°C variants showed comparable growth. However, increased temperature strongly influenced the cell viability later in the biotransformation phase. Starting at around 60 h, yeasts exposed to a higher temperature revealed loss in viability indicated by the drop in CO₂ formation resulting finally in reduced cell biomass (Table 3-2). Obviously, loss in cell viability during the biotransformation at 35°C led to significant decrease of the DDA productivity and thus, specific productivity (Table 3-2). To maintain high cell viability and cell biomass as the theoretical number of the biocatalysts, the upcoming DAME biotransformations were performed at 30°C.

Table 3-2: Overview of process parameters at different temperatures

| | Cell biomass [g/L] | Final DDA concentration [g/L] | Volumetric productivity [g/(L·h)] | Specific productivity [mg _{DDA} /(g ^{biomass} ·h)] |
|--------|-----------------------|-------------------------------------|--------------------------------------|---|
| 30°C* | 22.4 ± 2.6 | 37.3 ± 3.1 | 0.41 ± 0.03 | 18.5 ± 2.7 |
| 35°C** | 19.4 ± 1.4 | 25.4 ± 1.7 | 0.28 ± 0.02 | 14.9 ± 0.8 |

The experiment was performed using DASGIP 8x1L parallel bioreactor system as described in methods applying constant DAME feed of 0.5 g/(L·h). The data represent the mean ± standard deviation at the end of the production process (91 h). Sample size: * n = 3, ** n = 4.

**Figure 3-2: DDA production in dependency of the temperature**

Monitoring of the DDA concentration and CO₂ as detected in exhaust gas over time. CO₂ formation showed a typical peak in growth phase: increased CO₂ production followed by drastic decrease caused by depletion of glucose. Initiation of glucose feed in the biotransformation phase resulted in enhanced CO₂ formation. During the performance of the pH shift, the CO₂ level became more moderate and declined at the end of the major pH shift after 45 h independent on the temperature. DDA concentration was found to increase during the production process. The experiments were performed in triplicate using DASGIP 8x1L parallel bioreactor system as described in methods applying constant DAME feed of 0.5 g/(L·h). The error bars represent the standard deviations.

3.1.2.3 Determination of an optimal substrate feed rate

As mentioned earlier, application of DAME as the biotransformation substrate at feed rates higher than 0.5 g/(L·h) resulted in significant reduction of cell viability, accumulation of DAME and accordingly inhomogeneity of the cultivation broth [99]. Introduction of the pH shift to the biotransformation phase, however, resulted in increased specific productivity (Table 3-1), likely due to enhanced solubility of the product and substrate. Thus, increasing the substrate feed over 0.5 g/(L·h) was conceivable. Since the pH shift itself negatively affected the cell growth and viability (Table 3-1), the substrate feed was adjusted as follows. During the intensive pH shift, the substrate feed was kept constantly low at 0.5 g/(L·h). Close to the end of the pH shift (pH 7.7, 45 h after inoculation) the substrate feed was continuously increased in 0.05 g/(L·h) steps to identify the optimal DAME feed (Figure 3-3). During the biotransformation the production of DDA and possible accumulation of the DAME or DA was monitored by use of GC/FID.

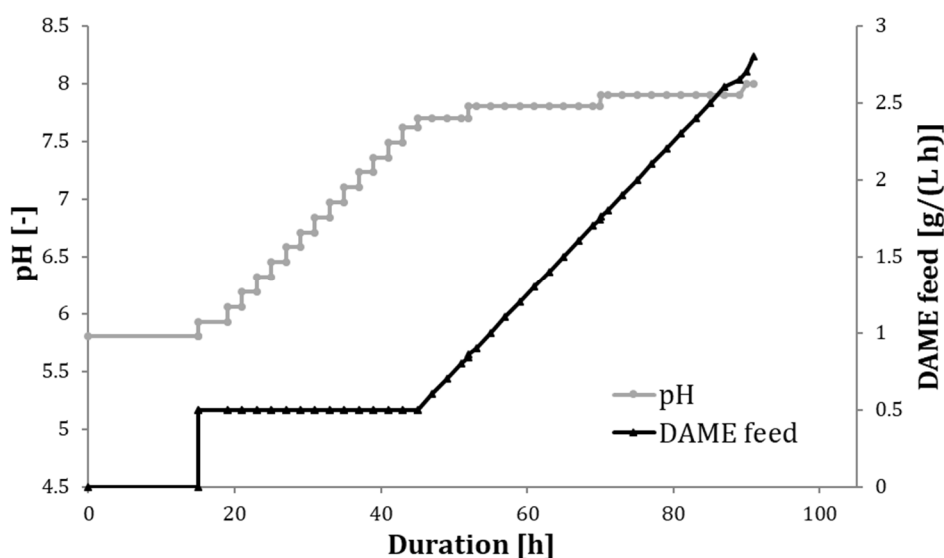


Figure 3-3: pH shift in combination with the increased DAME feed for evaluation of the maximal feed rate for bioconversion [100]

Towards the beginning of the biotransformation phase at 17 h the pH shift was initiated, and pH was gradually increased from 5.8 to 7.7 until 45 h. During this time DAME feed was kept constant at 0.5 g/(L·h). After 45 h the major pH shift was conducted and slow increase of pH up to 8.0 was performed. Simultaneously DAME feed was increased in 0.05 g/(L·h) steps, calculated relative to the present volume.

Applying an increased DAME feed in combination with the pH shift revealed first accumulations of DA after 55 h of the process, with a substrate feed of 1 g/(L·h) and accumulation of DAME after 60 h at the substrate feed rate of 1.3 g/(L·h) (Figure 3-4). Therefore, a substrate feed of 0.9 g/(L·h) was defined as the lowest substrate feed and 1.2 g/(L·h) as the highest feed within the acceptable range.

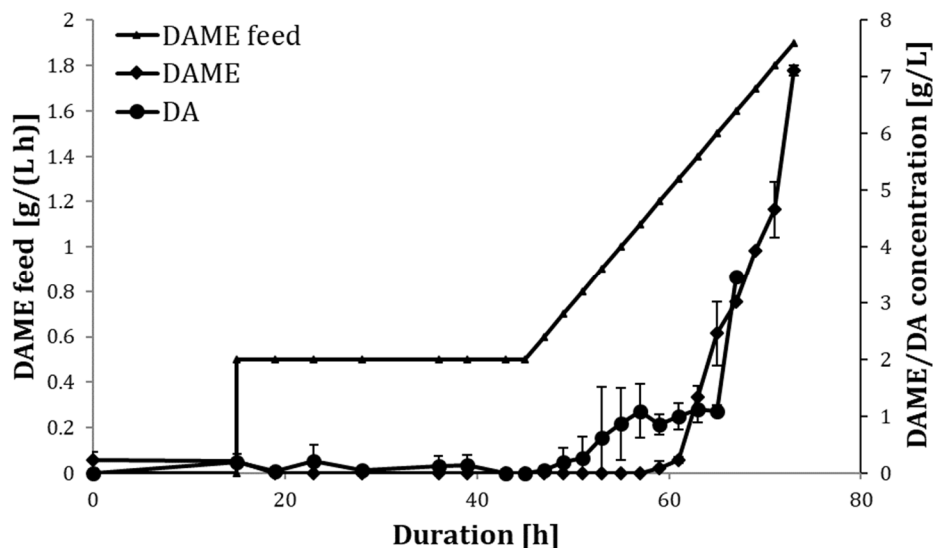


Figure 3-4: Accumulation of DAME and DA over the time displaying dependency on the applied increased DAME feed [100]

DAME feed was kept constant at 0.5 g/(L·h) from 17 h to 45 h, followed by a stepwise increase of 0.05 g/(L·h). Accumulation of DA occurred at around 55 h, followed by DAME accumulation after 60 h. The experiments were performed in duplicate using the DASGIP 8x1L parallel bioreactor system as described in the methods. The error bars represent the standard deviations.

In the next step, the identified thresholds of the optimal substrate feed rate range were verified by additional experiments. A similar strategy of combining the pH shift and an increased substrate feed rate in two different approaches, run A and run B, was applied. For run A the DAME feed rate was increased from 0.5 to 0.9 g/(L·h) and then kept constant. To confirm the upper limit in run B the substrate feed rate was increased until 1.2 g/(L·h) and then held constant. As a positive control to evaluate the effects of the substrate on cell viability, a control bioreactor was run at identical conditions, but in the absence of DAME feed. Since, the quantification of both substrate and product using GC/FID is laborious and time consuming, it was not appropriate for the real-time

monitoring of the biotransformation process. Therefore, to quickly verify DA and DAME accumulation, a qualitative analysis using thin-layer chromatography (TLC) was performed, which assured distinct separation of the desired components (DAME, DA, DDA) (Figure 3-5). During biotransformation, whenever DAME or DA accumulation was detected via TLC, the substrate feed was interrupted to minimize negative effects on cell viability. In case, the substrate or intermediates were no longer detected, the feed was restarted until DA or DAME accumulation were visible again (Figure 3-6).



Figure 3-5: Thin layer chromatography for the qualitative detection of DAME, DA and DDA

Standards of (1) DAME, (2) DA, (3) DDA and (4) mix of DAME, DA, DDA were dissolved in pyridine at 50mM. TLC was performed as described in the methods.

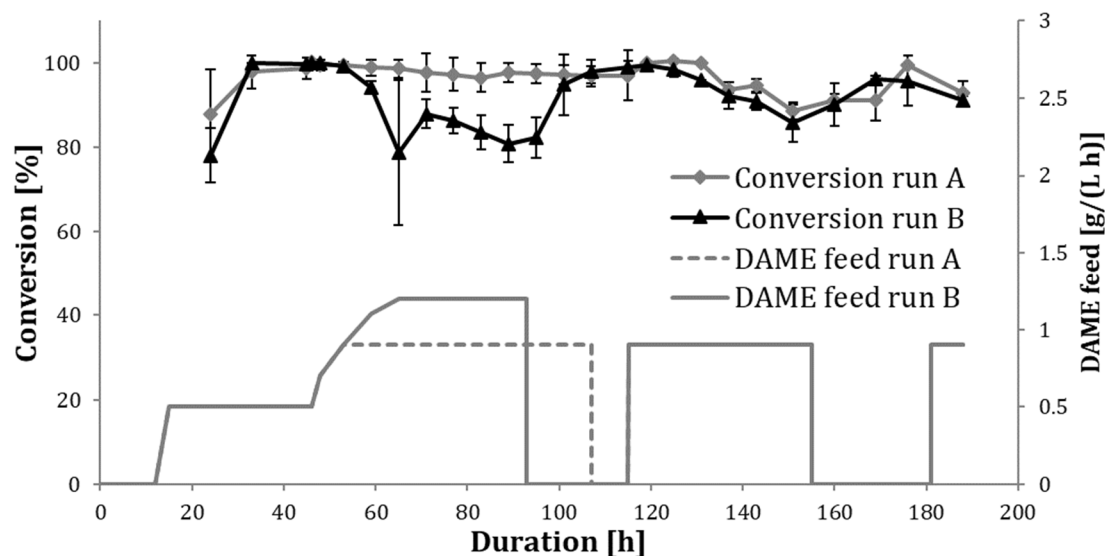


Figure 3-6: Conversion of DAME and profile of the DAME feed over time [100]

Both DAME feeds were initially held at a constant rate of 0.5 g/(L·h) and were increased at a rate of 0.05 g/(L·h) after 45 h. The feed rates were then increased until they reached 0.9 g/(L·h) (run A) or 1.2 g/(L·h) (run B) and then kept constant. After 93 h, run B was interrupted due to accumulating DAME and DA as monitored by TLC. Run A was interrupted after 107 h for the same reason. After full conversion, as identified by TLC, both runs were restarted and set to 0.9 g/(L·h). The same procedure was repeated after 155 h and restarted again at 181 h. The experiments were performed in quadruplicate for run A and in triplicate for run B (run B from 93 h on in duplicate) using the DASGIP 8x1L parallel bioreactor system as described in methods. Error bars represent the standard deviation.

The evaluation of optimal substrate feed rate revealed first accumulation of DAME in run B at 59 h as confirmed by TLC. Later these results were also verified by GC/FID and were illustrated as a conversion over the time (Figure 3-6). DAME feed in run B was interrupted at 93 h, due to accumulation of substrate and intermediate. In contrast, run A showed accumulation of DAME first after 107 h, consequently DAME feed was also interrupted. A direct comparison of both runs before interrupting DAME feed at 93 h revealed similar volumetric productivity for both runs, implying that an increased substrate feed rate did not lead to higher productivity (Table 3-3). Instead, it seems that the yeast cells can produce only a specific amount of DDA from DAME (specific productivity) leading to accumulation of substrate when the DAME feed exceeded the conversion capacity. Thus, the specific productivity remained highly similar in both cases (Table 3-3, Figure 3-7) indicating biomass as the limiting factor in the DAME conversion.

Interestingly, specific productivity decreased drastically after the major conduction of pH shift in the biotransformation phase and revealed to be almost constant at around of 14 $\text{mg}_{\text{DDA}}/(\text{g}_{\text{biomass}}\cdot\text{h})$ afterwards (Figure 3-7). These results highlight the importance of the pH shift, which enables enhanced productivity as a result of increased substrate and product solubility.

Table 3-3: Overview of process parameters in dependency of DAME feed [100]

| | Duration [h] | Cell biomass [g/L] | Final DDA concentration [g/L] | Volumetric productivity [g/(L·h)] | Specific productivity [$\text{mg}_{\text{DDA}}/(\text{g}_{\text{biomass}}\cdot\text{h})$] |
|-------|--------------|--------------------|-------------------------------|-----------------------------------|---|
| Run A | 93* | 29.9 ± 1.9 | 45.9 ± 6.3 | 0.48 ± 0.07 | 16.4 ± 3.1 |
| | 188* | 26.5 ± 2.3 | 65.9 ± 3.1 | 0.35 ± 0.02 | 13.4 ± 1.9 |
| Run B | 93** | 31.0 ± 1.7 | 46.2 ± 2.3 | 0.49 ± 0.02 | 15.7 ± 1.3 |
| | 188*** | 27.2 ± 0.9 | 60.9 ± 0.8 | 0.32 ± 0.01 | 11.9 ± 0.2 |

Run A: constant DAME feed of 0.5 g/(L·h) during the first 45 h followed by an increase until 0.9 g/(L·h), then held constant. Run B: constant DAME feed of 0.5 g/(L·h) during the first 45 h followed by an increase until 1.2 g/(L·h), then held constant. Run B was interrupted after 93 h restarted again later at 0.9 g/(L·h). The experiment was performed using DASGIP 8x1L parallel bioreactor system as described in the methods part. The data represent the mean \pm standard deviation. Sample size: * n = 4, ** n = 3, *** n = 2

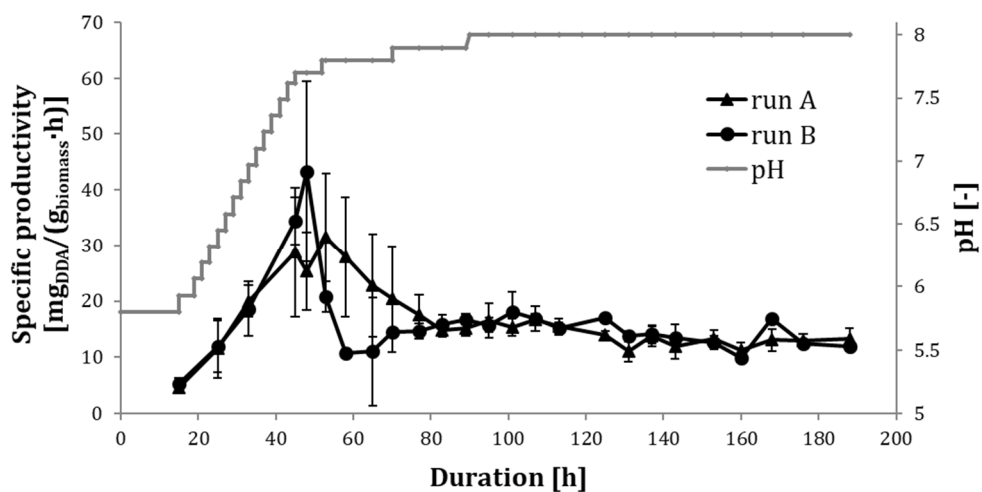


Figure 3-7: Specific productivity of DDA in dependency on pH shift

The specific productivity drastically increased during the major pH shift from 5.8 to 7.7. The experiments were performed in quadruplicate for run A and in triplicate for run B (run B from 93 h in duplicates) using the DASGIP 8x1L parallel bioreactor system as described in methods. Error bars represent the standard deviation.

On monitoring the DAME and DA accumulations further by TLC revealed full conversion at around 115 h, since accumulation in both runs was not detectable. Consequently, the DAME feed was restarted, but kept at the low feed rate of 0.9 g/(L·h) in both runs, considering the feed rate of 1.2 g/(L·h) as too high. From that time point on, both processes were run identically. After 131 h, an accumulation of DAME and DA in both runs was detected again. Consequently, after 155 h the feed was interrupted and restarted at 181 h (Figure 3-6). Interestingly, by interrupting the DAME feed yeast cells were always able to regain full conversion. Nevertheless, even a low DAME feed rate of 0.9 g/(L·h) finally resulted in substrate and intermediate accumulation representing the limit for maximum conversion. Operation of the control bioreactor at identical conditions as the runs A and B confirmed toxicity of DAME to the cells. Monitoring the biomass in the control bioreactor revealed up to 3-fold higher biomass production yielding 85 g/L at the end of the process.

3.1.3 Development of RT-qPCR method for gene expression

DCA production by *C. tropicalis* represents a very complex process including various harsh operational conditions, such as pH shift or feed of toxic substrates. Adaption of microorganisms to such stressful conditions usually involves remodeling of gene expression pattern [101, 102]. Insights into regulation of the selected genes in conjunction with response to different operational conditions can provide additional information for characterization and optimization of the DDA production process. To enable monitoring of expression of the corresponding genes RT-qPCR was developed as summarized in the following section.

3.1.3.1 Establishment of an appropriate RNA extraction method

Assessment of RNA quality is a crucial requirement for reproducible and reliable gene expression data. To guarantee a high quality of RNA an appropriate isolation method was established. Even though, RNA extraction was performed using Aurum™ Total RNA Mini Kit (Bio-Rad, USA) several steps required special attention. Enzymatic cell lysis (3.1.3.1.1) and gDNA degradation (3.1.3.1.2) were found to be critical and were

investigated in detail and optimized. To assure the quality of RNA its integrity was confirmed (3.1.3.1.3).

3.1.3.1.1 Enzymatic cell wall digestion

As contained in Aurum™ Total RNA Mini Kit (Bio-Rad, USA), Lyticase was used for the cell wall degradation at first. But the samples from the biotransformation were found to be less accessible for the degradation by Lyticase resulting in low amount and poor-quality RNA. Most of the samples from the biotransformation process contained cells from the stationary phase. Since the cell proliferation is not in the focus during the stationary phase, the cell walls become thicker and more resistant to β -1,3-glucanase digestion by Lyticase [103, 104]. Thus, Zymolyase, which additionally offers β -1,3-glucan-laminaripentaohydrolase and mannanase activities [105], was tested as a promising alternative enzyme.

Direct comparison of the enzymes was enabled by monitoring protoplast formation. Therefore, the cell broth was treated with the equivalent amount of enzyme (100 U) and the decrease in optical density at 600 nm (OD_{600}) was displayed (2.2.1.5). Starting with a sample at OD_{600} of 14, Zymolyase was able to reach OD_{600} ~0.9 after 10 min treatment, which is approximately ten times lower compared to OD_{600} of 11 observed by application of Lyticase. These results clearly revealed the ability of Zymolyase to degrade the cell walls very efficiently and thus, the amount of the enzyme could be reduced to 15 U. Moreover, the application of Zymolyase yielded in a higher RNA concentration in comparison to Lyticase (Table 3-4). Thus, Zymolyase enabled fast and efficient cell wall lysis, which allowed to reduce incubation time and therefore possible RNA degradation during the cell wall lysis.

Nevertheless, the monitored purity of RNA at A_{260}/A_{280} was found to be low applying both enzymes (Table 3-4). Obtained A_{260}/A_{280} ratios were mostly not in the acceptable range between 1.8-2.0, indicating possible contaminations with proteins or some aromatic substances. Since, these unwanted contaminations could interfere with the subsequent cDNA synthesis or qPCR, the RNA purity for the selected cell lysis method using Zymolyase needed to be optimized and was further targeted.

Table 3-4: Comparison of cell wall digestion by Lyticase and Zymolyase

| | Detected RNA [ng_{RNA}/mg_{biomass}] | A₂₆₀/A₂₈₀ [-] |
|------------------------|---|--|
| Lyticase, 50 U | 47 | 3.6 |
| Lyticase, 100 U | 148 | 1.6 |
| Lyticase, 200 U | 253 | 1.8 |
| Zymolyase, 15 U | 267 | 1.6 |

The protoplast formation was used to monitor the enzymatic cell wall degradation and was performed as described in methods. Sample size: n = 1.

3.1.3.1.2 gDNA degradation

gDNA contamination became an issue for the extracted RNA samples, when the cells from stationary phase were used. The RNA extraction from these samples yielded low RNA concentration. To achieve higher amounts of RNA the sample volume was increased, also leading to higher gDNA content. Degradation of gDNA on the silica column during the RNA extraction was not efficient. Since, even low amounts of gDNA in the RNA samples would lead to an inaccurate evaluation of the gene expression, gDNA degradation was optimized. gDNA contamination was monitored by qPCR assay (NRT samples, refer also to Table 2-3).

To reduce gDNA content in the RNA samples, DNase I treatment of the samples on the silica column as described by manufacturer was modified. First, the amount of applied DNase I was doubled, but did not lead to any improvement of the gDNA degradation, as displayed by even lower C_q value in NRT samples in comparison to the standard procedure (Table 3-5). These results allow to assume, that the DNase I activity was inhibited. Thus, the washing step as applied before DNase I treatment was repeated to remove any possible inhibitors, such as cell debris. Indeed, the extra washing step led to the reduction of gDNA amount, which was proved by an increased C_q value of the treated samples (Table 3-5).

Even by using an extra washing step the gDNA contamination was not completely removed. The elimination of the last gDNA was achieved by applying RapidOut DNA Removal kit (Thermo Fisher Scientific, USA) and no signal in NRT was found (Table 3-5).

To exclude complete inhibition of the qPCR, which would also result in no signals, RNA samples treated by RapidOut DNA Removal kit were spiked additionally with gDNA and measured by qPCR. An obtained signal at Cq of 22 (Table 3-5) indicates that the additional gDNA removal step is compatible with the following qPCR. Also, the RNA purity observed by absorbance after the additional gDNA degradation was within the acceptable range.

Table 3-5: Overview over gDNA contamination detected after various RNA extraction steps

| | Cq value in NRT [-] | A₂₆₀/A₂₈₀ [-] |
|---------------------------------|--------------------------------|--|
| Standard procedure | 26.72 ± 0.29** | 2.2 ± 0.1* |
| Double amount of DNase I | 21.64 ± 0.14* | 2.2**** |
| Extra washing step | 30.20 ± 1.72** | 2.2 ± 0.0* |
| gDNA removal kit | No signal*** | 2.0**** |
| Spike | 22.42 ± 0.08*** | |

The experiment was performed using CFX96 Touch™ Real-Time PCR Detection System as described in the methods part. The data represent the mean ± standard deviation. Sample size: * n = 2, ** n = 6, *** n = 3, ****n = 1.

3.1.3.1.3 RNA Integrity

Besides the assurance of the RNA purity, assessment of RNA quality includes a control of the RNA integrity. The integrity of RNA was confirmed by denaturing agarose gel electrophoresis (2.2.2.6.2).

RNA integrity was determined for the established RNA extraction method including cell wall digestion by Zymolyase, extra washing step before DNase I treatment on the silica column and additional gDNA degradation and revealed intact RNA. This was assured by observing of the major ribosomal RNA (rRNA) bands: 28S and 18S as obtained in lines one and two of the agarose gel (Figure 3-8). Once the RNA integrity for this RNA extraction method was guaranteed, it was not monitored for all the samples.



Figure 3-8: Extracted RNA samples on denaturing agarose gel

RNA samples extracted from sample of (1) run A, 0 h (2) run B, 0 h and (3) GeneRuler 100bp DNA Ladder (Fermentas) on the denaturing agarose gel. Electrophoresis was performed as described in methods.

3.1.3.2 Validation of qPCR assay

qPCR assay was performed by the application of SsoAdvanced™ Universal SYBR® Green Kit (Bio-Rad, USA) as described in 2.2.2.5. Nonetheless, all the primer pairs designed had to be tested for their suitability for qPCR amplification. Therefore, validation of qPCR including determination of the reaction specificity and efficiency for each gene of interest was carried out (3.1.3.2.1). Furthermore, determination of the appropriate reference genes was targeted to assure reliable and accurate gene expression data analysis by gene normalization (3.1.3.2.2)

3.1.3.2.1 Establishment of qPCR specificity and efficiency

As the most critical step of the PCR in general, appropriate annealing of primer to the template enables proper template amplification and thus requires special attention. The optimal primer concentration as well as annealing temperature was determined for each primer pair. In the following, results are displayed exemplarily for one of the genes.

The optimal primer concentration for the qPCR assay was determined by cDNA amplification at various primer concentrations in the range of 50 nM to 600 nM. As shown for the primer pair designed for amplification of *CYP52A13/14*, the resulting Cq values decreased with an increasing primer pair concentration until the 300 nM (Table

3-6). Since, afterwards no significant improvement of the C_q value was achieved, primer concentration of 300 nM was assigned to be optimal. Similar procedure was performed for all primer pairs, confirming primer concentration of 300 nM to be the most suitable concentration for the qPCR assay.

Using optimal primer concentrations, the temperature gradient in the range of 58-65°C, around melting temperature (T_m), was applied to investigate the optimal annealing temperature (T_a). Since all the primer pairs were initially designed with a T_m close to 60°C as recommended by SsoAdvanced™ Universal SYBR® Green (Bio-Rad, USA), the measured optimal T_a of all primer pairs was found to be at 61°C.

Table 3-6: Determination of the optimal primer concentration for the *CYP52A13/14*

| Primer concentration [nM] | C _q value [-] |
|------------------------------|-----------------------------|
| 50 | 23.71 ± 0.70 |
| 100 | 21.69 ± 0.72 |
| 200 | 20.87 ± 0.37 |
| 300 | 20.08 ± 0.23 |
| 400 | 20.09 ± 0.07 |
| 500 | 20.17 ± 0.21 |
| 600 | 20.12 ± 0.04 |

The experiment was performed using CFX96 Touch™ Real-Time PCR Detection System at annealing temperature of 55°C as described in methods. The data represent the mean ± standard deviation. Sample size: n = 2.

Following the investigation of the optimal conditions for the assay, the qPCR specificity was determined by a melting curve analysis of the PCR product for each primer pair (2.2.2.5.1). Exemplarily, the melting curve analysis of the *GAPDH* as presented below revealed one distinct peak, indicating specific binding of the primer pair (Figure 3-9). This peak at a melting temperature of 81.5°C represents the specific amplified qPCR product. To verify the melting curve analysis, the obtained qPCR products were run on a 1% agarose gel to confirm the expected length of the desired amplicons (2.2.2.6.1). Thus,

the primer pair for the control gene *GAPDH* was designed to amplify a specific region of 101 bp (Table 2-1), which could also be confirmed by gel electrophoresis (Figure 3-10).

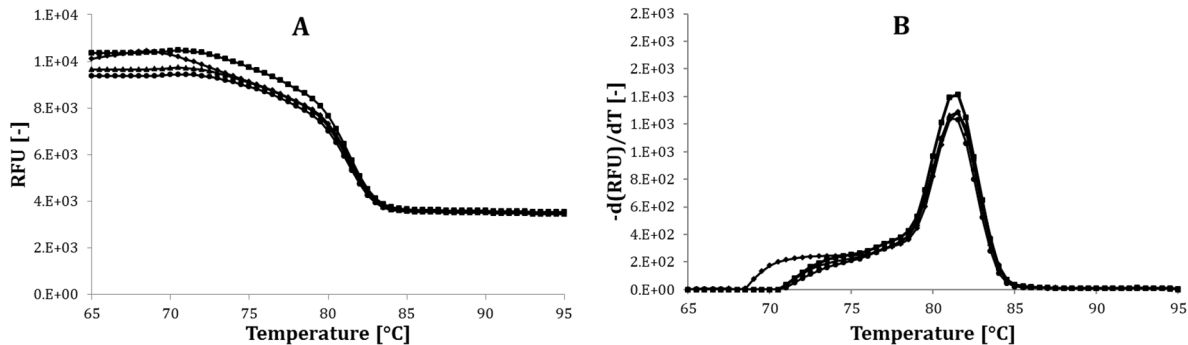


Figure 3-9: Melting curve analysis of *GAPDH*

(A) Melting curve and (B) negative first derivative of the melting curve were used to guarantee the specificity of the primers. The experiment was performed by use of CFX96 Touch™ Real-Time PCR Detection System, *GAPDH* primers at optimal conditions followed by analysis using Bio-Rad CFX Manager as described in methods.

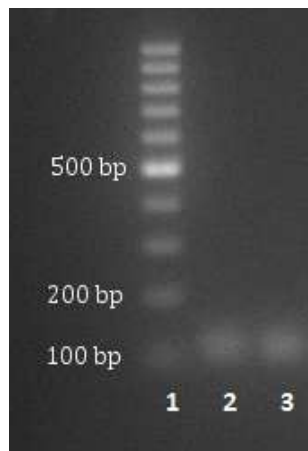


Figure 3-10: Agarose gel of amplified qPCR product of the *GAPDH*

(1) GeneRuler 100bp DNA Ladder (Fermentas) and (2), (3) amplified qPCR product of *GAPDH* on the 1% agarose gel. Electrophoresis was performed as described in methods.

After the determination of optimal qPCR conditions and verification of the qPCR specificity for each primer pair, the qPCR efficiency was established as described in 2.2.2.5.2. Ideally, an exact two-fold amplification of templates per cycle results in qPCR reaction efficiency of 100%. However, the acceptable range of a qPCR efficiency is determined to be between 90% and 110%. Thus, only the primer pairs within this range

were chosen and used for further gene expression studies. The following table summarizes all primer pairs with the corresponding efficiency (Table 3-7).

Table 3-7: qPCR efficiency of all genes investigated by qPCR

| Target gene | Efficiency [%] | Coefficient of determination, R ² [%] |
|--------------------|----------------|--|
| <i>CYP52A13/14</i> | 93.2 | 99.9 |
| <i>CYP52A17/18</i> | 91.7 | 99.7 |
| <i>CPR</i> | 105.2 | 99.3 |
| <i>GAPDH</i> | 101.2 | 99.4 |
| <i>ACT1</i> | 95.3 | 99.6 |
| <i>PGK1</i> | 92.8 | 99.5 |
| <i>PAM1</i> | 98.9 | 99.6 |

The standard curves were performed as described in methods, in the cDNA range of 30-0.05 ng and a dynamic range of 5-6 log₅.

3.1.3.2.2 Selection of reference genes for normalization

Application of RT-qPCR technique enables the monitoring of gene expression by comparing relative RNA levels in different samples. To control the variations across samples, the measured RNA level should be normalized to reference genes. Due to basic cellular functions housekeeping genes represent excellent reference genes. Several housekeeping genes were selected and analyzed for the suitability to serve as stable control genes under applied conditions in this study: *GAPDH*, *ACT1*, *PGK1* and *PMA1* (2.2.2.5.3).

The identification and selection of the appropriate control genes was performed by validation of the expression stability. The coefficient of variation (CV) and the expression stability (M) value were calculated as described in 2.2.2.5.3. The corresponding values are given in the following Table 3-8.

According to the calculations based on all four control genes, *ACT1* and *GAPDH* were the most stable expressed genes, since both exhibited the lowest CV as well M values. *PMA1* encoding H⁺-ATPase was identified to be the less stable expressed gene. By stepwise exclusion of the least stable genes, the remaining control genes (*ACT1* and *GAPDH*)

resulted in an average CV of 22.69% and M value of 0.6559. All the following gene expression profiles were normalized using these two control genes.

Table 3-8: CV and M values of reference genes

| Control gene | CV [%] | M [-] |
|--------------|--------|--------|
| <i>ACT1</i> | 28.66 | 0.7482 |
| <i>GAPDH</i> | 25.83 | 0.7536 |
| <i>PMA1</i> | 60.30 | 0.9885 |
| <i>PGK1</i> | 30.11 | 0.8040 |
| Mean | 36.22 | 0.8236 |

3.1.4 Monitoring of gene expression during DDA production process

Gene expression of allelic variants, *CYP52A13/14* and *CYP52A17/18*, and corresponding *CPR* was monitored to gain insight into the DDA production process and to investigate response to different operational conditions at the cellular level. The transcriptional level was determined during the biotransformation process of runs at two different DAME feeds: run A (0.9 g/(L·h)) and run B (1.2 g/(L·h)) as well as of a control bioreactor, which was operated under identical conditions as others, but in the absence of DAME feed (3.1.2.3).

Monitoring of the relative transcript amount revealed an increase of all investigated genes in both runs, which occurred after the start of DAME feed in the biotransformation phase at 17 h (Figure 3-11, A-C). Since, both *CYP52A* and *CPR* did not show any changes during the entire process in the non-induced control bioreactor (Figure 3-11, D), DAME and its demethylated product, DA, are responsible for the induction of these genes. As found in this study, *CPR* transcript levels revealed to be low during the production process in both runs and exhibited almost 20-fold lower expression in comparison to *CYP52A*. Considering the steady increase of expression of the *CYP52A* allelic variants at the beginning of the process, the decline of the volumetric productivity can be correlated with the reduced *CPR* expression after 30 h of the production process (Figure 3-12). Interestingly, the sudden decrease of the *CPR* expression levels can be clearly correlated

with the pH shift performed at the same time. Obviously, the initiation of the pH shift at 17 h led to a drastic reduction of *CPR* expression level, which remained low until the major pH shift was completed (pH 7.8 after 59 h).

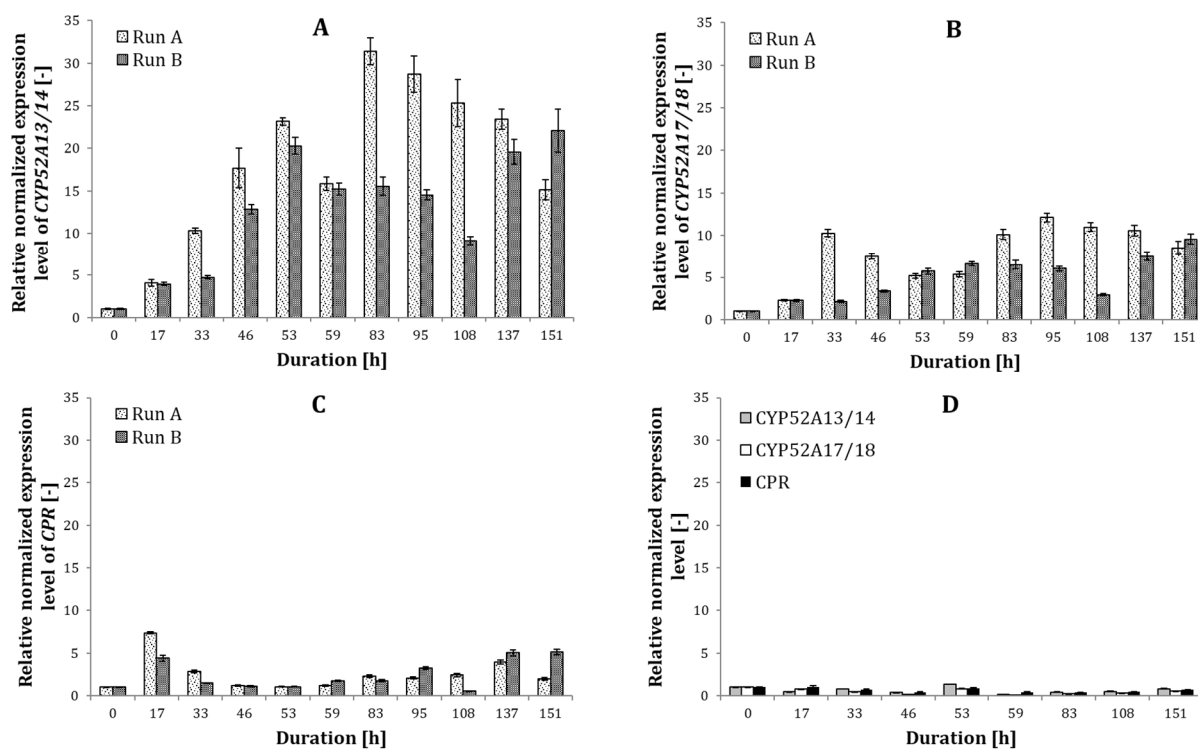


Figure 3-11: Relative normalized expression profiling of the genes during the DDA production process [100]

Expression profiles of (A) *CYP52A13/14*, (B) *CYP52A17/18* and (C) *CPR* genes during the runs A and B. (D) transcriptional profile of *CYP52A13/14*, *CYP52A17/18*, and *CPR* genes in the non-induced control bioreactor. All expression values were normalized toward the values of *ACT1* and *GAPDH* ($CV = 0.2269$, $M = 0.6559$). The error bars represent the standard error of the mean. Gene expression: p-value < 0.05 (except for following samples of *CPR* expression: Run A: 46 h, 53 h; Run B: 46 h, 53 h; and control bioreactor 17 h, 53 h).

The expression level of allelic variants *CYP52A13/14* was found to be up to 20-fold higher compared to *CYP52A17/18*. Both genes showed high expression levels until the end of the production process, leading to the assumption, that no product repression occurred, since at the end of the biotransformation process a product concentration of 66 g/L in run A and 61 g/L in run B was measured. However, an indication of the repression caused by the substrate could be identified. As applied in run B, an elevated substrate feed led to

substrate accumulation, which started at 59 h and reached a DAME concentration of 8.1 g/L at 89 h (Figure 3-6, Table 3-9). At the same time, the transcriptional level of both allelic variants, *CYP52A13/14* and *CYP52A17/18*, decreased and remained lower compared to run A until 108 h. However, the second occurrence of DAME accumulation started at 131 h and reached 7.7 g/L at 151 h in both runs and seems to have small impact on the expression level of *CYP52A*. Thus, the accumulated amounts of DAME and DA at both time points, 89 h and 151 h, were very similar to each other, whereas the duration of the accumulations differed greatly (Table 3-9). Compared to 151 h, the first accumulation persisted two times longer resulting in a decrease at the transcriptional level after 89 h. These findings confirm the importance of optimal substrate feed in combination with the pH shift, invigorated by the results of moderate *CPR* expression during the pH shift.

Table 3-9: Accumulation of DAME and DA during biotransformation of DAME

| Time [h] | DAME concentration [g/L] | DA concentration [g/L] | Duration of accumulation at specific time point [h] |
|-----------------|---------------------------------|-------------------------------|--|
| 89* | 8.1 ± 2.4 | 1.2 ± 0.2 | 30 |
| 151** | 7.7 ± 2.3 | 1.4 ± 0.5 | 14 |

The experiments were performed using DASGIP 8x1L parallel bioreactor system as described in methods. The error bars represent the standard deviations. Sample size: *n=3 (run A), **n=6 (runs A and B).

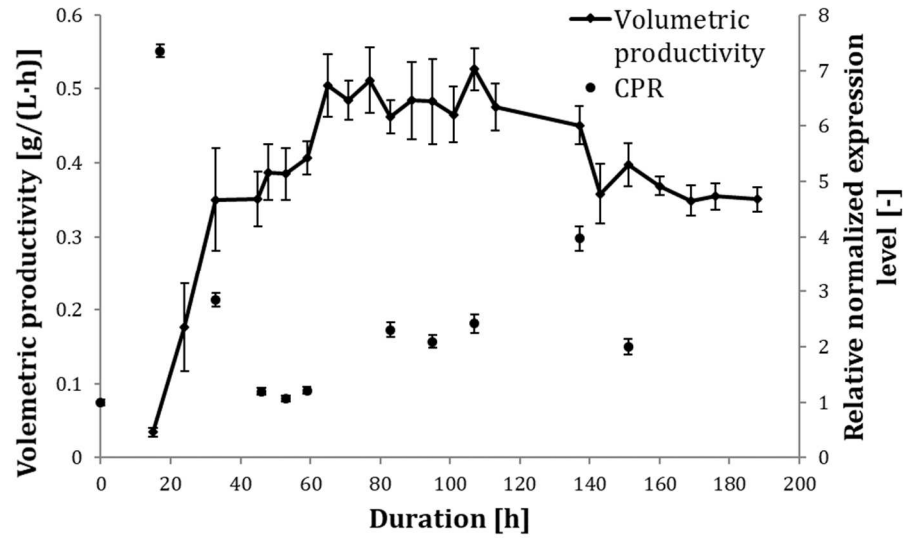


Figure 3-12: Volumetric productivity and expression levels of *CPR* over time [100]

Exemplarily shown for run A. After the pH shift initiation at 18 h, reduced expression of *CPR* was observed and can be correlated with the decline in volumetric productivity. All expression values are normalized to the values of *ACT1* and *GAPDH* ($CV = 0.2269$, $M = 0.6559$). The error bars represent the standard deviation of volumetric productivity and the standard error of the mean for gene expression. Gene expression: p -value < 0.05 (except for the following samples: Run A: 46 h, 53 h).

3.2 Characterization and optimization of the pre-culture

The biotransformation of fatty acids to their corresponding dicarboxylic acids relies on application of resting cells as whole-cell biocatalysts. Increasing number of theoretical biocatalysts by increasing the cell biomass should subsequently lead to enhanced biotransformation. Therefore, the preparation of the pre-culture for biotransformation experiments in a parallel bioreactor system was characterized in more detail starting with cultivation on agar plates (3.2.1) towards the liquid pre-culture in shake flasks (3.2.2) until the final biomass production step in the 2 L bioreactor (Table 2-7). The information on cell growth obtained by that approach was applied to optimize the cell growth in the pre-culture to gain higher cell biomass.

3.2.1 Cell growth on agar plates

The cell growth on agar plates represents just an intermediate step and allows cells to revitalize after cryopreservation before entering the liquid pre-culture. Usually this step is very simple and does not require a great attention. However, the observation of cell growth on plates led to an interesting discovery of changing cell morphology over the time. When grown on agar plates the colonies of *C. tropicalis* usually appears to be smooth and beige and later turns curly and wavy. Monitoring cell growth on YPD agar plates revealed the differentiation of colonies after prolonged incubation time (ca. 100 h). Some of the colonies turned reddish and remained smooth meanwhile others stayed beige and curly (Figure 3-13, B). Interestingly, the differentiation of these colonies at the earlier time point was not possible, since the cells looked alike (Figure 3-13, A). To identify the reddish microorganism on the agar plates and to describe the phylogenetic relationship with beige colonies, rRNA analysis was performed (2.2.2.4). The results revealed that both microorganisms on the agar plate were 100% similar to each other and according to a BLAST search were identified as *C. tropicalis* ATCC 20962 (refer to 7.4).

In the next step, beige and reddish colonies were separated and grown for several generations on agar plates, liquid cultures and then back to agar plates. It was noticed, that the yeast cells generated from reddish colonies showed lower cell growth in comparison to beige cells. Interestingly, after separation beige cells remained beige and

no repeated occurrence of the reddish colonies was observed. After successful separation of beige colonies from reddish ones, new glycerol stock containing only beige cells were prepared and used for all upcoming experiments.

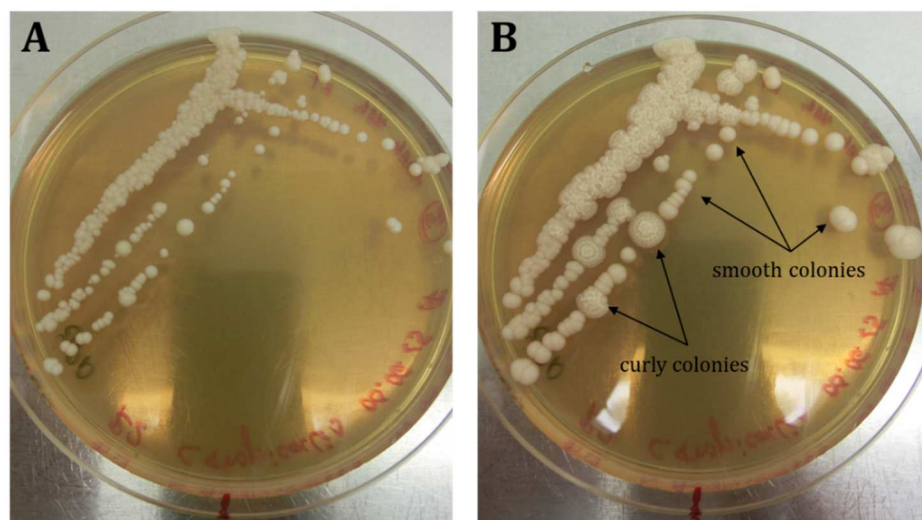


Figure 3-13: Streak of *C. tropicalis* from glycerol stock on YPD agar plates

Observation of the cell growth on YPD agar plates of *C. tropicalis* at 30°C after (A) 72 h and (B) 168 h.

3.2.2 Optimization of liquid pre-culture

The pre-culture used in this work was adapted from the DAME process [99], characterized and further optimized to reach higher cell biomass titers. Starting with a single colony from the agar plate, pre-culture I and subsequently pre-culture II were implemented for the final inoculation of a pre-culture in the 2 L bioreactor (2.2.4.1, 2.2.4.2).

Cell growth in a 2 L bioreactor, as performed earlier in a batch mode for 24 h (Table 3-10, A), was characterized in detail. Besides usual monitoring of dissolved oxygen consumption during the cultivation, investigation of the cell growth by determination of cell density was applied as well. Cell cultivation in a batch mode revealed the stagnation of the pO_2 values in the first half of the cultivation followed by a drastic increase (Figure 3-14). This observation presumes cells entering the stationary phase after 6-7 h and a starvation phase after 20 h. The transition of the cells into the starvation phase could be also verified by a sudden increase of the pH due to release of alkaline cell contents from lysed cells [106] as indicated by supply of phosphoric acid into the bioreactor to keep the

Results

pH value constant (Figure 3-14). Since the cells produced in the 2 L bioreactor serve as a starting material for the whole-cell biotransformation, not just high cell biomass, but also cell viability must be considered. Thus, cell biomass from the exponential phase exhibiting the highest cell viability is preferred for further inoculation. According to these results, cell cultivation in the 2 L bioreactor was shortened to 12 h (Table 3-10, B). Simultaneously with the reduction of the growth phase duration the exponential phase was prolonged by additional supply of glucose to achieve higher cell densities. The glucose feed was initiated at 8 h to the final concentration of 30 g/L, the same as at the beginning of the growth phase (Table 3-10, C). Application of the fed-batch mode led to almost a three-fold increase of the initial cell density and thus, was applied for all upcoming experiments for the biotransformation of oleic acid.

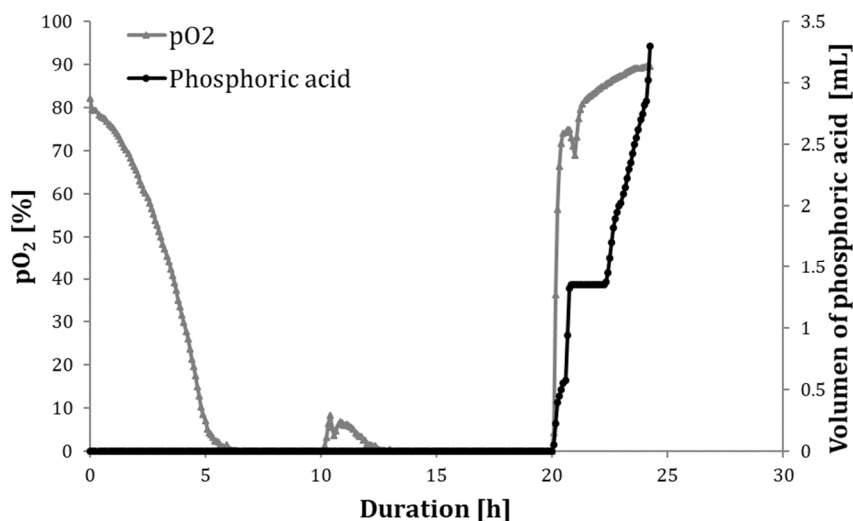


Figure 3-14: Monitoring of pO₂ and phosphoric acid in 2 L bioreactor

pO₂ and supply of phosphoric acid over the time. The experiment was performed using the 2 L bioreactor as described in methods.

Table 3-10: Comparison of several variants of the cell growth in 2 L bioreactor

| | A* | B** | C* |
|----------------------------------|-----------|-----------|---------------|
| Cultivation time [h] | 24 | 12 | 12 |
| Additional glucose supply | - | - | 30 g/L at 8 h |
| OD₆₀₀ [-] | 8.2 ± 3.2 | 9.4 ± 0.8 | 24.1 ± 4.7 |

The experiments were performed using 2 L bioreactor as described in methods. The data represent the mean ± standard deviation. Sample size: * n = 4, ** n = 2.

3.3 Biotransformation of oleic acid

The DDA production process as developed in the benchtop parallel bioreactor system was applied to produce *cis*-ODA by the biotransformation of oleic acid. During the transfer of the process into the bioreactor system the influence of several process parameters on the efficiency of oleic acid biotransformation was evaluated. The pH shift and glucose feed were considered as the most crucial parameters and were analyzed in detail. The characterization of the process was assured by a slightly modified GC/FID method enabling accurate separation of the desired product.

3.3.1 Establishment of suitable GC/FID method

For the production process of *cis*-ODA, technical grade oleic acid with a purity of 94.7% was used. This feedstock also contained other fatty acids, which were not specified further by the supplier. Applying the GC/FID method as developed for the DAME and DDA (C12 method, 2.2.3.1), the following fatty acids could be identified: palmitic acid (C16:0), stearic acid (C18:0) and linoleic acid (C18:2) (Figure 3-15, A). However, a complete separation of the linoleic acid and oleic acid using this method was not achieved. Therefore, the C12 method was further modified by applying additional ramps and a slow temperature increase (Table 2-5). This approach led to a distinct separation of all peaks (Figure 3-15, B) and resulted in the clear distinction between the oleic acid and its stereoisomer, elaidic acid (*trans* C18:1).

The modified GC/FID method was also tested for its ability to separate some of the dicarboxylic acids, which were present at this point of time: *trans*-ODA (C18:1) and C18:0. The peaks were found to be well separated and appeared in the same order as the corresponding fatty acids (Figure 3-15, C). Therefore, it was assumed, that by applying this method, a separation of *cis*- and *trans*-ODA would be possible as well. Since both corresponding fatty acids were present in the technical grade oleic acid that was used, correct assignment of the products was essential. The ability to separate *cis*- and *trans*-ODA using C18:1 method was confirmed later after the analytical standard of *cis*-ODA was produced, purified and characterized in the detail (3.3.4).

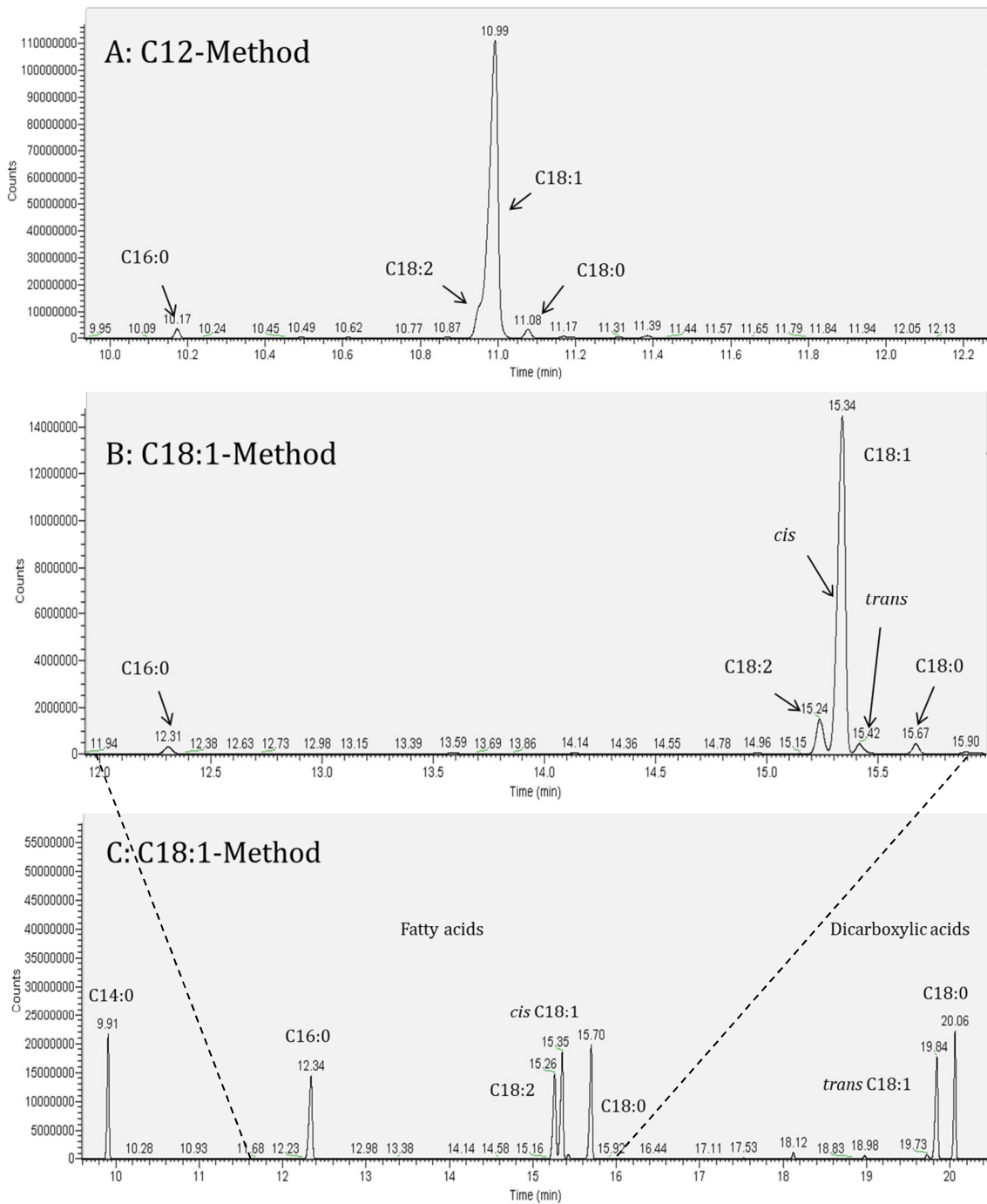


Figure 3-15: Separation of FAs and DCAs of various chain length by various GC/FID methods

Comparison of the separation ability of several fatty acids with various chain length by different GC/FID methods: (A) C12 method as established for the detection of the DAME, DA and DDA. (B) C18:1 method optimized for the detection of oleic acid and *cis*-ODA. (C) Using C18:1 a distinct separation also of the *cis* and *trans* stereoisomers of fatty acids as well as DCAs was achieved. The experiments were performed using appropriate GC/FID method as described in the methods.

3.3.2 *cis*-ODA production: from shake flask towards bioreactor scale

First attempts on the biotransformation of oleic acid by *C. tropicalis* started with the conversion experiments in a shake flask (3.3.2.1). The conversion in the bioreactor system (3.3.2.2) and 2 L bioreactor (3.3.2.3) revealed several crucial parameters, which influenced the efficiency of the process and thus, were investigated in more detail (3.3.3).

3.3.2.1 *Oleic acid biotransformation in the shake flask*

A simple conversion test in shake flask scale was used to confirm the ability of *C. tropicalis* to produce *cis*-ODA from oleic acid. To enable accurate evaluation of the experiment, DAME was applied as a positive control. Surprisingly, none of the substrates were converted into the corresponding DCAs. Both, oleic acid and DAME remained in the cell broth even after 4 h of biotransformation and no production of DDA or *cis*-ODA was observed (Figure 3-16). Since, pH shift was already identified to be the most crucial parameter affecting the biotransformation (3.1.2.1), the non-regulated conditions in the shake flask were assumed to be responsible for the missing conversion. Thus, biotransformation of oleic acid was transferred directly to controlled and regulated conversion in the parallel bioreactor system.

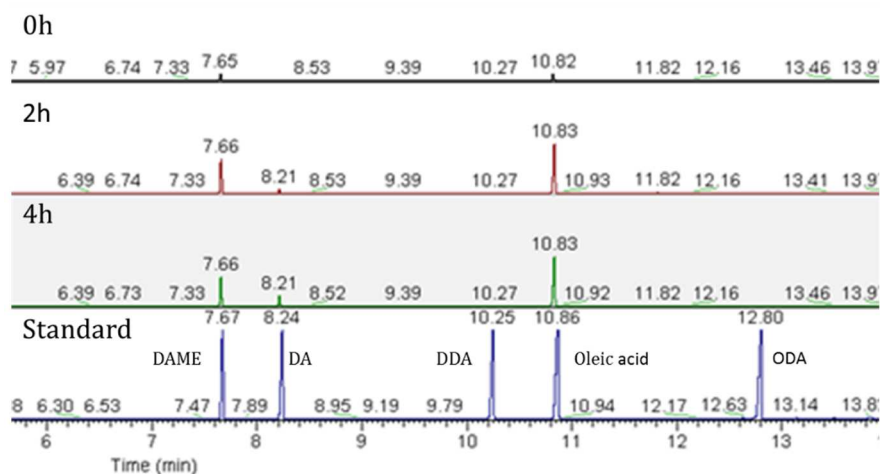


Figure 3-16: Chromatogram of biotransformation of DAME and oleic acid in shake flask

The GC/FID chromatogram visualizes the biotransformation efficiency of oleic acid and DAME in the shake flask. As showed over the time, the substrates peaks maintained the same and no product peaks were observed. The experiments were performed in the shake flask as described in the methods.

3.3.2.2 Conversion of oleic acid in the parallel bioreactor system

Biotransformation process in the parallel bioreactor system under regulated conditions established for the DDA production (3.1) was used to verify the ability of *C. tropicalis* to convert oleic acid to a *cis*-ODA. Besides oleic acid, DAME was used as a positive control enabling direct comparison of biotransformations.

Application of different substrates for the biotransformation process revealed a distinct difference in the cell growth as well as in DCA production. At the end of the growth phase, the variant supplied with DAME exhibited almost two-fold lower cell biomass of 7.9 g/L in comparison to oleic acid (14.3 ± 0.2 g/L, $n=3$). Obviously, the pre-induction of cells with DAME at the beginning of the growth phase (2.2.4.4) caused reduced cell growth due to high toxicity of DAME, meanwhile oleic acid seemed to be harmless.

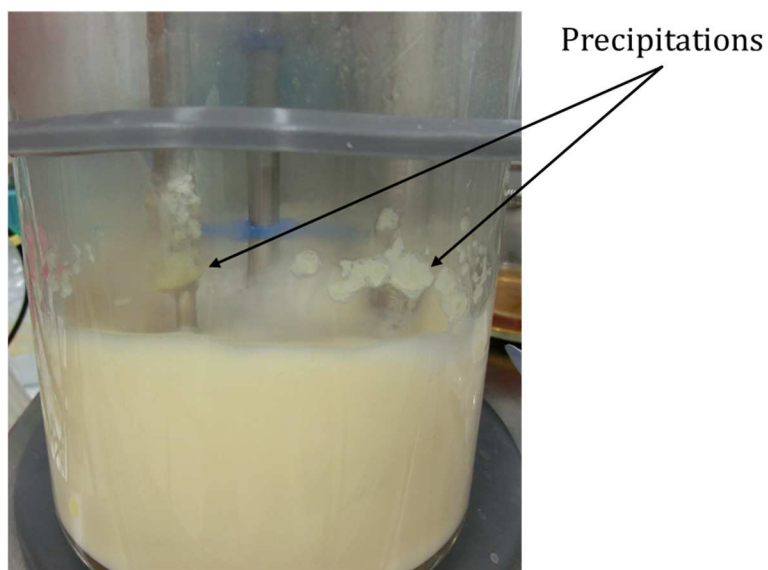


Figure 3-17: Precipitations of oleic acid observed during the biotransformation

Precipitation of oleic acid as observed during the biotransformation by *C. tropicalis* in parallel bioreactor system.

Even though, the application of oleic acid resulted in higher cell amount, only very poor substrate conversion was observed. DAME, however, was successfully converted to DDA yielding a 20-fold higher titer. Interestingly, oleic acid showed quite different solubility behavior in an aqueous environment, as the formation of visible precipitates of oleic acid during the biotransformation were detected (Figure 3-17). Obviously oleic acid with a

higher chain length showed lower solubility in water compared to DAME and thus, under applied conditions appeared to precipitate resulting in low substrate conversion. The pH shift, as applied for DAME biotransformation, showed a drastic increase in its solubility but seemed to be less suitable for conversion of oleic acid. To enhance oleic acid solubility, the pH shift was accelerated by initiation of the process at slightly higher pH values.

For this, the growth of *C. tropicalis* at various pH conditions was firstly tested in shake flasks. The results revealed that, raising the pH until 6.5 did not affect cell growth at all. In the next step, two variants of the pre-culture in the 2 L bioreactor at the pH of 5.8 and 6.5 were carried out followed by the biotransformation in a parallel bioreactor system with the growth phase starting at 5.8 and 6.5, respectively. The cell density in 2 L bioreactor at a pH of 6.5 reached slightly lower OD₆₀₀ of 7.1 compared to the pH 5.8 variant with an OD₆₀₀ of 8.7. But, by the end of the growth phase in bioreactor system both variants were found to achieve very similar amounts of cell biomass (Table 3-11). As assumed, due to the increased solubility of oleic acid, the biotransformation initiated at a pH of 6.5 led to a slightly, but obviously, higher production of *cis*-ODA compared to the 5.8 variant. However, even the 6.5 variant resulted in a very poor product yield of 1%.

Table 3-11: Overview over the production process initiated at pH 5.8 and 6.5

| pH of pre-culture and growth phase | Pre-culture in 2 L | Production process in bioreactor system | |
|------------------------------------|-----------------------|---|---|
| | OD ₆₀₀ [-] | Cell biomass by the end of growth phase [g/L] | Product yield after 41 h of biotransformation [%] |
| 5.8 | 8.7* | 5.3 ± 1.2** | 0.60 ± 0.03** |
| 6.5 | 7.1* | 6.2 ± 0.6*** | 1.11 ± 0.12*** |

The pre-culture was performed in 2 L bioreactor and the biotransformation with the preceding growth phase using DASGIP 8x1L parallel bioreactor system as described in methods. The data represent the mean ± standard deviation. Sample size: * n = 1, ** n = 3, ***n = 2.

Furthermore, monitoring the glucose levels during the production process revealed glucose accumulation at concentrations of around 11 g/L for both variants (Figure 3-18). Interestingly, no such issues were observed during the DDA production process. Thus, these findings of accumulation of glucose and low solubility of oleic acid mediated by

medium pH, indicated that the biotransformation process in a parallel bioreactor system needed essential modifications. In particular, the pH shift and glucose feed should be analyzed in more detail and optimized for the conversion of oleic acid. To access this, a biotransformation in the 2 L bioreactor was set up to minimize the preparation effort in comparison to the parallel bioreactor system.

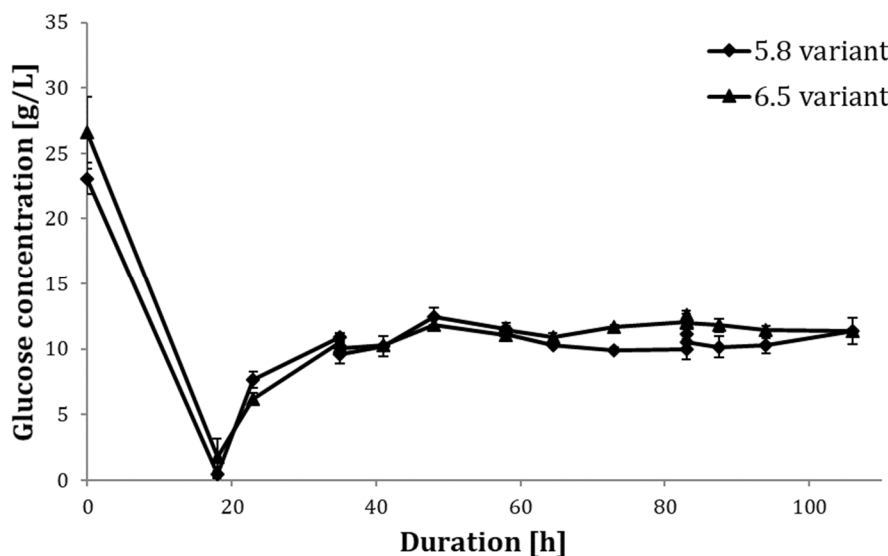


Figure 3-18: Glucose accumulation observed during the biotransformation phase

Accumulation of glucose as observed during the biotransformation phase independent of the starting pH of the growth phase (5.8 or 6.5). The experiments were performed in duplicate for the 6.5 variant and in triplicate for the 5.8 variant using the DASGIP 8x1L parallel bioreactor system as described in methods. The error bars represent the standard deviations.

3.3.2.3 Biotransformation of oleic acid in 2 L bioreactor scale

Biotransformation of oleic acid in 2 L bioreactor was performed similar to the application of the parallel bioreactor system (2.2.4.5). Unfortunately, several operations could not be performed the same way as the parallel bioreactor system due to limited regulation possibilities of the software and therefore, the following adjustments were implemented. Continuous supply of the substrate and glucose was substituted by application of both in batch mode. More critical, however, was the performance of the pH shift, since the regulation system of the 2 L bioreactor was incapable to perform the pH shift automatically. Therefore, the pH shift was conducted manually and had to be drastically shortened to 12 h. During this time the cell growth was monitored in detail. Surprisingly,

the pH adjustment within 12 h did not show any negative impact on cell growth unlike during the DDA production [99]. Even more interesting was the observation of the *cis*-ODA production in correlation to the pH shift. Conversion of oleic acid towards the corresponding *cis*-ODA was found to take place first after reaching a pH of 8.0 (Figure 3-19). Thus, solubility issues, which occurred during oleic acid biotransformation, seemed to depend on the pH value. At a pH of approximately 7.0, oleic acid was found to form precipitates on the walls and installations of the bioreactor. But further increase of the pH towards a value of 8.0 resulted in re-dissolution of oleic acid. The investigation on pH mediated solubility and conversion of oleic acid was further analyzed to enable an efficient biotransformation process.

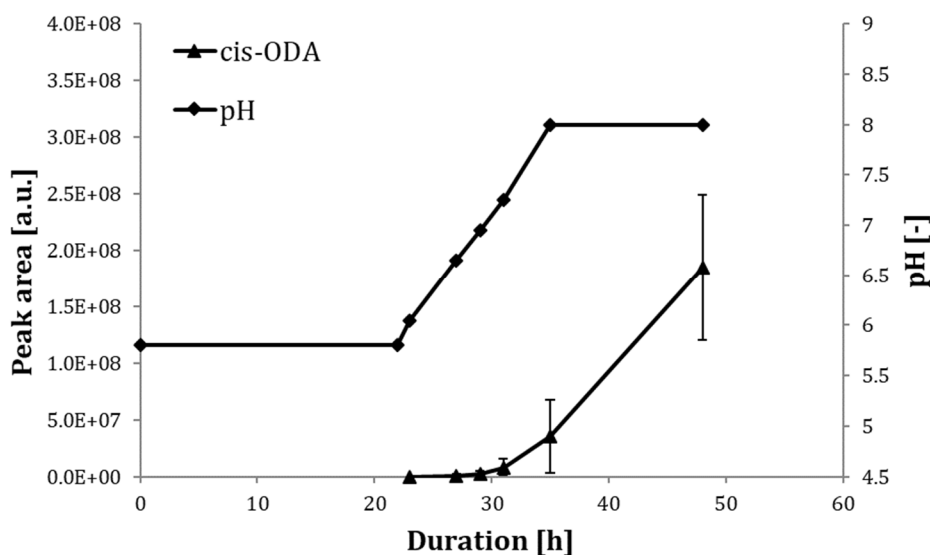


Figure 3-19: Production of *cis*-ODA in dependency of pH [107]

Enhanced production of *cis*-ODA was observed at slightly basic pH (~8.0) during application of a reduced pH shift in the 2 L bioreactor. The experiments were performed in duplicate using the 2 L bioreactor as described in methods. The error bars represent the standard deviation.

3.3.3 Optimization of *cis*-ODA production in parallel bioreactor system

First experiments regarding the biotransformation of oleic acid showed crucial differences to the production process using DAME as a substrate. Addressing the low water solubility of oleic acid, the conversion process strongly depended on the pH of the medium. Fortunately, due to the absence of any toxicity effects of oleic acid on the yeast cells, the reduction of the time for the pH shift was conceivable and was further targeted (3.3.3.2). Furthermore, glucose feed (3.3.3.3) and oleic acid feed (3.3.3.4) were also found to have a great influence on the productivity of *cis*-ODA and were aimed in the optimization.

3.3.3.1 Biomass production in the growth phase

The first step in the growth phase of the dicarboxylic acid production process involves efficient production of biocatalysts. Thus, the growth phase in parallel bioreactor system was optimized towards enhanced cell biomass production. Therefore, the exponential cell growth was extended in the similar manner by supplying additional glucose after 8 h as described for the preparation of the pre-culture in 2 L bioreactor (3.2.2).

Additional glucose supply resulted in enhanced cell growth as indicated by the expansion of the specific CO₂ peak in comparison to the batch approach (Figure 3-20, Figure 3-2). Application of a fed-batch operational mode led to a final cell biomass of 22.5 ± 2.3 g/L, which is 1.5-fold higher compared to the growth phase performed in batch mode (Table 3-12). However, the fed-batch approach led to a biomass yield coefficient of 0.37 g/g (Table 3-12), which is slightly lower compared to the theoretical maximal value of 0.5 g/g based on the aerobic metabolism of glucose [51, 108]. This observation indicates the occurrence of the Crabtree effect during the growth phase. Thus, exemplarily samples obtained throughout the entire process were analysed for ethanol production using HPLC (2.2.3.3). This analysis revealed an average ethanol concentration of 3.2 ± 0.6 g/L (n=4) at the end of the growth phase. Interestingly, ethanol was consumed thereafter and no ethanol was detected during the biotransformation phase (3.3.3.3.2). Since the produced ethanol concentration was very low, it was not considered as an issue and the fed-batch approach was applied in the growth phase.

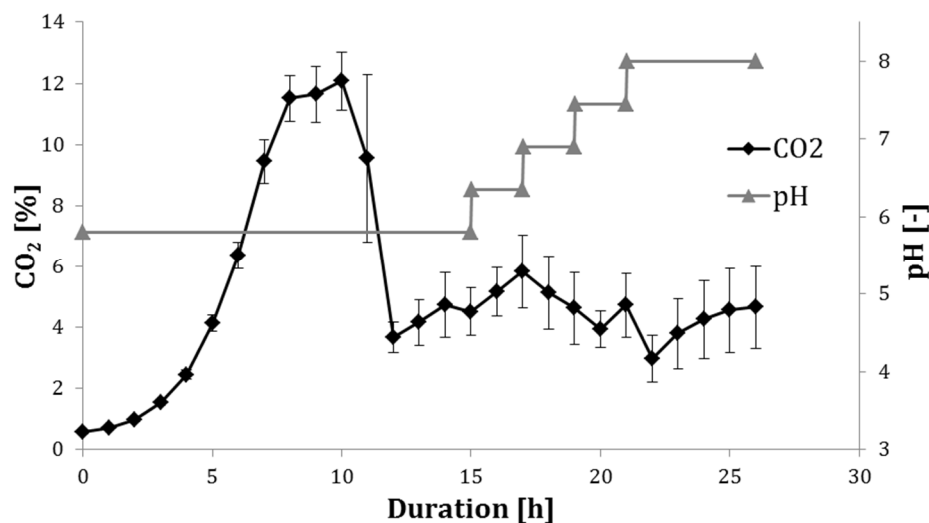


Figure 3-20: Monitoring of CO₂ in exhaust gas as an indicator for cell viability

Application of the pH shift and extended cell growth by additional supplementation of glucose in the growth phase. CO₂ production showed a typical peak around 8 h. Due to additional supply of glucose, the CO₂ peak lasted until 10 h followed by a drastic decrease caused by the depletion of glucose. During application of the pH shift the CO₂ level became more moderate. The experiments were performed using DASGIP 8x1L parallel bioreactor system as described in methods. The data summarizes growth phase of eight independent experiments. The error bars represent the standard deviations.

3.3.3.2 Design of the pH shift strategy

As observed in the 2 L bioreactor scale, solubility of oleic acid and the *cis*-ODA productivity greatly relies on the pH of the medium (Figure 3-19). Since, oleic acid did not show any toxic effect on *C. tropicalis* (3.3.2.2), the duration of the pH shift in the parallel bioreactor system was gained for reduction from 45 h to 6 h (Figure 3-21, A, B).

Even though, the cell viability during the biotransformation experiment in the 2 L bioreactor scale was not affected by the fast pH shift within 12 h (3.3.2.3), a further reduction to 6 h could increase the possibility of an alkaline stress. Therefore, during the performance of the pH shift the cell viability was indirectly monitored by CO₂ production in the exhaust gas (Figure 3-20). As the results revealed, CO₂ formation remained almost constant during the pH increase indicating no negative effect of the fast pH shift on the cell viability. Obviously, application of the shortened pH shift in combination with reduced glucose feed of 0.4 g/L led to a drastic increase of *cis*-ODA productivity yielding

in a final concentration of 40 g/L with a product yield of 77.8% (Table 3-13), which is almost 80 times higher than applying the pH shift over 45 h with a glucose feed rate of 1 g/h (Table 3-11). The role of the glucose feed in the increased product yield was studied further (3.3.3.3).

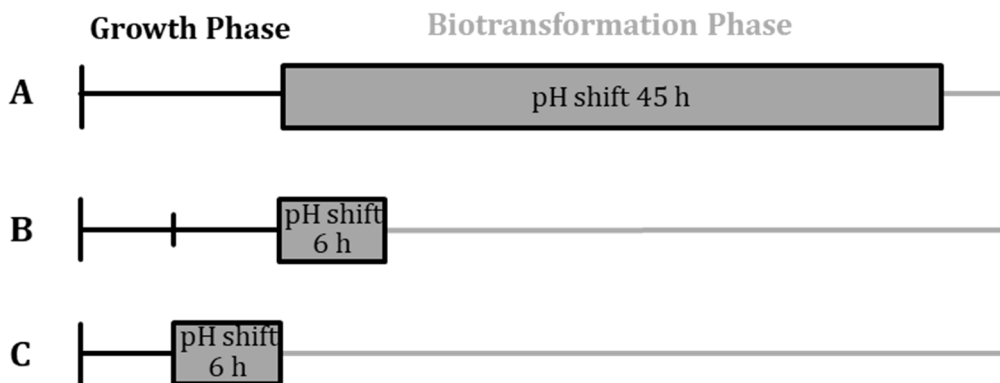


Figure 3-21: Overview over the various pH shift strategies

(A) production process as described for the DAME biotransformation comprising of the growth phase in batch mode and the biotransformation phase initiated by prolonged pH shift over 45 h and DAME feed. (B) Growth phase in fed-batch mode with subsequent biotransformation initiated with reduced pH shift and simultaneous application of the oleic acid feed. (C) pH shift transferred into the growth phase and initiated with the second supplement of glucose at 8 h to gain an initiation of the oleic acid feed at pH of 8.0 allowing higher solubility of oleic acid.

However, complete avoidance of the oleic acid accumulation could not be achieved by using this method. To minimize the solubility issues the biotransformation phase was initiated at a basic pH of 8.0. Therefore, a reduced pH shift was transferred into the growth phase and started with the feed of glucose at 8 h (Figure 3-21, C). This strategy allowed visible reduction in oleic acid precipitation. Interestingly, no substantial improvement of *cis*-ODA productivity could be achieved. The pH shift in the growth phase resulted in similar product concentration of approximately 40 g/L after 68 h as the pH shift during the biotransformation phase (Figure 3-22). Nonetheless, increased homogeneity of biotransformation broth due to reduction of oleic acid accumulation allowed more reliable and reproducible characterisation of the entire process (Figure 3-22).

Transfer of reduced pH shift in the growth phase did not affect the cell growth and viability as indicated by consistency in cell dry weight and CFU (Table 3-12). Therefore, application of the reduced pH shift within the growth phase was defined as standard method.

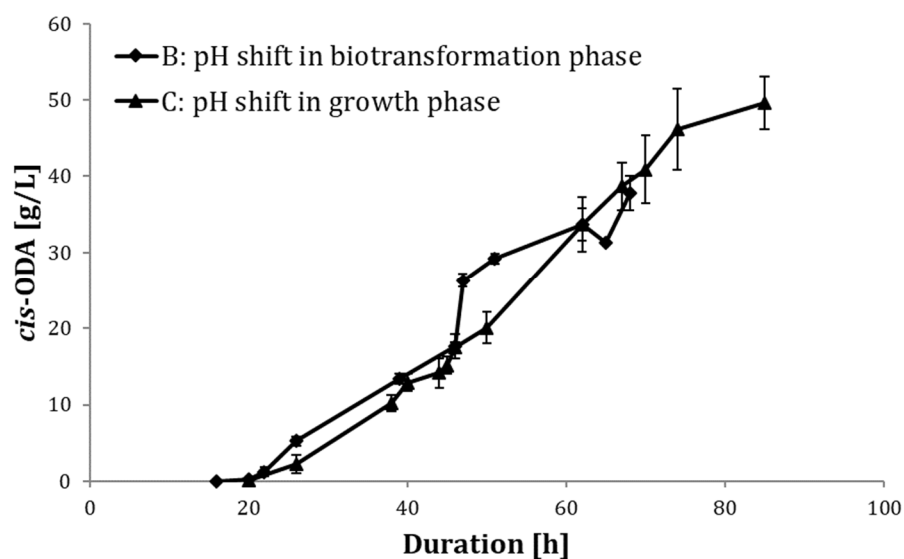


Figure 3-22: cis-ODA production in dependency on the pH shift strategy [107]

Investigation of the effect of (B) pH shift applied in biotransformation phase and (C) pH shift applied in growth phase on the production of *cis*-ODA. The experiments were performed at least in duplicate using DASGIP 8x1L parallel bioreactor system as described in methods. The error bars represent the standard deviations.

Table 3-12: Overview over the various growth phase models [107]

| Variant | Operational mode | pH shift | Cell biomass [g/L] | Colony forming units [CFU/mL] | Specific growth rate [h ⁻¹] | Doubling time [h] | Biomass yield coefficient [g ^{biomass} /g ^{glucose}] |
|---------|------------------|----------|--------------------|--|---|-------------------|---|
| A* | Batch | no | 14.3 ± 0.2 | - | 0.14 ± 0.02 | 5.2 ± 0.6 | 0.44 ± 0.01 |
| B** | Fed-Batch | no | 22.5 ± 2.3 | 6.01 × 10 ⁸ ± 1.47 × 10 ⁸ | 0.26 ± 0.02 | 2.7 ± 0.2 | 0.37 ± 0.03 |
| C** | Fed-Batch | yes | 24.8 ± 2.2 | 8.53 × 10 ⁸ ± 1.85 × 10 ⁸ | 0.26 ± 0.05 | 2.7 ± 0.5 | 0.39 ± 0.04 |
| | Ø Fed-Batch *** | | 23.6 ± 2.5 | 6.95 × 10⁸ ± 2.03 × 10⁸ | 0.26 ± 0.04 | 2.7 ± 0.4 | 0.38 ± 0.04 |

The assignment of the variants A, B and C as described in the methods. The experiments were performed using the DASGIP 8x1L parallel bioreactor system. The data represent the mean ± standard deviation. Sample size: * n = 3, ** n = 10, ***n = 20. Ø Fed-Batch represents the mean value of both fed-batch variants (B and C).

3.3.3.3 *Product yield in dependency of glucose feed*

Application of the genetically engineered *C. tropicalis* strain, which lacks the fatty acid utilization pathway, requires additional supply of a carbon source to maintain cell viability, as well as biotransformation. Thus, the biotransformation phase was initiated by using oleic acid feed as a substrate for *cis*-ODA production and by glucose feed as the energy source. Earlier, glucose accumulation was identified to interfere with the biotransformation efficiency (3.3.3.2). Therefore, to gain insight on this issue the effect of glucose feed on the *cis*-ODA production was studied in detail.

First biotransformation experiments on oleic acid revealed accumulation of glucose in the medium at high concentrations of around 11 g/L (Figure 3-18). Obviously, the application of a glucose feed rate of 1 g/h, as it was applied for the biotransformation of DAME, was too high for this process. To avoid glucose accumulation several feed rates in the range of 0.4 to 0.75 g/h were investigated (Table 3-13). Also, a distinctly higher glucose feed rate of 1.25 g/h was used to evaluate the effect of the elevated glucose feed on the production process at the transcriptional level using RT-qPCR (3.3.3.3.2).

The application of various glucose feed rates was found to influence several parameters, such as cell growth and cell viability. As expected, by increasing the glucose supply during biotransformation phase, the cell growth and proliferation was supported resulting in an increased cell biomass and CFU (Table 3-13). The highest glucose feed of 1.25 g/h resulted in almost four-fold higher biomass and two-fold higher viable cells compared to 0.4 g/h variant. However, increased biocatalysts production as represented in the form of the cell biomass did not lead to enhanced *cis*-ODA production. Contrarily, elevated glucose feed levels resulted in a drastic decrease of product yield. Lower glucose feed of 0.4 g/h yielded an almost 34 times higher *cis*-ODA concentration compared to the glucose feed of 1.25 g/h. Surprisingly, substrate conversion remained at 100% in all variants (Table 3-13) indicating the existence of an alternative oleic acid metabolic pathway, which strongly depends on the glucose concentration.

In general, there are several possibilities of fatty acids utilization within the yeast cells. A common degradation of fatty acids via β -oxidation pathway is not applicable for the

C. tropicalis strain ATCC 20962 (2.1.6). Thus, ω -oxidation remains the alternative fatty acid metabolic pathway for the production of the DCAs. However, several oleaginous yeast strains possess alternative routes of fatty acid utilization: production of lipid bodies (LBs). These lipid bodies consist of neutral lipids, such as triacylglycerols (TAGs) and sterol esters (SEs) and are usually surrounded by a monolayer of phospholipids (PLs) [31]. Synthesis of TAGs requires an excess of free fatty acids and glucose [31], both provided during the *cis*-ODA production process. Since *C. tropicalis* is also described to be an oleaginous yeast [109, 110], the possible incorporation of oleic acid into TAGs and subsequent storage in LBs was investigated in more detail.

Table 3-13: Characterization of *cis*-ODA production process at various glucose feed rates [107]

| Glucose feed [g/h] | Cell biomass [g/L] | Colony forming units [CFU/mL] | Final <i>cis</i> -ODA concentration [g/L] | Volumetric productivity [g/(L·h)] | Specific productivity [mg _{<i>cis</i>-ODA} /(g _{biomass} ·h)] | Product yield [%] | Substrate conversion [%] |
|--------------------|--------------------|---|---|-----------------------------------|---|-------------------|--------------------------|
| 0.4 | 29.9 ± 0.1 | 3.57 × 10 ⁸ ± 1.15 × 10 ⁸ | 37.78 ± 2.29 | 0.56 ± 0.03 | 20.18 ± 1.29 | 77.8 ± 6.5 | 99.9 ± 0.09 |
| 0.5 | 37.7 ± 2.3 | 2.49 × 10 ⁸ ± 3.97 × 10 ⁷ | 26.38 ± 1.40 | 0.39 ± 0.02 | 11.22 ± 1.27 | 62.6 ± 2.7 | 100 ± 0 |
| 0.75 | 72.8 ± 6.2 | 6.28 × 10 ⁸ ± 1.32 × 10 ⁸ | 19.23 ± 2.14 | 0.28 ± 0.03 | 4.25 ± 0.82 | 32.2 ± 6.1 | 100 ± 0 |
| 1.25 | 118.3 ± 1.3 | 7.86 × 10 ⁸ ± 1.56 × 10 ⁸ | 1.17 ± 0.14 | 0.02 ± 0.00 | 0.16 ± 0.02 | 2.3 ± 0.07 | 99.3 ± 0.07 |

The experiments were performed in duplicate using the DASGIP 8x1L parallel bioreactor system as described in the methods. The data represent the mean ± standard deviation at the end of the production process (68 h).

3.3.3.3.1 Incorporation of oleic acid into the lipid bodies

The production of LBs by oleaginous yeasts is a very well described process. Some yeasts are capable of storing lipids up to 70% of their cell dry weight [111] resulting in visible changes of cell morphology. Thus, the yeast cells that exhibited lowest (0.4 g/h) and highest (1.25 g/h) glucose feed during the biotransformation were examined using light microscopy. Obviously, the application of an elevated glucose feed resulted in yeast cells with double the size as compared to the ones grown at a lower glucose feed rate (Figure 3-23). More interesting was the appearance of large vesicles within the cells obtained from cultivations at the glucose feed rate of 1.25 g/h. These vesicles were of 3.7 ± 0.9 μm (n=43) in diameter and filled almost the whole cell.

Since the production of lipid bodies will increase the overall lipid content of the cells, the total lipid extraction from cell pellets was applied. To enable direct comparison samples obtained under the lowest and the highest glucose feed were used for extraction (2.2.1.6). As a control, cells cultured in the absence of oleic acid were used. The elevated glucose feed rate of 1.25 g/h resulted in almost a two-fold higher lipid content of 183.6 ± 9.6 mg per gram of cell wet weight compared to the 0.4 g/h variant (Figure 3-24). These results allow to assume that the observed vesicles were indeed LBs. As mentioned before, elevated glucose feed led to four times higher cell biomass in comparison to lower glucose feed (Table 3-13). Interestingly, only a two-fold increase in the number of viable cells (CFU) was detected. Obviously, accumulation of lipid bodies increased the weight of individual yeast cells. However, compared to the control sample, the variant exposed to the lowest glucose feed of 0.4 g/h also showed a five times higher lipid content, suggesting the formation of lipid bodies under these conditions as well. This assumption is reinforced by the fact that even at the lowest glucose feed only substrate conversion of 77% could be achieved (Table 3-13).

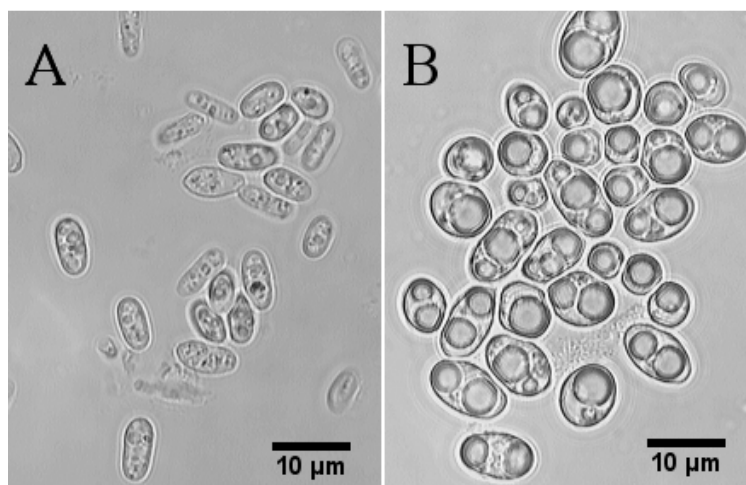


Figure 3-23: Microscopic views at 1,000×magnification of *C. tropicalis* process at various glucose feeds [107]

(A) Glucose feed of 0.4 g/h, cell length: $6. \pm 0.9$ μm , area: 17.5 ± 4.9 μm^2 (n=22). (B) Glucose feed of 1.25 g/h, cell length: 7.3 ± 2.0 μm , area: 33.6 ± 12.3 μm^2 (n=31). The data represent the mean \pm the standard deviation obtained from cell measurements using ImageJ software at a process time of 62 h. Sample size n is giving in brackets.

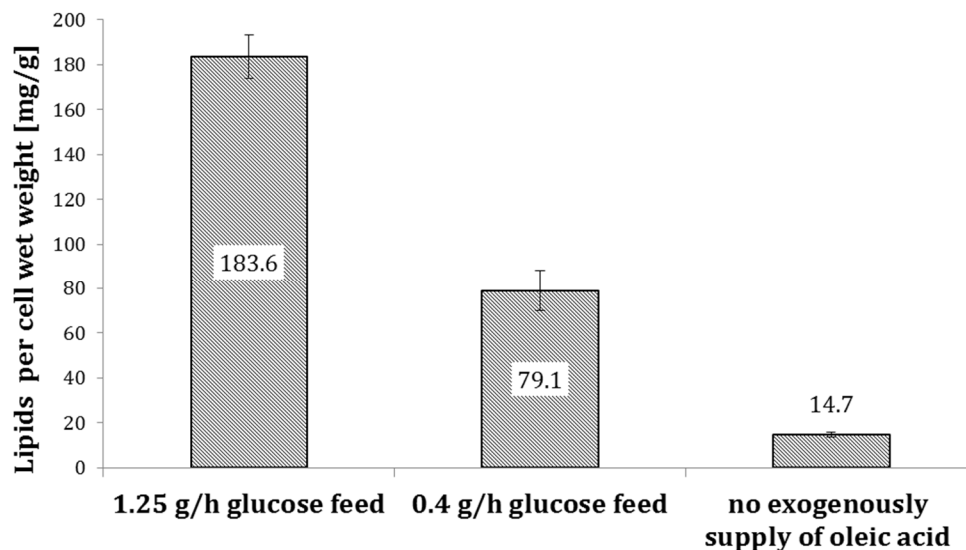


Figure 3-24: Extracted total lipids from samples exposed to various glucose feed rates [107]

Lipid concentration is expressed per cell wet weight. Lipid extraction was performed as described in methods. The error bars represent the standard deviations from three independent samples.

Furthermore, the composition of the extracted lipids was investigated in detail by thin-layer chromatography (2.2.3.4). This method enabled a qualitative analysis by distinct separation of the four main lipid groups: triacylglycerols (TAGs), sterol esters (SEs), sterols (Ss) and phospholipids (PLs) (Figure 3-25). The extracted lipids from cells exposed to both low and high glucose feed rates contained all the expected lipids in various amounts. As the main components of the LBs, TAGs and SEs were found in highly unequal proportions. Independent of the glucose feed rate, the SE level was very moderate while TAGs accounted for the major fraction. Nevertheless, cells exposed to higher glucose feed rate conferred a remarkable increase in TAG level compared to the 0.4 g/h variant. Since, the high TAG levels were observed simultaneously with a low product yield, the incorporation of the oleic acid into the TAGs production was assumed.

To confirm the channelling of oleic acid into the TAG synthesis saponification of the extracted lipids was targeted. Saponification relies on the treatment of triglycerides with a strong base, which accelerates cleavage of the ester bond and releases fatty acid salts and glycerol (Figure 2-1). As identified by GC/FID, 80% of the released FAs after TAG hydrolysis were accounted to oleic acid (7.5), verifying the incorporation of oleic acid

into LBs. Also, the presence of glycerol in the hydrolysed lipids samples was confirmed by HPLC (7.5).

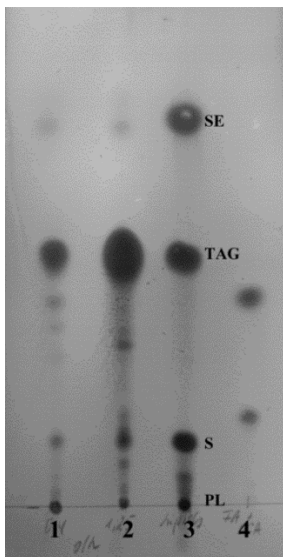


Figure 3-25: TLC of extracted lipids from samples exposed to various glucose feeds rates [107]

Lipids obtained from samples exposed to (1) 0.4 g/h glucose feed rate or (2) 1.25 g/h glucose feed rate in comparison to (3) standards (PL, S, TAG, SE) at 4 mg/ μ L and (4) oleic acid (top) and *cis*-ODA (bottom) at 25 mM. TLC was performed as described in methods.

3.3.3.3.2 Effect of glucose on the transcriptional level

High glucose concentration within the cell lead to facilitated LBs production and storage within the cells. To explore the role of glucose in more detail, the expression level of the genes important for the ω -oxidation, *CYP52A13/14*, *CYP52A17/18* and *CPR* (1.5) in correlation to the various glucose feed rates was monitored.

Interestingly, the transcriptional analysis revealed only a modest difference in expression levels of all investigated genes in the samples exposed to various glucose feed rates (Figure 3-26). Independent of the glucose feed, *CYP52A17/18* was found to be induced at higher expression rates than the *CYP52A13/14* and *CPR*. However, towards the end of the process a two- to three-fold decrease in the expression levels of all genes at the highest glucose feed rate compared to the lowest was observed. Since, the production of the LBs directly occurred at the beginning of the biotransformation, no

repression of *CYP52A* on the transcriptional level by glucose in the presence of oleic acid could be confirmed.

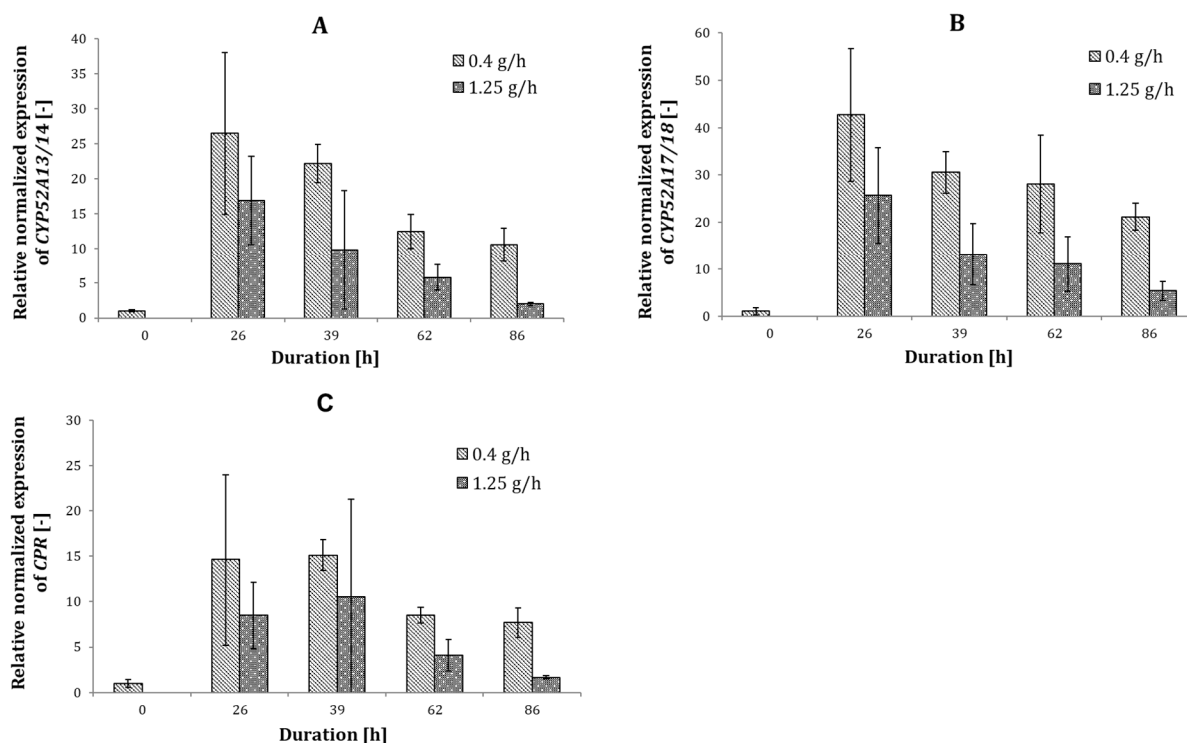


Figure 3-26: Monitoring of gene expression in dependency of glucose feed rates [107]

Relative normalized expression profiles of (A) *CYP52A13/14*, (B) *CYP52A17/18* and (C) *CPR*. All expression values were normalized to *ACT1* and *GAPDH* (CV=0.3333, M=0.9626). The error bars represent the standard error of the mean of two biological samples measured in triplicate. Gene expression: p-value < 0.05 (except for the following sample of *CPR* expression: 1.25 g/h for 86 h).

3.3.3.3 Production of DDA in dependency of glucose feed

During DDA production, channeling of the substrate into the TAGs synthesis was never an issue since the mass balance of the substrate and product was always comprehensive. The product yield remained constant around 100% despite the high glucose feed of 1 g/h. Contrarily, during oleic acid biotransformation glucose feed of 0.75 g/h resulted in high reduction of the product yield to 32% (Table 3-13). The comparison of both processes raised the question as to whether DAME could not be stored in TAGs or applied glucose feed rate was too low to initiate LBs production. Thus, to investigate the effect of the glucose feed rate on the DDA product yield, the DDA production process was repeated

applying accelerated pH shift during the growth phase and two different glucose feed rates of 1 g/h and 3 g/h.

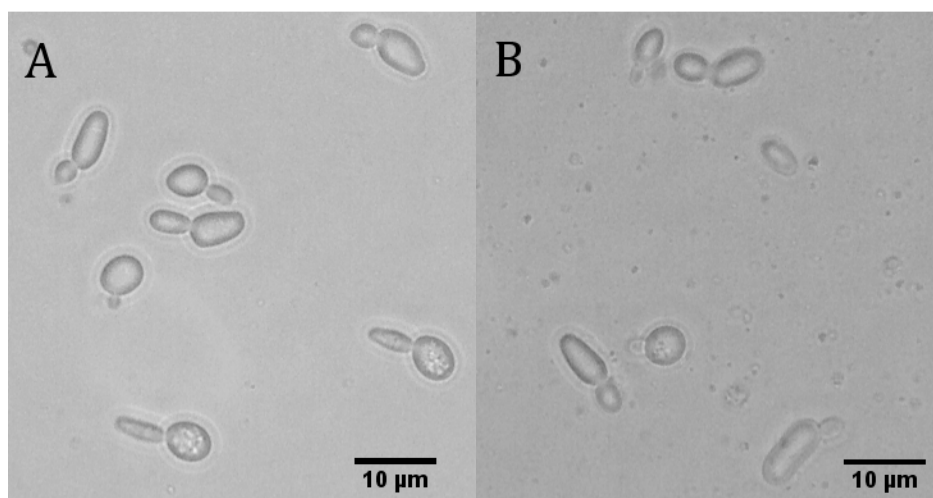


Figure 3-27: *C. tropicalis* during DAME biotransformation exposed to various glucose feed rates [107]

The microscopic views of *C. tropicalis* exposed to glucose feed rates at (A) 1 g/h and (B) 3 g/h during DDA production process. The microscopic observation was taken after 67 h of DAME biotransformation at 1,000×magnification.

During DAME biotransformation cell morphology was monitored by microscopy and none of the variants, both high and low glucose feed, showed any inclusions within the cell (Figure 3-27). Also, a comprehensive mass balance of the substrate and product was achieved regardless of the glucose feed rate (Figure 3-28). These findings clearly refute the theory of DAME incorporation into TAGs and subsequently LBs formation during the DDA production.

Table 3-14: Characterization of DDA production in correlation to glucose feed

| Glucose feed [g/h] | Cell biomass [g/L] | Final DDA concentration [g/L] | Volumetric productivity [g/(L·h)] | Specific productivity [mg _{DDA} /(g _{biomass} ·h)] | Product yield [%] | Substrate conversion [%] |
|--------------------|--------------------|-------------------------------|-----------------------------------|--|-------------------|--------------------------|
| 1 | 23.2 ± 3.1 | 10.7 ± 0.3 | 0.56 ± 0.03 | 8.35 ± 2.25 | 34.0 ± 1.1 | 35.9 ± 15.4 |
| 3 | 20.0 ± 1.7 | 6.6 ± 2.3 | 0.39 ± 0.02 | 10.01 ± 3.27 | 21.6 ± 7.6 | 39.4 ± 7.5 |

The experiments were performed in duplicate using DASGIP 8x1L parallel bioreactor system as described in methods. The data represent the mean ± standard deviation at the end of the production process (62 h).

Even if no LB accumulation was observed, glucose did affect the efficiency of DAME biotransformation. Results revealed, that an elevated glucose feed of 3 g/h led to a lower DDA productivity in comparison to the 1 g/h variant (Table 3-14). Interestingly, applying the optimized production process including the extended growth phase with the reduced pH shift resulted in a low substrate conversion of 35%.

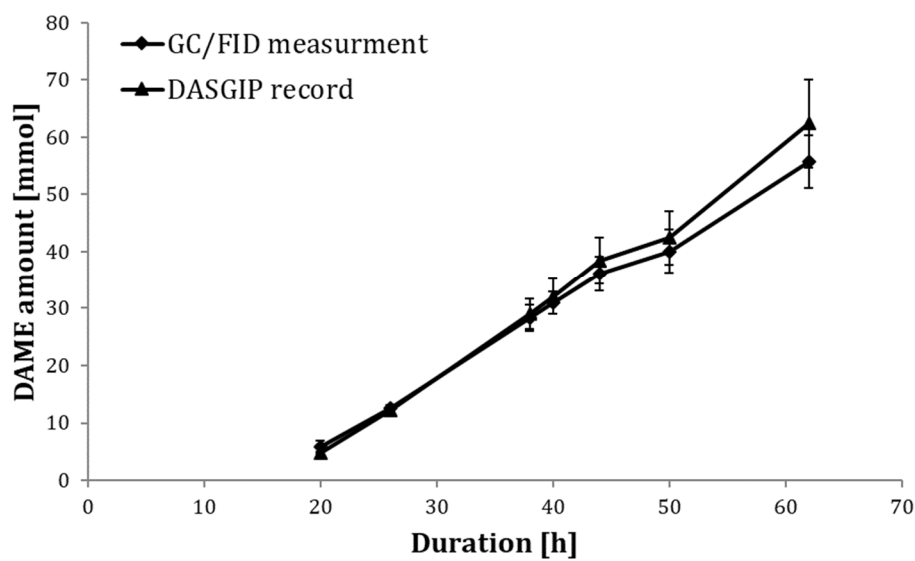


Figure 3-28: Mass balance of the substrate and product during DAME biotransformation [107]

Comparison of the amount of DAME as supplied and registered by calibrated DASGIP feed rates to the summarized amounts of DAME, DA, and DDA as measured by GC/FID. The experiments of four biological samples were performed GC/FID as described in methods. The error bars represent the standard deviations.

3.3.3.4 *cis*-ODA production in correlation to substrate feed

TAG synthesis is driven by the availability of the corresponding precursors: FAs and glycolysis-derived glycerol-3-phosphate or DHAP. While excess glucose was identified to be responsible for the channelling of oleic acid toward TAG production, the availability of oleic acid itself as a second important precursor can also promote LB accumulation. Thus, the concentration of oleic acid accessible for TAG production was limited by decreasing the oleic acid feed rate. The experiments were performed at the lowest possible glucose feed rate of 0.4 g/h in constant mode.

Surprisingly, limiting the oleic acid supply did not lead to the desired increase of product yield. On the contrary, reduced oleic acid feed rate of 0.3 g/(L·h) resulted in low

productivity (Figure 3-29). With subsequent increase of oleic acid feed rate, the product yield also increased and reached a final value of $60.6 \pm 2.5\%$ at $1.0 \text{ g}/(\text{L}\cdot\text{h})$.

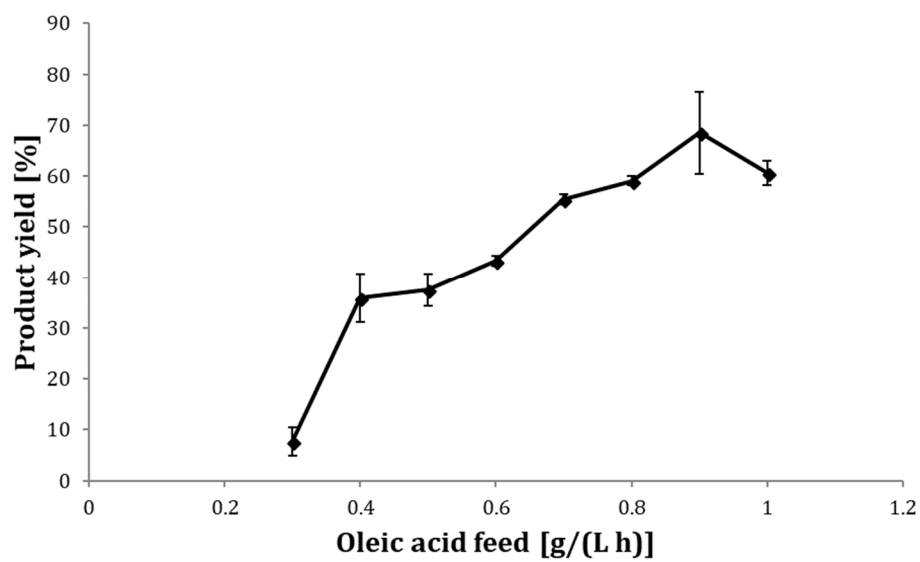


Figure 3-29: *cis*-ODA product yield in dependency on oleic acid feed rate [107]

The experiments were performed in duplicate using DASGIP 8x1L parallel bioreactor system as described in methods. The error bars represent the standard deviations.

3.3.4 Recovery and purification of *cis*-ODA

The cell broth as obtained after oleic acid biotransformation was used for the purification process of *cis*-ODA as described in 2.2.5. The alteration of pH value of the supernatant by acidification led to immediate precipitation of the desired product (Figure 3-30, B). Further purification and dehydration of *cis*-ODA resulted in formation of white powder (Figure 3-30, D). In this way, purified *cis*-ODA was used as analytical standard for GC/FID measurements.

The purification was performed using a part of the cell broth containing 3.4 g of *cis*-ODA according to GC/FID measurement. After the purification, 2.9 g of the product with a purity of 94% was recovered as confirmed by GC/FID (Figure 3-31). Thus, applying optimal conditions for oleic acid biotransformation with product yield of 77% and subsequent purification with recovery of 85%, 1 g of oleic acid should yield in 0.7 g of *cis*-ODA.

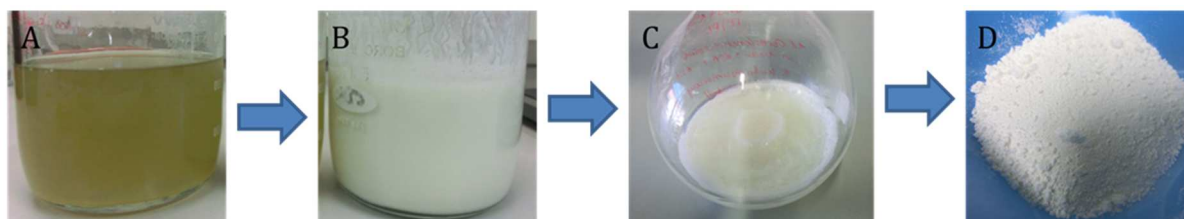


Figure 3-30: Purification steps of *cis*-ODA

As described in methods, the supernatant obtained after centrifugation step (A) was acidified with 2N HCl leading to precipitation of *cis*-ODA (B). The precipitate was further purified by hot-filtration and recrystallization, which led to formation of white crystals (C). Subsequently crystals were dried under vacuum and *cis*-ODA as a white powder (D) was obtained.

Further, *cis*-ODA was analyzed by several analytical techniques. First, the melting point of the purified *cis*-ODA and also of *trans*-ODA was determined as described in 2.2.3.7. *cis*-ODA was found to have a melting point of 70.2°C. In contrast, *trans*-ODA exhibited much higher melting temperature of 99.5°C. In addition, both stereoisomers were analyzed by GC/MS (Figure 3-32). The retention time of *cis* isomer was slightly earlier at 18.44 min compared to *trans*-ODA with the retention time at 18.51 min. GC/MS data showed comparable fragmentation of both molecules underlining their identical structure.

Results

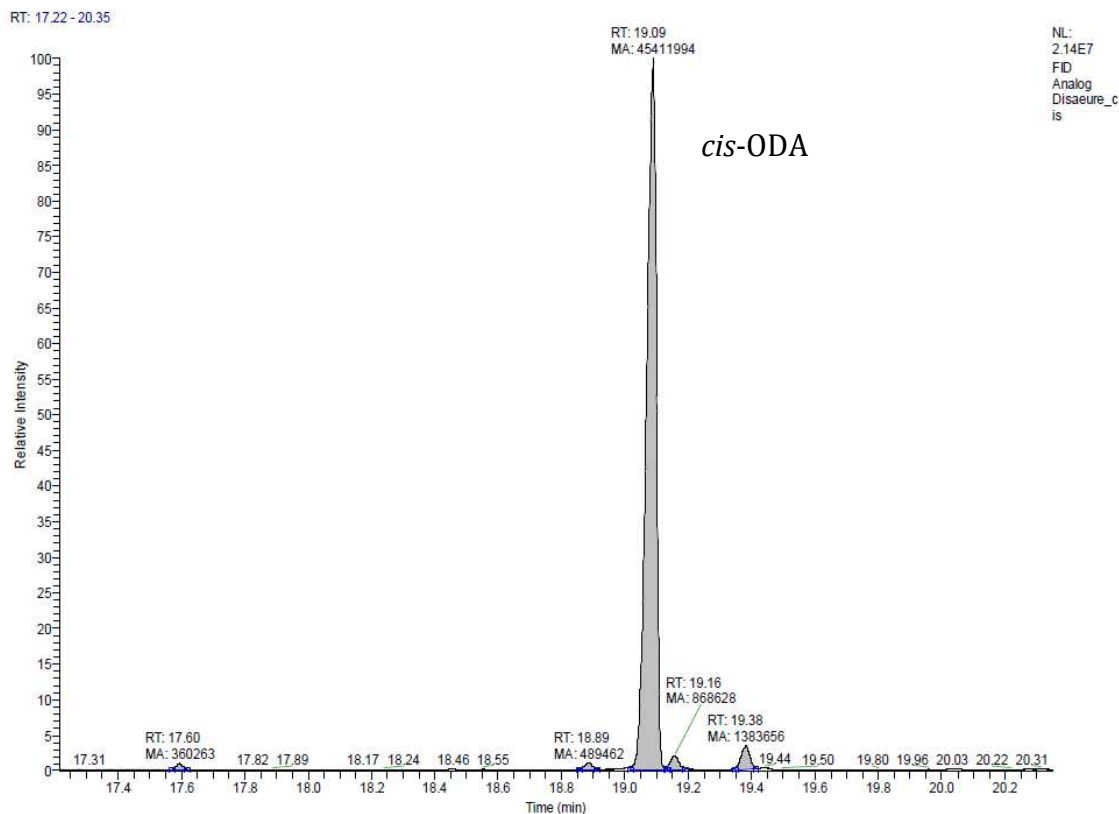


Figure 3-31: GC/FID chromatogram of purified *cis*-ODA

Purification using hot-filtration as described in methods resulted in ca. 94% pure *cis*-ODA. Purity was calculated based on the peak area.

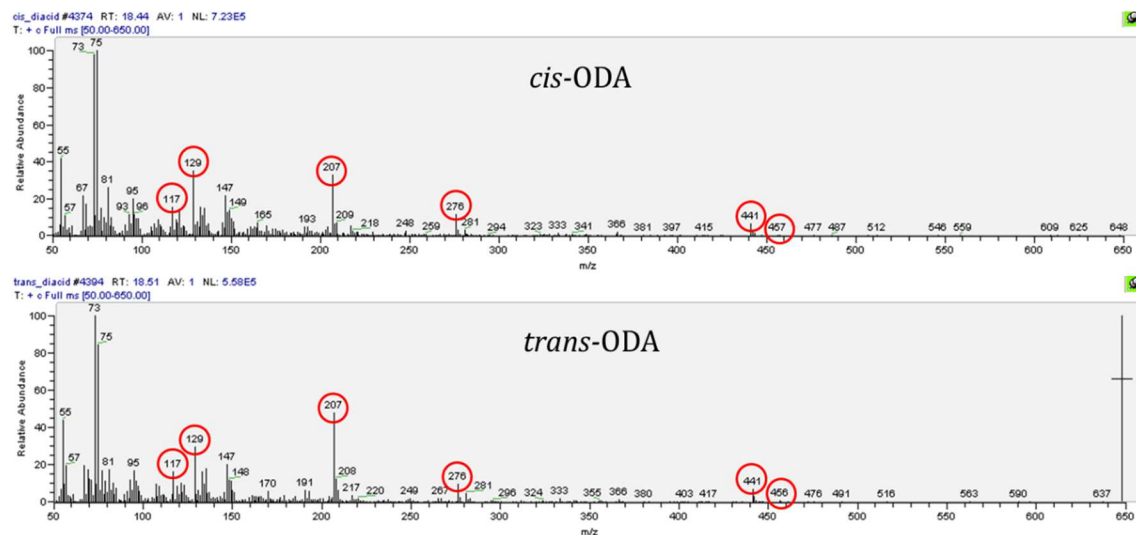


Figure 3-32: Comparison of the GC/MS of *cis*- and *trans*-ODA

Where 456 m/z is the molar mass (M) of derivatized ODA, 441 m/z missing one methyl group (M-15), 276 m/z missing both silyl groups including neighboring oxygen molecule (M-178), 207 m/z missing CO, CH₂ in addition to M-178 (M-249). The experiment was performed as described in methods.

4 Discussion

The parallel bioreactor system enabled the identification of critical process parameters and allowed fast and reliable process development and optimization for the production of the desired dicarboxylic acids. Applying this system, the production process of DDA and *cis*-ODA could be successfully implemented.

4.1 Enhanced biomass production supporting biotransformation

Characterization of the cell growth in the pre-cultures enabled optimization of the process resulting in highly reproducible and reliable process. The detailed observation of the cell growth revealed morphological differentiation of *C. tropicalis* after prolonged cultivation on the agar plates (Figure 3-13). For the observed color patterns of the yeast cells (3.2.1), a contamination could be excluded by rRNA analysis. As described in literature, adenine auxotrophic yeast cells tend to accumulate a red pigment within the cells and are used as typical auxotrophic markers in yeast engineering [112-114]. In general, adenine represents an important intermediate of the nucleotide *de novo* synthesis and can be directly converted to adenosine monophosphate (AMP) by a single step [115]. When adenine is not present, the cells are able to produce AMP from phosphoribosyl-pyrophosphate (PRPP) by a pathway comprising 12 enzymatic steps. Known mutations in *ade1/ade2* genes of this pathway lead to the accumulation of an intermediate of PRPP pathway, ribosylaminoimidazole (AIR). When, exposed to air, the intermediate is oxidized leading to the production of a red pigment [112]. A similar effect was observed for the *C. tropicalis* strain used in this work. Cells grown on complex YPD agar containing adenine didn't turn reddish, since there was no need for AMP production from PRPP. However, after prolonged cultivation over 100 h, adenine in the media was obviously consumed and cells were dependent on the PRPP pathway. At this time point the adenine auxotrophic yeast cells start to accumulate AIR and changed the color enabling the differentiation between auxotrophic and prototrophic colonies. Interestingly, after the isolation of the prototrophic yeast cells (3.2.1), no occurrence of reddish auxotrophic cells was observed, indicating that the adenine-requiring mutation was likely not spontaneous. Usually, adenine auxotroph mutants are generated by using

of harsh conditions, such as antimicrobial agents [116, 117], UV light [114] or γ -radiation[117]. Thus, the glycerol stocks should have contained both, auxotrophic and prototrophic, cells from the beginning on. The origin of different *C. tropicalis* cells in the glycerol stock remained unclear.

Within the usual cultivation time on the agar plates of 48 h no differentiation of the cell types could be made. This revealed a risk of using different yeast cell types for various experiments during DAME conversion. Fortunately, adenine-requiring mutants showed a very moderate cell growth in liquid culture, likely due to accumulation of a toxic intermediate [113]. By rechecking cell growth of all pre-cultures used for DAME biotransformation process, the application of prototrophic yeast cells was assured. Thus, the comparison between the various experiments and processes can be guaranteed. This observation highlights the significance of cell morphology and cell growth characterization to avoid genetic inhomogeneities and to perform reliable process. Finally, the cross contamination by adenine-requiring mutants was eliminated by the preparation of new glycerol stock which contained only the prototrophic *C. tropicalis* cells. To prove the absence of adenine-requiring mutants, all agar plates were stored after inoculation of the pre-cultures and were incubated for more than 100 h.

The detailed characterization of the pre-culture in the 2 L bioreactor (3.2.2) enabled the reduction of the cultivation time and thus, a significant decrease of the entire process time. By changing the operational mode of the cultivation from batch to fed-batch, enhanced cell growth was achieved (Table 3-10). Application of the same strategy for the growth phase in the parallel bioreactor system led to almost a two-fold increase of the cell biomass (Figure 3-12). Nevertheless, the cultivation in fed-batch mode revealed distinct limitation as well. As described in 3.3.3.1, the occurrence of ethanol accumulation as a result of the Crabtree effect [50, 51] was observed. As shown for *S. cerevisiae*, glucose concentration higher than 0.15 g/L results in ethanol production by channelling pyruvate into the fermentation pathway [51]. The limit of the glucose concentration might vary from species to species, but the applied glucose concentration of 30 g/L is 200-fold higher than the limit determined for *S. cerevisiae* and will surely lead to ethanol production in Crabtree-positive yeasts. To increase the amount of biomass by avoiding

Crabtree effect, the growth phase as well as pre-culture can be performed in continuous mode. This approach will allow the supply of glucose at low feed rates to prevent glucose accumulation and therefore ethanol formation. Nevertheless, during the biotransformation phase no ethanol production was observed most likely due to application of the continuous glucose feed.

4.2 DCA productivity in dependency on the pH

The application of the designed pH shift from 5.8 to 8.0 over 45 h in biotransformation phase revealed distinct differences directly related to the substrate used. DDA productivity could be greatly increased using this pH shift strategy (Table 3-1). However, application of an identical pH shift for biotransformation of oleic acid was less efficient. Only drastic time range reduction of the pH shift to 6 h enabled enhanced *cis*-ODA production (3.3.3.2).

The huge difference of the optimal pH conditions is likely related to the chain length and thus the physical properties of the corresponding substrate (Table 4-1). As fatty acids are weak carboxylic acids, their dissociation in aqueous environment strongly depends on the pH value [118]. Carboxylic acids with a logarithmic acid dissociation constant (pKa value) lower than the pH value of the medium prefer ionized form and thus, are more water soluble. Therefore, oleic acid with a pKa value of around 7.5 [118, 119] will exist rather in a protonated than ionized form at a pH as applied in the production process ($\text{pH} < \text{pKa}$). Obviously, the application of a prolonged pH shift resulted in the precipitation of oleic acid and therefore a poor conversion rate. Kanicky *et al.* described oleic acid to form crystals in aqueous medium at pH values around pKa (~ 7.5) [119] as observed in this study as well, during the biotransformation of oleic acid in the 2 L bioreactor (3.3.2.3). Reduction of the pH shift to 6 h and starting the biotransformation phase at pH of 8.0 enabled enhanced solubility of oleic acid and thus, efficient substrate conversion. A reasonable question arose from the observed dependency of the oleic acid conversion on the medium pH: would further increase of the pH result in even higher solubility of oleic acid and thus enhanced productivity? At a pH value higher than 9.0 also long-chain fatty acids should be completely ionized leading to formation of micelles,

thermodynamically stable aggregates (saponification) [120]. This event might drastically decrease the availability of the oleic acid for the cells reducing the product yield. Theoretically, increasing of medium pH up to 9.0 should be possible, when no negative effects on the cell viability will occur.

Table 4-1: Overview over the pKa values and solubility of fatty acids

| Fatty acid | pKa (20°C) | Water solubility (pH 7.4, 37°C) [121] |
|-----------------|---------------------|--|
| Dodecanoic acid | 5.3 [122] | > 1 mM |
| Oleic acid | 7.5-9.85 [118, 119] | < 1 μM |

The pKa value of oleic acid is difficult to estimate and varies depending on the method and concentration [118].

Successful increase of oleic acid solubility from beginning on was enabled by transfer of the reduced pH shift into the growth phase (Figure 3-21). However, the same strategy applied for DDA production led to an almost two-fold decrease of specific productivity in comparison to prolonged pH over 45 h (Table 4-2). In general, the application of pH shift is expected to negatively influence yeast cell viability. The alteration of surrounding pH strongly affects H⁺ gradients [123, 124] and thus the regulation of the internal pH (pH_i) [123]. Although, yeast cells are known to be able to adapt to a wide pH range [102, 123], cells in the stationary phase are less susceptible to environmental stress factors in comparison to still growing cells in the exponential phase [125]. Consequently, the application of pH shift in the growth phase is more stressful for the yeast cells compared to the pH shift in biotransformation phase. Thus, the subsequent feeding of the toxic substrate DAME after pH shift in growth phase resulted in additional stress and led to a reduced cell activity. Application of oleic acid did not show any further negative effects on the cell viability (Figure 3-12), since this substrate is not toxic to the *Candida* cells. A slightly different explanation for the reduced productivity can be given based on the research of Liu *et al.* The authors demonstrated, that the pH shift itself stimulates the activity of the P450 enzymes, catalyzing the first step of ω-oxidation [47]. According to this study, application of the constant pH during the biotransformation should be less efficient than applying the pH shift. Obviously, this statement applies for the production

process using DAME as a substrate. Both, the constant pH of 5.8 and of 8.0 during the biotransformation resulted in marginal product titer, whereas application of the pH shift drastically enhanced productivity (Table 4-2). These results clearly support the study of Liu *et al.* However, biotransformation of oleic acid at constant pH of 8.0 resulted in remarkable high specific productivity compared to conversion of DAME by using of the pH shift strategy (Table 4-2). To clarify the effect of pH shift stimulation on oleic acid conversion, a pH shift during the growth phase until pKa of oleic acid (7.5) can be applied to enhance oleic acid solubility in the biotransformation phase followed by an additional pH shift from 7.5 up to 9.0 in the biotransformation phase.

Table 4-2: Summary of specific productivity in dependency of pH and applied substrate

| Substrate applied | pH during biotransformation | Specific Productivity [mg _{product} /(g _{biomass} ·h)] |
|-------------------|--|---|
| DAME | Constant pH at 5.8* | 5.0 ± 0.2 |
| | Constant pH at 8.0** (after pH shift in growth phase) | 8.35 ± 2.25 |
| | pH shift (45 h)*** | 13.36 ± 1.87 |
| Oleic acid | Constant pH at 8.0**** (after pH shift in growth phase) | 20.18 ± 1.29 |

*Sample size n=2, constant DAME feed rate at 0.5 g/(L·h), constant glucose feed rate at 1.0 g/L

**Sample size n=2, increased DAME feed rate, constant glucose feed rate at 1.0 g/L

***Sample size n=4, increased DAME feed rate, constant glucose feed rate at 1.0 g/L

****Sample size n=2, constant oleic acid feed rate at 1g/(L·h), constant glucose feed rate at 0.4 g/L

4.3 Effect of temperature on DCA production

As an essential parameter, the optimal temperature affects the cell growth and viability and has an impact on the metabolic processes of microbial cells. Also, the process economy strongly depends on the choice of the appropriate temperature. From the industrial point of view, especially for the scale-up possibilities, removal of process heat, mainly produced by chemical reactions, pumps or mechanical agitation, represents a bottleneck [126, 127]. Cooling down the system and the maintenance of constant temperature consumes large amounts of energy and cooling water. High process temperature requires less energy for cooling the system and thus, makes processes more

sustainable. But application of slightly higher temperature of 35°C for biotransformation of DAME by *C. tropicalis* led to a significant decrease in the specific productivity compared to the process variant at 30°C (Table 3-2). Since the temperature strongly affects the fluidity of the cell membrane [128, 129], the permeability of the yeast cell also depends on this process parameter. Increased temperatures might have led to a facilitated uptake of DAME and thus increased toxic effects on the cells resulting in the reduced viability and specific productivity (Figure 3-2, Table 3-2). Besides, a possible impact on the fatty acid transport, higher temperature leads to decreased solubility of oxygen and thus lowers transfer to cells [126, 127]. Since, the biotransformation of fatty acids relies on the oxidation by implementation of molecular oxygen (Figure 1-2), a decrease of oxygen uptake could also affect the conversion process, especially at an industrial scale. Thus, 30°C was further used in this study for the fatty acid biotransformation. However, for industrial manufacturing the negative impact of lower productivity at 35°C must be confronted with energy costs compared to the process at 30°C.

4.4 Feed strategies in biotransformation phase

Being the most crucial parameters of fatty acids biotransformation by *C. tropicalis*, glucose feed and substrate feed were found to strongly affect the product yield. Depending on the applied substrates, these parameters influenced the corresponding production processes differently and were investigated in detail.

4.4.1 Effects of the glucose concentration on the product yield

The DDA production process was performed at a glucose feed rate of 1 g/h, which did not show any negative impacts on DAME conversion. In contrast, the application of a similar glucose feed of 1.25 g/h for the *cis*-ODA production resulted in very poor product yield accompanied by LBs formation (3.3.3.3.1). Commonly, LBs production is induced by nitrogen limitation, which can be achieved by increasing molar ratio of glucose to nitrogen (C/N). When nitrogen becomes unavailable, cell proliferation terminates and all accessible carbon is channeled directly into lipid synthesis with subsequent storage in LBs [111]. To initiate LBs formation the C/N ratio was described to be greater than

20 [109, 110]. Since the nitrogen content during the biotransformation of oleic acid by *C. tropicalis* was not determined, theoretical values were estimated. Starting conditions of biotransformation possess a C/N molar ratio of 8, which is theoretically the highest ratio possible during the whole process. Unlike glucose, additional nitrogen source was not provided during the biotransformation, which could result in an increase of the ratio towards the end of the process. However, applying a high glucose feed rate at 1.25 g/h, LBs production was observed at the beginning of the biotransformation phase (Figure 4-1). Certainly, nitrogen limitation is not expected directly at the beginning of the process and thus, cannot be responsible for the LBs formation during *cis*-ODA production. Similar observations were also found for the LBs production by *Y. lipolytica*. The authors proposed formation of LBs without nitrogen limitation when hydrophobic substrates, mainly FAs, were supplied as the carbon source [111, 130].

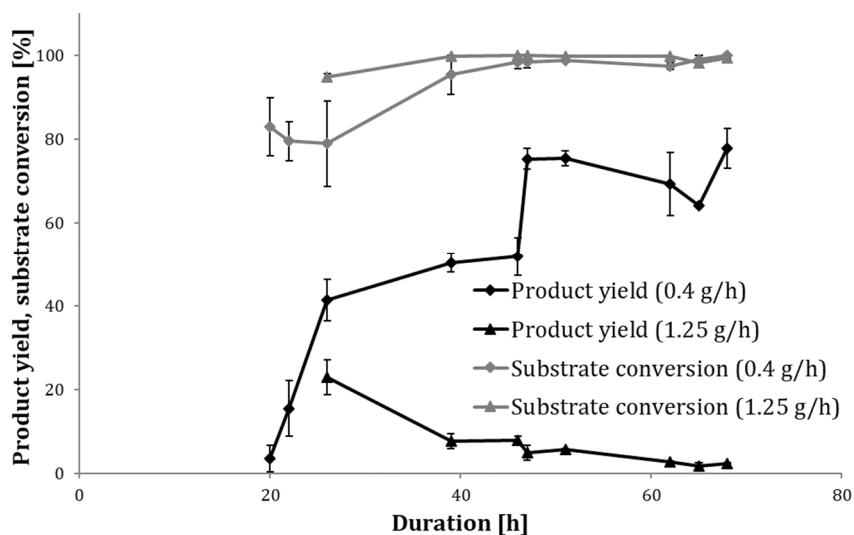


Figure 4-1: Product yield and conversion of oleic acid over the time at different glucose feed rates during the production process [107]

The experiments were performed at least in duplicate using DASGIP 8x1L parallel bioreactor system as described in methods. The error bars represent the standard deviations.

Beside nitrogen limitation, the presence of ethanol in the surrounding environment is described to promote LBs formation by repressing the synthesis of the core enzymes of β -oxidation [131]. Nevertheless, neither glucose nor ethanol accumulation in the media was observed at any glucose feed rate used during oleic acid biotransformation. It seems

that the supplied glucose is fully transported from the media into the yeast cell and remains the driving force in the LBs formation. Several studies described glucose to interfere with the DCA production pathway [26, 29, 41, 44, 52, 53]. So, Seghezzi *et al.* showed complete repression of *CYP52A* family genes of *C. tropicalis* by glucose as detected via northern blot [53]. On the contrary, in this study no glucose-mediated repression of *CYP52A13/14* and *CYP52A17/18* genes was observed (Figure 3-26). Due to lack of information about the pre-induction or simultaneous supply of FAs in the studies of Seghezzi, no direct comparison with the results obtained in this study is possible. However, transcriptional analysis does not describe the effect of glucose on the activity of enzymes of the ω -oxidation pathway. Thus, an inhibition on the enzyme level can be assumed, as suggested in other studies for *Candida sp.* [26, 44].

Using lowest possible glucose feed rate of 0.4 g/h a loss of around 30% of oleic acid to LBs formation seems to be unavoidable. During the biotransformation phase the glucose feed was interrupted assuming LBs and TAGs degradation and usage of released glycerol as a carbon source. The degradation of TAGs would also lead to release of oleic acid, which could be easily monitored by GC/FID. However, neither increase of oleic acid nor of *cis*-ODA levels could be detected. As an option, Kohlwein *et al.* suggested the degradation of TAGs by transferring the cells into the fresh media containing glucose [31]. More promising approach, however, includes prevention strategies of LB formation. An efficient production of DCA could be achieved by application of alternative carbon sources, such as glycerol or sucrose. Also, using genetic engineering tools, *C. tropicalis* strain could be further modified towards enhanced fatty acid biotransformation. As proposed earlier, a knockout of the major regulator of TAG synthesis, phosphohydrolase, can reduce TAG production up to 70% [31]. Also, deletion of the *Faa1p* gene, encoding long-chain acyl-CoA synthetase (ACS), can enable drastic reduction of lipid accumulation, as described for *Y. lipolytica* [58].

4.4.1.1 LBs formation in dependency on substrate

The assumed glucose-mediated formation of LBs raised a reasonable question: Why does a comparably high glucose feed rate of 1.0 g/h during DAME biotransformation not interfere with the conversion process? As the major source of essential TAG precursors, the fatty acid itself has a great influence on production of LBs. Prior to the incorporation of fatty acids into TAGs, they are activated to acyl-CoAs catalysed by ACS (EC 6.2.1.3) [31]. Obviously, activation of DAME is hindered by its methyl group disabling subsequent formation of TAGs. Surprisingly, the demethylated intermediate DA was also not incorporated into TAGs (3.3.3.3). As shown by Froissard *et al.*, medium-chain fatty acids (MCFAs) in general are rarely incorporated into the LBs accounting for only 0.5% of total FA content of the LBs [132]. On the other hand, oleic acid being a long-chain fatty acid (LCFA) was described to be the major component of LBs [31]. Interestingly, the activation of the oleic acid in the cytosol is catalysed by a long-chain ACS, the only cytosolic ACS, which is strongly induced by oleate [58]. Thus, constrained activation of oleic acid in the cytosol to acyl-CoA in combination with the high glucose feed rate favoured enhanced TAGs formation (Figure 4-2). Also, the facilitated oleic acid solubility as enabled by reduced pH shift could enhanced their incorporation into the LBs. There are several researches describing transport mechanism of the fatty acids by free diffusion through the membrane [28, 56, 57]. Therefore, an increased oleic acid solubility in the medium could result in an increased passive diffusion of oleic acid into the cell. Since, application of high glucose feed rate obviously leads to the partial inhibition of ω -oxidation, oleic acid content within the cell would increase. Thus, the disability of utilization of FFA through the ω -oxidation seems to be compensated by the activation of oleic acid to acyl-CoAs and incorporation into TAGs for subsequent storage in LBs.

An interesting correlation between the fatty acids chain and their ability to be stored in LBs can be expanded to the subject on their toxicity. Elevated levels of free fatty acids within the cell are known to induce lipotoxicity [31, 60]. The oleaginous yeasts are able to control FFA flux by several pathways: ω -oxidation, β -oxidation and obviously TAGs formation (Figure 4-2). Using *C. tropicalis* ATCC 20962 strain the β -oxidation can be excluded from the regulation of the FFA concentration. So, in case of oleic acid

biotransformation, yeast cells are left with two possibilities to either metabolize fatty acids by ω -oxidation or incorporate them into LBs. Solely, the cytosolic activation of oleic acid enabled by long-chain ACS may also function as a viable means of detoxification. Combining all these possibilities, oleic acid is utilized rapidly. And thus, the viability of *C. tropicalis* seems to be not affected by this fatty acid. On the other hand, neither DAME nor DA can be stored in LBs, thus ω -oxidation remains the only possibility to control the fatty acid concentration within the cell. Transportation of the DA into the medium, as observed during DAME biotransformation, can also be interpreted as an attempt to regulate the FFA concentration within the cell. Given only one possibility to be utilized, DAME and DA strongly affect cell viability. Kabara *et al.* also illustrated antifungal properties of DA [81, 82]. DAME, on the other hand, seems to be less toxic than DA, but still negatively affects the biological activity [133].

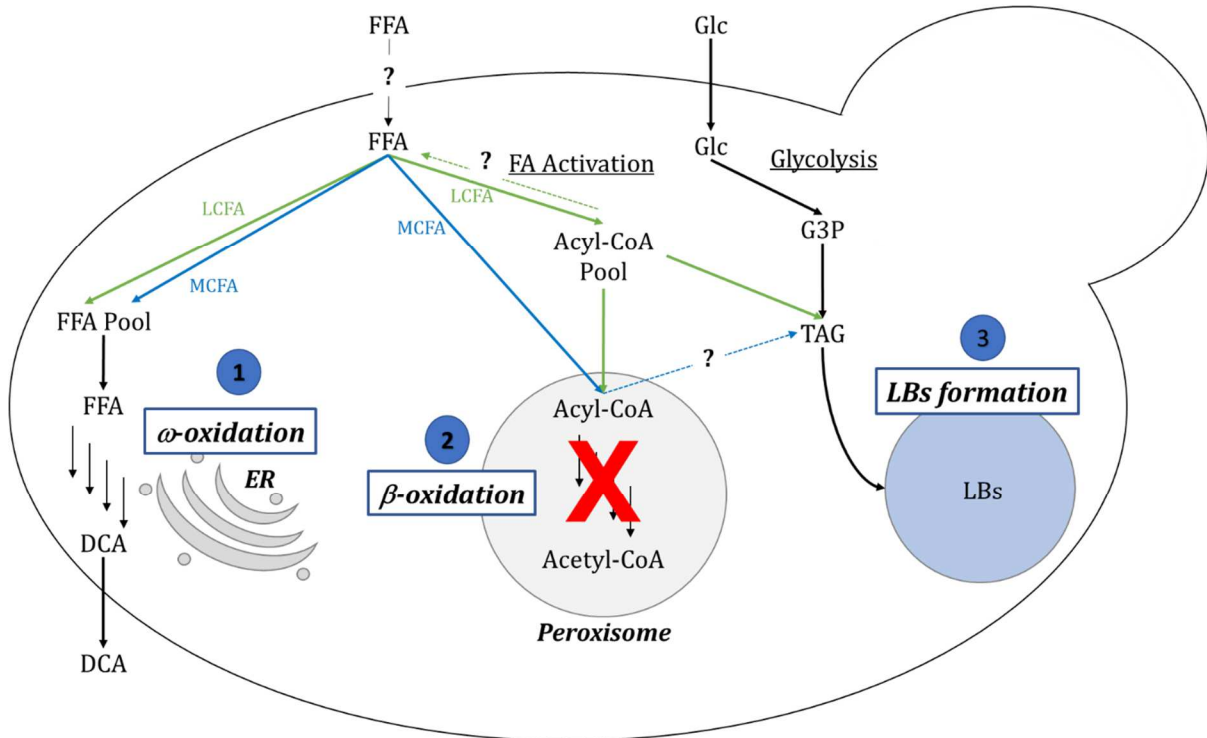


Figure 4-2: Proposed pathway of ω -oxidation and LB formation in dependency on the fatty acids chain-length in *C. tropicalis*

The transport mechanism of fatty acid still remains poorly understood and differs greatly among the yeast species [58]. *S. cerevisiae* is described to transport the fatty acids into the cell by simultaneously activation them to acyl-CoAs [58-61]. Meanwhile the oleaginous yeast, *Y. lipolytica*, activate the fatty acids first after their transport, however exact transport pathway remains unclear [58, 59]. After entering the cell FFA can be further metabolized by ω -oxidation (1), which requires free FA for the further conversion to DCA in ER [134]. β -oxidation (2) instead requires application of activated FAs, acyl-CoAs. The activation of FAs depends on its chain-length: LCFAs are activated in cytosol, whereas MCFA are activated by entering the peroxisome for further β -oxidation [31, 58, 111]. As LCFA are activated to acyl-CoA, further formation to TAGs with subsequent storage in LBs can be initiated (3) and will be favoured by high glucose concentration.

FFA - free fatty acid, **MCFA** - medium-chain fatty acid, **LCFA** - long-chain fatty acid, **DCA** - dicarboxylic fatty acid, **Glc** - glucose, **G3P** - glycerol-3-phosphate

4.4.2 Substrate feed

Application of highly hydrophobic substrates possessing antifungal properties requires special attention. Depending on the individual characteristics of each fatty acid, suitable substrate feed strategies were developed.

From the beginning on, DAME feed accounted to be the most important parameter of the production process. An investigation of the feed strategy revealed low DAME feed at 0.5 g/(L·h) during the major pH shift with subsequently slightly increase to 0.9 g/(L·h) to be the optimal variant (Table 3-3, Run A). Nonetheless, the application of this feed strategy led eventually to the accumulation of DAME and DA (Figure 3-6). To prevent substrate accumulation and its negative impact on the cell viability and biotransformation efficiency the feed strategy should be modified further. As a possible approach, DAME feed can be initiated at slightly higher feed of 1.2 g/(L·h), which showed full conversion at the beginning of the process. Knowing the approximate timing of the accumulation, the feed strategy can be performed by repeated start/stop cycles. This approach can enable long-term biotransformation process reducing set-up time and thus, the process costs. However, possible DAME and DA accumulations must be monitored. In this work, frequent sampling and analysis using TLC was performed. To assure an automated process, the regulation of the DAME feed can be triggered to other parameters, which can be correlated with substrate accumulation. Unfortunately, none of the on-line measured parameters in this study showed any distinct correlation with the DAME accumulation. Thus, the manual sampling with subsequent monitoring by TLC remains the only possibility to monitor fatty acid biotransformation.

Application of fatty acids methyl ester as a substrate led to efficient biotransformation to corresponding DDA highlighting the ability of the *C. tropicalis* to demethylate the substrate. Detection of DA, but not the methylated products of dicarboxylic acid, confirms demethylation of DAME prior to conversion to DDA. Biotransformation of DAME to DA, for example by carboxyl methyl esterase [135], would lead to production of methanol, which can be further metabolized to water and CO₂ [136]. Thus, demethylation of DAME seems to explain enhanced CO₂ formation in comparison to control bioreactor (Figure 4-3).

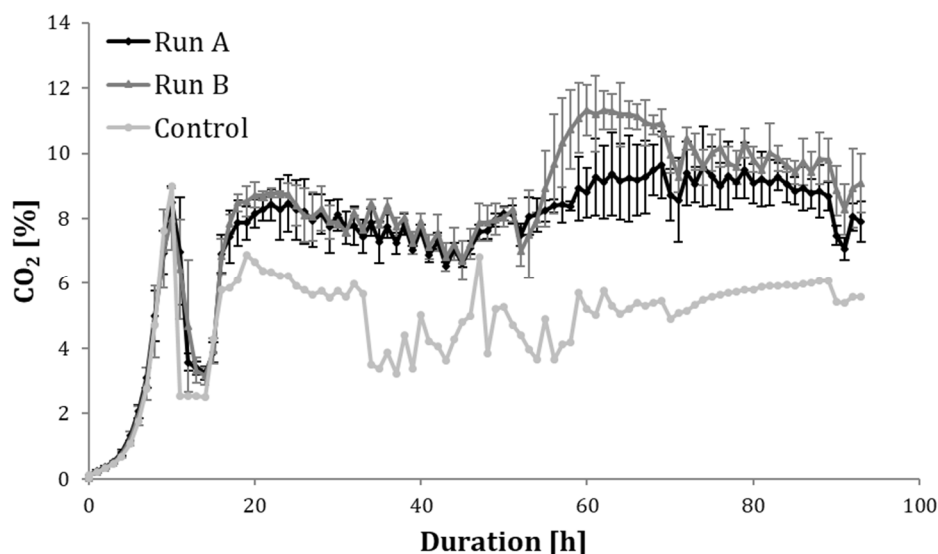


Figure 4-3: Comparison of CO₂ in exhaust gas in dependency on DAME feed in comparison to control bioreactor

CO₂ in exhaust gas as monitored for various DAME feed strategies. Constant DAME feed of 0.5 g/(L·h) was applied during the first 45 h followed by increase until 0.9 g/(L·h) for run A and 1.2 g/(L·h) for run B, which were subsequently held. Control: no DAME feed. The experiments were performed in duplicate using DASGIP 8x1L parallel bioreactor system as described in methods. The error bars represent the standard deviations.

Application of oleic acid for the biotransformation process did not require implementation of a complex feed strategy, as in the case of DAME conversion. At the beginning, oleic acid feed rate was set for 1 g/(L·h) and other parameters, which were highly essential for the process, such as pH shift or glucose feed, were investigated. However, the awareness of the incorporation of oleic acid into LBs led to decision to investigate the feed strategy in more detail. As described above, TAGs synthesis is activated by the availability of both precursors, glucose and oleic acid. Thus, decreasing the overall oleic acid concentration, its excess for LBs production was expected to be reduced leading to a higher biotransformation rate. Contrarily, the low oleic acid feed rate of 0.3 g/(L·h) applied at the constant glucose feed rate of 0.4 g/h resulted in surprisingly low product yield of 10%. Full conversion of oleic acid indicated LBs production. Further increase of the substrate feed led to an enhanced product yield (Figure 3-29). This observation allows to assume that oleic acid induction of the ω -oxidation can be competitive with the glucose-mediated suppression of this pathway.

As glucose supply was constant during the biotransformation phase, increasing the oleic acid feed rate resulted in decrease of the ratio of the glucose to oleic acid (C/S) and subsequently in enhanced *cis*-ODA production. Thus, a certain molar C/S ratio seems to be required to initiate formation of LBs. Since, reducing glucose feed rate below 0.4 g/h led to immediate loss of cell viability, the lowest possible molar ratio of 1.5 could be achieved in this study. Further increase oleic acid feed rate and its influence on the biotransformation and LBs formation will be an interesting attempt. However, the increase must be performed carefully, since poorly water-soluble oleic acid can precipitate leading to less efficient biotransformation process.

4.5 Monitoring biotransformation at transcriptional level

The transcriptional level of the genes encoding for enzymes of the first and rate-limiting step of the ω -oxidation pathway, *CYP52A13/14*, *CYP52A17/18* and *CPR* (Figure 1-2), was monitored during DAME and oleic acid biotransformation by RT-qPCR.

As an essential part of the RT-qPCR, normalization of the obtained data to reference genes is necessary for identification of the real gene-specific variation [65, 92, 137]. Being involved in the maintenance of the basic cellular functions, housekeeping genes represent excellent reference genes due to their stable expression across the samples. Several housekeeping genes were selected and analyzed for the ability to be reference genes: *GAPDH*, *ACT1*, *PGK1* and *PMA1*. Interestingly, *PMA1*, encoding H⁺-ATPase involved in pHi homeostasis, was found to vary strongly during the production process. Obviously, the application of a pH shift during DCA production led to an increased external pH and thus, might have partially disrupted the transport of protons by H⁺-ATPase [123, 138]. The pHi homeostasis and uptake of nutrients can be regulated by overexpression of *PMA1* resulting in unstable expression levels. Also *S. cerevisiae* was described to upregulate *ENA1*, encoding ATPase, as a response to alkaline pH stress [102]. Thus, being strongly dependent on the operational conditions *PMA1* is not classified as a reference gene. Several studies in the past also reported on the unstable expression of various housekeeping genes considerably and strongly depending on the experimental conditions [65, 139-141]. Obviously, robust and accurate RNA level profiling requires

multiple control genes for the normalization of gene expression. Thus, *GAPDH* and *ACT1* were found to be the most stable genes expressed by *C. tropicalis* during the DDA production process (Table 3-8). The stability of these two reference genes was also assured during oleic acid biotransformation.

Not just the expression of a potential reference gene *PMA1* was found to respond to an alkaline stress, also transcriptional level of *CPR* drastically decreased during the pH shift (Figure 3-11). Since NADPH reductase plays an essential role in the fatty acid and alkanes biotransformation [40], its limitation was assumed to be the main reason of the reduced DAME conversion (Figure 3-12). As applied for oleic acid biotransformation, the reduction of pH shift could minimize the negative effect on the *CPR* expression (Figure 3-26). Interestingly, the application of pH shift in the growth phase for DDA production, did not lead to expected facilitated productivity. Obviously, pH shift during DAME biotransformation has a great influence on the DDA production process (Table 4-2) confirming the optimal combination of the DAME feed and pH shift (Figure 3-3).

The conversion of fatty acids is enabled by efficient interaction of cytochrome P450 and reductase. Several studies reported 10- to 20-fold lower abundance of CPR in comparison to P450 enzymes. Based on these findings, researchers proposed clustering of P450 monooxygenases around the reductases in ER [142, 143]. Interestingly, the *CYP52A* genes in this study showed up to 30-fold higher expression in comparison to *CPR* (Figure 3-11, Figure 3-26). As low gene expression will consequently lead to moderate enzyme production, the obtained results confirm the clustering theory of previous studies. Being a minority CPR plays a crucial role in the conversion process. As observed by Picataggio *et al.*, the overexpression of *CYP52A* did not have any significant influence on the production process, whereas the *CPR* overexpression resulted in drastic increase in DCA productivity [40].

The induction pattern of the *CYP52A13/14* and *CYP52A17/18* differed greatly along the production processes. During DAME biotransformation, the expression level of *CYP52A13/14* was distinctly higher compared to *CYP52A17/18* (Figure 3-11). Meanwhile, the application of oleic acid as a substrate showed contrary transcriptional profile of the *CYP52A* genes. Obviously, oleic acid induced *CYP52A17/18* more strongly than

CYP52A13/14 (Figure 3-26). Interestingly, Craft *et al.* showed a slightly different induction pattern of both alleles by oleic acid [64], which is similar to the transcriptional profiles observed during DAME biotransformation. Oleic acid applied in this study was of technical grade and thus contained several other fatty acids (3.3.1), which could have influenced the induction pattern. In comparison to fatty acids, alkanes were found to induce the *CYP52A* genes strongly [64]. This valuable observation might explain the higher product concentration obtained for the processes using alkanes as substrates (Table 1-1). Thus, occasionally supply of alkanes of the same chain length during the biotransformation to support distinct transcriptional level of *CYP52A* genes could lead to a higher DCA productivity.

4.6 Purification of *cis*-ODA

The downstream process in the lab scale was successfully applied for the purification of *cis*-ODA, which was further used an appropriate analytical standard for GC/FID analysis. The separation of the product from the aqueous phase was performed simply by altering of the pH towards acidic conditions, leading immediately to the precipitation of the product. This observation highlights the importance of the pH shift to enable the solubility of the DCAs yet again. Subsequent purification using hot-filtration recrystallization resulted in *cis*-ODA with a purity of 94% (Figure 3-31). This approach is rather laborious and can be applied for purification of the product at low amounts. An efficient downstream process at industrial scale, however, requires the use of an alternative technique. Earlier, Körner *et al.* proposed a continuous purification of *cis*-ODA with up to 95% (w/w) purity using a distillation facility [144]. The authors did not describe the capacity of the equipment, nonetheless, due to the application of the continuous mode certainly high amounts of the *cis*-ODA can be processed.

cis-ODA obtained in this study was further analyzed by several analytical methods (3.3.4). Also, analysis of the *trans* stereoisomer was gained to enable a direct comparison. The GC/MS data revealed similar fragmentation pattern of both stereoisomers indicating identical structure. Different retention times, however, caused by different interaction of the molecules with the stationary phase emphasizes the difference in the orientation of

the double bond. Also, the analysis of the melting temperature underlined the orientation of the double bonds. Since *cis* orientation is less stable, it was expected to melt at a rather lower temperature when compared to the *trans* isoform. Indeed, the melting point of *cis*-ODA at 70.2°C is clearly lower than the melting temperature of *trans*-ODA at 99.5°C. Similarly, Pardal *et al.* applied the determination of the melting point to distinguish between these two stereoisomers and obtained comparable results, 66°C for *cis*-ODA and 99°C for *trans*-ODA [25]. In addition, NMR analysis, as a part of the corporate project with Chair of Organic and Analytical Chemistry (University of Applied Science Weihenstephan-Triesdorf), underlined the position of the double bond to be in *cis* configuration [145] (refer also to 7.6).

4.7 Comparison of DDA and *cis*-ODA production processes

The optimization of the DDA production process revealed the implementation of pH shift at the beginning of the biotransformation phase with the combination of an increased DAME feed until 0.9 g/(L·h) and operation at 30°C to be most advantageous for the process. Applying optimal conditions, the final DDA titer of 65.9 ± 3.1 g/L and a final volumetric productivity of 0.35 ± 0.02 g/(L·h) were reached, which is almost 1.5 higher compared to initial process at constant pH of 5.8 and constant DAME feed of 0.5 g/(L·h). Along with other studies published on the production of DDA (Table 1-1), the final concentration obtained in this study seems to be rather low. However, the approaches described until now rely on the conversion of petroleum-derived *n*-dodecane, application of DAME for DDA production was described for the first time in this study [100]. Using *C. tropicalis* Liu *et al.* showed the production of DDA from *n*-dodecane with a final titer of 166 g/L [47]. Also using the recently isolated *C. viswanathii* ipe-1 strain, an efficient DDA production process resulting in 181.6 g/L was described [48]. Interestingly, both research groups applied NaOH titration for the determination of the DDA concentration [47, 48]. Thus, the reported concentrations refer to the total DCAs concentration, regardless of carbon chain-length. Obviously, this method is less sensitive than the GC/FID method used in this study, which allows precise and accurate measurements of the substrate and product. Moreover, some of the studies reported the final concentration calculated based on the initial volume [40, 146], or in case of a two

phase system, based on the volume of the aqueous phase [48]. Due to the pH shift and the fed-batch mode in combination with a prolonged duration of the process, the volume of the cell broth at the end showed more than a two-fold increase compared to the initial volume. Thus, the amounts calculated on the initial volume yields a final DDA concentration is 162 g/L (Table 4-3), which is comparable to the other reported values. However, from a bioprocess engineering point of view the final concentration of the product, as well as the corresponding final volume are highly important, since both affect the bioreactor scale as well as the scale of downstream processing.

Table 4-3: Comparison of the DAME and oleic acid biotransformation processes

| Product | Cell biomass [g/L] | Final product concentration [g/L] | Final product concentration based on initial volume [g/L] | Volumetric productivity [g/(L·h)] | Specific productivity [mg _{product} /(g _{biomass} ·h)] |
|-------------------|--------------------|-----------------------------------|---|-----------------------------------|--|
| DDA* | 26.5 ± 2.3 | 65.9 ± 3.1 | 162.3 ± 5.5 | 0.35 ± 0.02 | 13.36 ± 1.87 |
| <i>cis</i> -ODA** | 39.7 ± 2.7 | 49.6 ± 3.4 | 74.7 ± 8.0 | 0.58 ± 0.04 | 14.80 ± 1.73 |

*Duration 188 h, final volume 740 mL, initial volume 300 mL, sample size: n=4

**Duration 85 h, final volume 400 mL, initial volume 270 mL, sample size: n=3

The optimal process conditions of oleic acid biotransformation differed greatly from the DDA production process. A reduced pH shift in the growth phase and low glucose feed consequently enabled efficient biotransformation of oleic acid. Applying a constant glucose feed of 0.4 g/h and oleic acid feed of 1 g/(L·h) a final concentration of 49.6 ± 3.4 g/L was achieved. Final volumetric productivity of 0.58 ± 0.04 g/(L·h) as obtained in this study was found to be higher than the values described so far in the literature for *C. tropicalis* ATCC 20962 (Table 1-1). Nevertheless, using *C. tropicalis* AR40, with an amplified monooxygenase and an associated reductase, Piccatagio *et al.* was able to achieve a volumetric productivity of 1.5 g/(L·h) [40].

Despite the great difference in the optimal operating conditions (Table 4-4), the production process of DDA and *cis*-ODA showed a similar specific productivity. 1 g of yeast cells was able to produce around 14 mg of either DDA or *cis*-ODA within one hour

(Table 4-3). The great difference in the final product concentration was caused by the different duration of the biotransformation.

Table 4-4: Comparison of the optimal operational conditions for DDA and *cis*-ODA production

| Product | pH shift | | Substrate feed | Glucose feed |
|-----------------|-------------------------|----------|---|--------------|
| | start | duration | | |
| DDA | Biotransformation phase | 45 h* | Constant 0.5 g/(L·h) After 45h increasing until 0.9 g/(L·h) Constant at 0.9 g/(L·h) | 1 g/h |
| <i>cis</i> -ODA | Growth phase | 6 h | 1 g/(L·h) | 0.4 g/h |

*pH was gradually increased from 5.8 to 7.7 until 45 h, followed by a reduced rate of increase up to pH 8.0 within the next 45 h.

5 Outlook

A lab-scale biotransformation platform was successfully applied for the evaluation, characterization, and optimization of DCA production process using DAME and oleic acid as substrates. Regulation and control of the production process at this scale is highly complex. To assure suitability and feasibility of the process including a pH shift and specific feeding strategies for industrial application, performance of a scale-up approach is an essential point. Limited mass transfer and marginal homogeneity would represent the main obstacles of application at a large scale. Also, the solubility of fatty acids can be assumed to be the major limitation, especially when oleic acid is used. To maintain the solubility of fatty acids and enable an efficient DCA production the substrate feed strategy should be properly adopted for large-scale production.

Application of *C. tropicalis*, as a potential pathogen, in industrial scale is undesirable. Several alternative production routes have been studied by various research groups. Non-pathogenic microorganisms, such as *E. coli* can be used to produce DCAs or related products. *E. coli* featuring a monooxygenase system has been used for the production of hydroxy-fatty acids, which are also valuable intermediates in the polymer industry. Until now only marginal product levels could be achieved, mostly due to by-product formation [133]. Furthermore, the uptake of fatty acids and subsequent export of the product still represents a critical issue applying *E. coli* [133]. To overcome limitations caused by poor fatty acids transport, *Y. lipolytica* also as a non-pathogenic yeast, can be applied for DCA production [147]. Nonetheless, *Y. lipolytica* is a common oleaginous yeast strain used for the production of microbial oils [130, 148, 149] and thus, undesired LBs accumulation pathway has to be eliminated. Application of the whole-cell biocatalysts, in general, comes with several drawbacks, such as the occurrence of unwanted side-pathways and by-products. These issues can be overcome by using cell-free ω -oxidation by CYP52 enzymes. So, Scheller *et al.* demonstrated a conversion cascade of hexadecane to corresponding DCA by purified CYP52A3 enzyme. Despite low concentration of the produced DCA, the overoxidation of fatty acids represents a promising cell free DCA production method [150]. Unfortunately, purification of

membrane-bound CYP52 enzymes faces several limitations such as low enzyme stability and poor yield hindering cell-free industrial production of DCAs. Thus, *C. tropicalis* remains until now the best possibility of sustainable and efficient fatty acids biotransformation to corresponding DCAs.

6 References

1. Andrady, A.L. and M.A. Neal, *Applications and societal benefits of plastics*. Philos. Trans. R. Soc. Lond., B, Biol. Sci., 2009. **364**(1526): p. 1977-1984.
2. Dake, M., *Biodegradable polymers: Renewable nature, life cycle, and applications*, in *Microbial Factories*, V.C. Kalia, Editor. 2015, Springer India.
3. PlasticsEurope, *Plastics – the Facts 2016*. The special presentation is organised jointly by Messe Düsseldorf and PlasticsEurope Deutschland e.V., 2016.
4. Sabbah, M. and R. Porta, *Plastic pollution and the challenge of bioplastics*. J. Appl. Biotechnol. Bioeng., 2017. **2**(3): p. 00033.
5. Sheldon, R.A., *Green and sustainable manufacture of chemicals from biomass: State of the art*. Green Chem., 2014. **16**(3): p. 950-963.
6. Sillanpää, M. and C. Ncibi, *A sustainable bioeconomy, The green industrial revolution*. 2017: Springer International Publishing. XI, 343.
7. Birner, R., *Bioeconomy Concepts*, in *Bioeconomy: Shaping the transition to a sustainable, biobased economy*, I. Lewandowski, Editor. 2018, Springer International Publishing: Cham. p. 17-38.
8. McCormick, K. and N. Kautto, *The bioeconomy in Europe: An overview*. Sustainability, 2013. **5**(6): p. 2589.
9. Presidency, G., *En route to the knowledge-based bio-economy*. German Presidency of the Council of the European Union: Cologne, Germany, 2007.
10. BÖR, *Bioeconomy policies and strategies established by 2017*, in *Bioökonomierat – BÖR, Berlin*. 2017.
11. Bardi, U., *Peak oil: The four stages of a new idea*. Energy, 2009. **34**(3): p. 323-326.
12. Carus, M., *Sustainable biomass potential for food, feed, bio-based materials, bioenergy and biofuels* ESPOO, nova-Institut GmbH, 2017.
13. Scarlat, N., et al., *The role of biomass and bioenergy in a future bioeconomy: Policies and facts*. Environ. Development, 2015. **15**: p. 3-34.
14. Bugnicourt, E., et al., *Polyhydroxyalkanoate (PHA): Review of synthesis, characteristics, processing and potential applications in packaging*. eXPRESS Polymer Letters 2014. **8**(11): p. 791-808.
15. Slater, S., et al., *Evaluating the environmental impact of biopolymers*, in *Biopolymers Online*. 2005, Wiley-VCH Verlag GmbH & Co. KGaA.
16. Schaffer, S. and T. Haas, *Biocatalytic and fermentative production of α,ω -bifunctional polymer precursors*. Org. Process. Res. Dev., 2014. **18**(6): p. 752-766.
17. Loeffler, M. and J. Hinrichs, *Processing of biobased resources*, in *Bioeconomy: Shaping the Transition to a Sustainable, Biobased Economy*, I. Lewandowski, Editor. 2018, Springer International Publishing: Cham. p. 177-228.
18. Shin, J., et al., *Characterization of a whole-cell biotransformation using a constitutive lysine decarboxylase from Escherichia coli for the high-level production of cadaverine from industrial grade l-lysine*. Appl. Biochem. Biotechnol., 2018. **185**(4): p. 909-924.
19. Roth, S., et al., *Chemoenzymatic synthesis of a novel borneol-based polyester*. Chem. Sus. Chem., 2017. **10**(18): p. 3574-3580.

20. Polen, T., M. Spelberg, and M. Bott, *Toward biotechnological production of adipic acid and precursors from biorenewables*. J. Biotechnol., 2013. **167**(2): p. 75-84.
21. Guzman, D.D., *Bio-adipic acid prepares for entry*. ICIS Chemical Business, 2010.
22. Beardslee, T. and S. Picataggio, *Bio-based adipic acid from renewable oils*. Lipid Technol., 2012. **24**(10): p. 223-225.
23. Ngo, H.L., K. Jones, and T.A. Foglia, *Metathesis of unsaturated fatty acids: Synthesis of long-chain unsaturated- α,ω -dicarboxylic acid*. J. Am. Oil Chem. Soc., 2006. **83**(7): p. 629-634.
24. Elmkaddem, M.K., et al., *Ultrasound-assisted self-metathesis reactions of monounsaturated fatty acids*. OCL, 2016. **23**(5): p. D507.
25. Pardal, F., et al., *Unsaturated polyamides from bio-based Z-octadec-9-enedioic acid*. Macromol. Chem. Phys., 2008. **209**(1): p. 64-74.
26. Huf, S., et al., *Biotechnological synthesis of long-chain dicarboxylic acids as building blocks for polymers*. Eur. J. Lipid. Sci. Tech., 2011. **113**(5): p. 548-561.
27. Cheng, Q., et al., *Candida yeast long chain fatty alcohol oxidase is a c-type haemoprotein and plays an important role in long chain fatty acid metabolism*. Biochim. Biophys. Acta, 2005. **1735**(3): p. 192-203.
28. Werner, N. and S. Zibek, *Biotechnological production of bio-based long-chain dicarboxylic acids with oleogenic yeasts*. World J. Microbiol. Biotechnol., 2017. **33**(194).
29. Shiio, I. and R. Uchio, *Microbial production of long-chain dicarboxylic acids from n-alkanes. Part I: Screening and properties of microorganisms producing dicarboxylic acids*. Agric. Biol. Chem., 1971. **35**(13): p. 2033-2042.
30. Uchio, R. and I. Shiio, *Microbial production of long-chain dicarboxylic acids from n-alkanes. Part II: Production by Candida cloacae mutant unable to assimilate dicarboxylic acid*. Agric. Biol. Chem., 1972. **36**(3): p. 426-433.
31. Kohlwein, S.D., M. Veenhuis, and I.J. van der Klei, *Lipid droplets and peroxisomes: key players in cellular lipid homeostasis or a matter of fat-store 'em up or burn 'em down*. Genetics, 2013. **193**(1): p. 1-50.
32. Yi, Z.-H. and H.-J. Rehm, *Metabolic formation of dodecanedioic acid from n-dodecane by a mutant of Candida tropicalis*. European J. Appl. Microbiol. Biotechnol., 1982. **14**: p. 254-258.
33. Yi, Z.-H. and H.-J. Rehm, *Formation of α,ω -dodecanedioic acid and α,ω -tridecanedioic acid from different substrates by immobilized cells of a mutant of Candida tropicalis*. European J. Appl. Microbiol. Biotechnol., 1982. **16**: p. 1-4.
34. Yi, Z.-H. and H.-J. Rehm, *Formation and degradation of Δ^9 -1,18-octadecenedioic acid from oleic acid by Candida tropicalis*. Appl. Microbiol. Biotechnol., 1988. **28**: p. 520-526.
35. Yi, Z.-H. and H.-J. Rehm, *Identification and production of Δ^9 -cis-1,18-octadecenedioic acid by Candida tropicalis*. Appl. Microbiol. Biotechnol., 1989. **30**: p. 327-331.
36. Yi, Z.-H. and H.-J. Rehm, *Bioconversion of elaidic acid to Δ^9 -trans-1,18-octadecenedioic acid by Candida tropicalis*. Appl. Microbiol. Biotechnol., 1988. **29**: p. 305-309.

37. Fabritius, D., H.J. Schäfer, and A. Steinbüchel, *Biotransformation of linoleic acid with the Candida tropicalis M25 mutant*. Appl. Microbiol. Biotechnol., 1997. **48**(1): p. 83-87.
38. Fabritius, D., H.J. Schäfer, and A. Steinbüchel, *Bioconversion of sunflower oil, rapeseed oil and ricinoleic acid by Candida tropicalis M25*. Appl. Microbiol. Biotechnol., 1998. **50**(5): p. 573-578.
39. Fabritius, D., H.J. Schäfer, and A. Steinbüchel, *Identification and production of 3-hydroxy- Δ^9 -cis-1,18-octadecenedioic acid by mutants of Candida tropicalis*. Appl. Microbiol. Biotechnol., 1996. **45**(3): p. 342-348.
40. Picataggio, S., et al., *Metabolic engineering of Candida tropicalis for the production of long-chain dicarboxylic acids*. Nat. Biotechnol., 1992. **10**(8): p. 894-8.
41. Mishra, P., et al., *Genome-scale metabolic modeling and in silico analysis of lipid accumulating yeast Candida tropicalis for dicarboxylic acid production*. Biotechnol. Bioeng., 2016. **113**(9): p. 1993-2004.
42. Hill, F.F., I. Venn, and K.L. Lukas, *Studies on the formation of long-chain dicarboxylic acids from puren-alkanes by a mutant of Candida tropicalis*. Appl. Microbiol. Biotechnol., 1986. **24**(2): p. 168-174.
43. Zibek, S., et al., *Fermentative Herstellung der α,ω -Dicarbonsäure 1,18-Oktadecendisäure als Grundbaustein für biobasierte Kunststoffe*. Chem. Ing. Tech., 2009. **81**(11): p. 1797-1808.
44. Green, K.D., M.K. Turner, and J.M. Woodley, *Candida cloacae oxidation of long-chain fatty acids to dioic acids*. Enzyme Microb. Technol., 2000. **27**(3-5): p. 205-211.
45. Yang, Y., et al., *Two-step biocatalytic route to biobased functional polyesters from ω -carboxy fatty acids and diols*. Biomacromolecules, 2010. **11**(1): p. 259-268.
46. Gangopadhyay, S., S. Nandi, and S. Ghosh, *Biooxidation of fatty acid distillates to dibasic acids by a mutant of Candida tropicalis*. J. Oleo Sci., 2006. **56**(1): p. 13-17.
47. Liu, S., et al., *Optimal pH control strategy for high-level production of long-chain α,ω -dicarboxylic acid by Candida tropicalis*. Enzyme Microb. Technol., 2004. **34**(1): p. 73-77.
48. Cao, W., et al., *High-level productivity of α,ω -dodecanedioic acid with a newly isolated Candida viswanathii strain*. J. Ind. Microbiol. Biotechnol., 2017. **44**(8): p. 1191-1202.
49. Liu, S., et al., *Intracellular pH and metabolic activity of long-chain dicarboxylic acid-producing yeast Candida tropicalis*. J. Biosci. Bioeng., 2003. **96**(4): p. 349-53.
50. Broach, J.R., *Nutritional control of growth and development in yeast*. Genetics, 2012. **192**(1): p. 73-105.
51. Pfeiffer, T. and A. Morley, *An evolutionary perspective on the Crabtree effect*. Front. Mol. Biosci., 2014. **1**(17): p. 17.
52. Mauersberger, S., W.-H. Schunck, and H.-H. Müller, *The induction of cytochrome P-450 in Lodderomyces elongisporus*. Z. Allg. Mikrobiol., 1981. **21**(4): p. 313-321.
53. Seghezzi, W., et al., *Identification and characterization of additional members of the cytochrome P450 multigene family CYP52 of Candida tropicalis*. DNA Cell Biol., 1992. **11**(10): p. 767-780.
54. Cao, Z., et al., *Engineering the acetyl-CoA transportation system of Candida tropicalis enhances the production of dicarboxylic acid*. Biotechnol. J., 2006. **1**(1): p. 68-74.

55. Sagehashi, Y., et al., *Identification and characterization of a gene encoding an ABC transporter expressed in the dicarboxylic acid-producing yeast Candida maltosa*. Biosci. Biotechnol. Biochem., 2013. **77**(12): p. 2502-2504.
56. Kamp, F., et al., *Rapid flip-flop of oleic acid across the plasma membrane of adipocytes*. J. Biol. Chem., 2003. **278**(10): p. 7988-95.
57. Nakagawa, T., et al., *Peroxisomal membrane protein Pmp47 is essential in the metabolism of middle-chain fatty acid in yeast peroxisomes and is associated with peroxisome proliferation*. J. Appl. Biol. Chem., 2000. **275**(5): p. 3455-3461.
58. Dulermo, R., et al., *Unraveling fatty acid transport and activation mechanisms in Yarrowia lipolytica*. Biochim. Biophys. Acta, 2015. **1851**(9): p. 1202-1217.
59. Dulermo, R., et al., *The fatty acid transport protein Fat1p is involved in the export of fatty acids from lipid bodies in Yarrowia lipolytica*. FEMS Yeast Res., 2014. **14**(6): p. 883-896.
60. Black, P.N. and C.C. DiRusso, *Yeast acyl-CoA synthetases at the crossroads of fatty acid metabolism and regulation*. Biochim. Biophys. Acta, 2006. **1771**(3): p. 286-98.
61. Zou, Z., et al., *Fatty acid transport in Saccharomyces cerevisiae: directed mutagenesis of FAT1 distinguishes the biochemical activities associated with Fat1p*. J. of Biol. Chem., 2002. **277**(34): p. 31062-31071.
62. Seghezzi, W., D. Sanglard, and A. Fiechter, *Characterization of a second alkane-inducible cytochrome P450-encoding gene, CYP52A2, from Candida tropicalis*. Gene, 1991. **106**(1): p. 51-60.
63. Schulze, A. and J. Downward, *Navigating gene expression using microarrays - a technology review*. Nat. Cell. Biol., 2001. **3**(8): p. E190-E195.
64. Craft, D.L., et al., *Identification and characterization of the CYP52 family of Candida tropicalis ATCC 20336, important for the conversion of fatty acids and alkanes to α,ω -dicarboxylic acids*. Appl. Environ. Microbiol. , 2003. **69**(10): p. 5983-5991.
65. Vandesompele, J., et al., *Accurate normalization of real-time quantitative RT-PCR data by geometric averaging of multiple internal control genes*. Genome Biol., 2002. **3 RESEARCH0034**(7): p. 1-12.
66. Eschenfeldt, W.H., et al., *Transformation of fatty acids catalyzed by cytochrome P450 monooxygenase enzymes of Candida tropicalis*. Appl. Environ. Microbiol., 2003. **69**(10): p. 5992-5999.
67. Jiao, P., et al., *Effects and mechanisms of H₂O₂ on production of dicarboxylic acid*. Biotechnol. Bioeng., 2001. **75**(4): p. 456-62.
68. Ogata, N. and Y. Hosoda, *Synthesis of hydrophilic polyamide by active polycondensation*. J. Polym. Sci. , 1974. **12**(6): p. 355-358.
69. Hough, M. and R. Dolbey, *The plastics compendium: Key properties and sources*. 1995: Rapra Technology, Billingham.
70. Andrade, J., K. Köhler, and G. Prescher, *Process for the manufacture of 1,12-dodecandioic acid EP0258535A2*, 1986.
71. Schaffer, S., et al., *Biotechnological synthesis process of omega-functionalized carbon acids and carbon acid esters from simple carbon sources*. EP2744897A2, 2011.
72. Tetzlaff, D., *Verdezyne signs agreement with major european chemicals distributor Will & Co*. Press release: Verdezyne, 2015.
73. Welton, D.E., *Process for production of 1,12-dodecanedioic acid US3907883A*, 1972.

74. Klein, D.A., *Process for purifying 1,12-dodecanedioic acid* US4149013A, 1978.
75. Evonik-Industries-AG, *Evonik startet Innovationsoffensive* Press release: Evonik Industries AG, 2013.
76. Evonik-Industries-AG, *Evonik stellt die Weichen bei Polyamid 12* Press release: Evonik Industries AG, 2014.
77. DuPont, *DuPont™ Zytel® Long Chain and Zytel® RS Long Chain*. Press release: DuPont, 2010.
78. Tetzlaff, D., *Verdezyne earns USDA certified biobased product certification and label*. Press release: Verdezyne, 2015.
79. Cathay-Industrial-Biotech, *Cathay Industrial Biotech Ltd. announces ground-breaking and agreement signing for significant expansion in bio-produced monomer and polyamide production*. Press release: Cathay Industrial Biotech Ltd., 2016.
80. Dayrit, F.M., *The properties of lauric acid and their significance in coconut oil*. J. Am. Oil Chem. Soc., 2014. **92**(1): p. 1-15.
81. Kabara, J.J., *Antimicrobial agents derived from fatty acids*. J. Am. Oil Chem. Soc., 1984. **61**(2): p. 397-403.
82. Kabara, J.J., et al., *Fatty acids and derivatives as antimicrobial agents*. Antimicrob. Agents Chemother. , 1972. **2**(1): p. 23-28.
83. Gervajio, G.C., *Fatty acids and derivatives from coconut oil*, in *Kirk-Othmer encyclopedia of chemical technology*. 2012.
84. Guzman, D.D., *Elevance sells C18 diacids*, in *Elevance sells C18 diacids*. 2013, Green Chemicals Blog.
85. Kroha, K., *Industrial biotechnology provides opportunities for commercial production of new long-chain dibasic acids*. Cover Feature E, Inform, 2004. **15**(9): p. 568-571.
86. BASF, *BASF completes acquisition of Cognis*. Press release: BASF, 2010.
87. Beuhler, A., et al., *Elevance makes ODDA a commercial reality*. Bioplastics magazine, 2013. **8**(05/13).
88. Mobley, D.P., *Biosynthesis of long-chain dicarboxylic acid monomers from renewable resources*. US Department of Energy Report, in *Other Information: PBD: 30 Apr 1999*. 1999.
89. Chirgwin, J.M., et al., *Isolation of biologically active ribonucleic acid from sources enriched in ribonuclease*. Biochemistry, 1979. **18**(24): p. 5294-5299.
90. Bligh, E.G. and W.J. Dyer, *A rapid method of total lipid extraction and purification*. Can. J. of Biochem. Phys., 1959. **37**(8): p. 911-917.
91. Ichihara, K. and Y. Fukubayashi, *Preparation of fatty acid methyl esters for gas-liquid chromatography*. J. Lipid Res., 2010. **51**(3): p. 635-40.
92. Bustin, S.A., et al., *The MIQE guidelines: minimum information for publication of quantitative real-time PCR experiments*. Clin. Chem., 2009. **55**(4): p. 611-22.
93. Taylor, S., et al., *A practical approach to RT-qPCR - Publishing data that confirms to the MIQE guidelines*. Bio-Rad Laboratories, 2011.
94. Life-Technologies, *Real-time PCR handbook*. 2012.
95. Delgado, M.L., et al., *The glyceraldehyde-3-phosphate dehydrogenase polypeptides encoded by the Saccharomyces cerevisiae TDH1, TDH2 and TDH3 genes are also cell wall proteins*. Microbiol., 2001. **147**(2): p. 411-417.

96. Waingeh, V.F., et al., *Glycolytic enzyme interactions with yeast and skeletal muscle F-actin*. Biophys. J., 2006. **90**(4): p. 1371-1384.
97. Goossens, A., et al., *Regulation of yeast H⁺-ATPase by protein kinases belonging to a family dedicated to activation of plasma membrane transporters*. Mol. Cell. Biol., 2000. **20**(20): p. 7654-7661.
98. Bernstein, B.E. and W.G.J. Hol, *Crystal structures of substrates and products bound to the phosphoglycerate kinase active site reveal the catalytic mechanism*. Biochemistry, 1998. **37**(13): p. 4429-4436.
99. Rimmel, N., *Selektive ω -Oxidation aliphatischer Substrate –Charakterisierung von Monoxygenasen und Etablierung einer Biotransformationsplattform*. 2016. **Ph.D. thesis, Technical University Munich**.
100. Funk, I., et al., *Production of dodecanedioic acid via biotransformation of low cost plant-oil derivatives using Candida tropicalis*. J. Ind. Microbiol. Biotechnol., 2017. **44**(10): p. 1491-1502.
101. Denison, S.H., *pH regulation of gene expression in fungi*. Fungal. Genet. Biol., 2000. **29**(2): p. 61-71.
102. Serrano, R., et al., *The transcriptional response to alkaline pH in Saccharomyces cerevisiae: Evidence for calcium-mediated signalling*. Mol. Microbiol., 2002. **46**(5): p. 1319-1333.
103. Klis, F.M., et al., *Dynamics of cell wall structure in Saccharomyces cerevisiae*. FEMS Microbiol. Rev., 2002. **26**(3): p. 239-256.
104. Scott, J.H. and R. Schekman, *Lyticase: endoglucanase and protease activities that act together in yeast cell lysis*. J. Bacteriol., 1980. **142**(2): p. 414-423.
105. Suzuki, T. and Y. Iwahashi, *RNA preparation of Saccharomyces cerevisiae using the digestion method may give misleading results*. Appl. Biochem. Biotechnol., 2013. **169**(5): p. 1620-1632.
106. Vosti, D.C. and M.A. Joslyn, *Autolysis of baker's yeast*. Appl. Microbiol. , 1954. **2**(2): p. 70-78.
107. Funk, I., V. Sieber, and J. Schmid, *Effects of glucose concentration on 1,18-cis-octadec-9-enedioic acid biotransformation efficiency and lipid body formation in Candida tropicalis*. Sci. Rep., 2017. **7**(1): p. 13842.
108. Vieira É, D., M. da Graça Stupiello Andrietta, and S.R. Andrietta, *Yeast biomass production: A new approach in glucose-limited feeding strategy*. Braz. J. Microbiol., 2013. **44**(2): p. 551-558.
109. Dey, P. and M.K. Maiti, *Molecular characterization of a novel isolate of Candida tropicalis for enhanced lipid production*. J. Appl. Microbiol., 2013. **114**(5): p. 1357-68.
110. Lamers, D., et al., *Selection of oleaginous yeasts for fatty acid production*. BMC Biotechnol., 2016. **16**(1): p. 1-10.
111. Beopoulos, A., T. Chardot, and J.M. Nicaud, *Yarrowia lipolytica: A model and a tool to understand the mechanisms implicated in lipid accumulation*. Biochimie, 2009. **91**(6): p. 692-696.
112. Kokina, A., J. Kibilds, and J. Liepins, *Adenine auxotrophy-be aware: some effects of adenine auxotrophy in Saccharomyces cerevisiae strain W303-1A*. FEMS Yeast Res., 2014. **14**(5): p. 697-707.

113. Ugolini, S. and C.V. Bruschi, *The red/white colony color assay in the yeast Saccharomyces cerevisiae epistatic growth advantage of white ade8-18, ade2 cells over red ade2 cells*. Curr. Genet., 1996. **30**: p. 485-492.
114. Tsang, P.W.K., et al., *Loss of heterozygosity, by mitotic gene conversion and crossing over, causes strain-specific adenine mutants in constitutive diploid Candida albicans*. Microbiol., 1999. **145**: p. 1623-1629.
115. Ljungdahl, P.O. and B. Daignan-Fornier, *Regulation of amino acid, nucleotide, and phosphate metabolism in Saccharomyces cerevisiae*. Genetics, 2012. **190**(3): p. 885-929.
116. Gleeson, M.A.G., L.O.C. Haas, and J.M. Cregg, *Isolation of Candida tropicalis auxotrophic mutants*. Appl. Environ. Microbiol., 1990. **56**(8): p. 2562-2564.
117. Corner, B.E. and R.T.M. Poulter, *Interspecific complementation analysis by protoplast fusion of Candida tropicalis and Candida albicans adenine auxotrophs*. J. Bacteriol., 1989. **171**(6): p. 3586-3589.
118. Vila-Vicosa, D., et al., *Constant-pH MD simulations of an oleic acid bilayer*. J. Chem. Theory Comput., 2015. **11**(5): p. 2367-76.
119. Kanicky, J.R. and D.O. Shah, *Effect of degree, type, and position of unsaturation on the pKa of long-chain fatty acids*. J. Colloid. Interface Sci., 2002. **256**(1): p. 201-207.
120. Small, D.M., *Physical properties of fatty acids and their extracellular and intracellular distribution*. Polyunsaturated Fatty Acids in Human Nutrition, 1992. **28**: p. 25-39.
121. Vorum, H., et al., *Solubility of long-chain fatty acids in phosphate buffer at pH 7.4*. Biochim. Biophys. Acta, 1992. **1126**: p. 135-142.
122. Nyren, V. and E. Back, *The ionization constant, solubility product and solubility of lauric and myristic acid* Acta Chem. Scand., 1952. **12**(6): p. 1305-1311.
123. Orij, R., S. Brul, and G.J. Smits, *Intracellular pH is a tightly controlled signal in yeast*. Biochim. Biophys. Acta, 2011. **1810**(10): p. 933-44.
124. Imai, T. and T. Ohno, *The relationship between viability and intracellular pH in the yeast Saccharomyces cerevisiae*. Appl. Environ. Microbiol., 1995. **61**(10): p. 3604-8.
125. Valli, M., et al., *Intracellular pH distribution in Saccharomyces cerevisiae cell populations, analyzed by flow cytometry*. Appl. Environ. Microbiol., 2005. **71**(3): p. 1515-21.
126. Chotani, G.K., et al., *Industrial biotechnology: Discovery to delivery*, in *Handbook of Industrial Chemistry and Biotechnology*, J.A. Kent, T.V. Bommaraju, and S.D. Barnicki, Editors. 2017, Springer International Publishing: Cham. p. 1495-1570.
127. Storhas, W., *Bioverfahrensentwicklung*. 2013: Wiley-VCH.
128. Murata, N. and D.A. Los, *Membrane fluidity and temperature perception*. Plant Physiol., 1997. **115**(3): p. 875-879.
129. Quinn, P.J., *The fluidity of cell membranes and its regulation*. Prog. Biophys. Molec. Biol., 1981. **38**: p. 1-104.
130. Papanikolaou, S. and G. Aggelis, *Modeling lipid accumulation and degradation in Yarrowia lipolytica cultivated on industrial fats*. Curr. Microbiol., 2003. **46**(6): p. 398-402.
131. Titorenko, V.I. and S.R. Terlecky, *Peroxisome metabolism and cellular aging*. Traffic, 2011. **12**(3): p. 252-259.

132. Froissard, M., et al., *Lipids containing medium-chain fatty acids are specific to post-whole genome duplication Saccharomycotina yeasts*. BMC Evol. Biol., 2015. **15**(97): p. 1-16.
133. Kadisch, M., et al., *Maximization of cell viability rather than biocatalyst activity improves whole-cell ω -oxyfunctionalization performance*. Biotechnol. Bioeng., 2017. **114**(4): p. 874-884.
134. Novak, M., et al., *Oleic acid metabolism via a conserved Cytochrome P450 System-mediated ω -hydroxylation in the bark beetle-associated fungus *Grosmannia clavigera**. PLOS ONE, 2015. **10**(3): p. e0120119.
135. Wu, J., et al., *Carboxyl methylation of the phosphoprotein phosphatase 2A catalytic subunit promotes its functional association with regulatory subunits in vivo*. EMBO J., 2000. **19**(21): p. 5672-5681.
136. van der Klei, I.J., et al., *The significance of peroxisomes in methanol metabolism in methylotrophic yeast*. Biochim. Biophys. Acta, 2006. **1763**(12): p. 1453-1462.
137. Bustin, S.A., *Quantification of mRNA using real-time reverse transcription PCR (RT-PCR): trends and problems*. J. Mol. Endocrinol., 2002. **29**(1): p. 23-39.
138. Ke, R., P.J. Ingram, and K. Haynes, *An integrative model of ion regulation in yeast*. PLoS Comput. Biol., 2013. **9**(1): p. e1002879.
139. Nailis, H., et al., *Development and evaluation of different normalization strategies for gene expression studies in *Candida albicans* biofilms by real-time PCR*. BMC Mol. Biol., 2006. **7**(25).
140. Teste, M.A., et al., *Validation of reference genes for quantitative expression analysis by real-time RT-PCR in *Saccharomyces cerevisiae**. BMC Mol. Biol., 2009. **10**(99).
141. Roth, C.M., *Quantifying gene expression*. Curr. Issues Mol. Biol., 2002. **4**: p. 93-100.
142. Backes, W.L. and R.W. Kelley, *Organization of multiple cytochrome P450s with NADPH-cytochrome P450 reductase in membranes*. Pharmacol. Ther., 2003. **98**(2): p. 221-233.
143. Farooq, Y. and G.C. Roberts, *Kinetics of electron transfer between NADPH-cytochrome P450 reductase and cytochrome P450 3A4*. Biochem. J., 2010. **432**(3): p. 485-93.
144. Körner, H.J. and G. Deerberg, *Untersuchungen zum Downstream-Processing bei der biotechnologischen Herstellung von 1,18-Octadecendisäure*. Chem. Ing. Tech., 2009. **81**(11): p. 1823-1828.
145. Huber, T., *Neue Nahtstellen zwischen Silicium- und Oleochemie: Übergangsmetallkatalysierte isomerisierende Silylierungsreaktionen an ungesättigten Fettchemikalien*. 2017. **Ph.D. thesis, Technical University Munich**.
146. Lu, W., et al., *Biosynthesis of monomers for plastics from renewable oils*. J. Am. Chem. Soc., 2010. **132**(43): p. 15451-15455.
147. Mishra, P., et al., *Genome-scale model-driven strain design for dicarboxylic acid production in *Yarrowia lipolytica**. BMC Syst. Biol., 2018. **12**(2): p. 12.
148. Beopoulos, A., et al., *Control of lipid accumulation in the yeast *Yarrowia lipolytica**. Appl. Environ. Microbiol., 2008. **74**(24): p. 7779-7789.
149. Rakicka, M., et al., *Lipid production by the oleaginous yeast *Yarrowia lipolytica* using industrial by-products under different culture conditions*. Biotechnol. Biofuels, 2015. **8**(104).

References

150. Scheller, U., et al., *Oxygenation cascade in conversion of n-alkanes to α,ω -dioic acids catalyzed by cytochrome P450 52A3*. J. Biol. Chem., 1998. **273**(49): p. 32528-32534.

7 Attachments

7.1 List of tables

| | |
|---|----|
| Table 1-1: Overview of studies on biotransformation of fatty acids, alkanes and their derivatives as substrates to the corresponding DCAs | 19 |
| Table 2-1: Sequences of primer pairs used for RT-qPCR and accession numbers of target genes | 24 |
| Table 2-2: PCR conditions for DNA amplification | 31 |
| Table 2-3: Templates and controls applied for qPCR | 32 |
| Table 2-4: qPCR conditions..... | 32 |
| Table 2-5: GC/FID parameters applied for different methods..... | 37 |
| Table 2-6: Conditions applied for GC/MS..... | 38 |
| Table 2-7: Pre-culture preparation: from agar plate to a 2 L bioreactor | 40 |
| Table 2-8: 2 L bioreactor set up | 41 |
| Table 2-9: Operational conditions of pre-culture in 2 L bioreactor | 42 |
| Table 2-10: Set up of DASGIP parallel bioreactor system | 43 |
| Table 2-11: Assignment of the pumps and corresponding supplements (DASGIP) | 43 |
| Table 2-12: General parameters and their regulation during the biotransformation process | 44 |
| Table 2-13: Operational parameters of various variants of growth phase | 45 |
| Table 2-14: Operational parameters of the biotransformation of DAME and oleic acid | 46 |
| Table 3-1: Overview of process parameters at constant pH in comparison to pH shift during the biotransformation | 51 |
| Table 3-2: Overview of process parameters at different temperatures..... | 52 |
| Table 3-3: Overview of process parameters in dependency of DAME feed [100] | 57 |
| Table 3-4: Comparison of cell wall digestion by Lyticase and Zymolyase..... | 60 |
| Table 3-5: Overview over gDNA contamination detected after various RNA extraction steps | 61 |
| Table 3-6: Determination of the optimal primer concentration for the <i>CYP52A13/14</i> .. | 63 |
| Table 3-7: qPCR efficiency of all genes investigated by qPCR..... | 65 |

| | |
|---|-----|
| Table 3-8: CV and M values of reference genes..... | 66 |
| Table 3-9: Accumulation of DAME and DA during biotransformation of DAME..... | 68 |
| Table 3-10: Comparison of several variants of the cell growth in 2 L bioreactor | 72 |
| Table 3-11: Overview over the production process initiated at pH 5.8 and 6.5 | 77 |
| Table 3-12: Overview over the various growth phase models [107] | 83 |
| Table 3-13: Characterization of <i>cis</i> -ODA production process at various glucose feed rates [107]..... | 85 |
| Table 3-14: Characterization of DDA production in correlation to glucose feed..... | 90 |
| Table 4-1: Overview over the pKa values and solubility of fatty acids | 98 |
| Table 4-2: Summary of specific productivity in dependency of pH and applied substrate | 99 |
| Table 4-3: Comparison of the DAME and oleic acid biotransformation processes..... | 112 |
| Table 4-4: Comparison of the optimal operational conditions for DDA and <i>cis</i> -ODA production | 113 |

7.2 List of figures

| | |
|---|----|
| Figure 1-1: Overview over the possibilities of bio-based polymer production from biomass..... | 7 |
| Figure 1-2: Fatty acid degradation pathway in <i>Candida tropicalis</i> | 10 |
| Figure 2-1: General saponification procedure..... | 29 |
| Figure 2-2: Schematic overview over the sampling procedure during the DCA production | 46 |
| Figure 3-1: pH shift in the biotransformation phase applied for DDA production | 50 |
| Figure 3-2: DDA production in dependency of the temperature | 52 |
| Figure 3-3: pH shift in combination with the increased DAME feed for evaluation of the maximal feed rate for bioconversion [100]..... | 53 |
| Figure 3-4: Accumulation of DAME and DA over the time displaying dependency on the applied increased DAME feed [100]..... | 54 |
| Figure 3-5: Thin layer chromatography for the qualitative detection of DAME, DA and DDA..... | 55 |
| Figure 3-6: Conversion of DAME and profile of the DAME feed over time [100] | 56 |
| Figure 3-7: Specific productivity of DDA in dependency on pH shift..... | 57 |
| Figure 3-8: Extracted RNA samples on denaturing agarose gel | 62 |
| Figure 3-9: Melting curve analysis of <i>GAPDH</i> | 64 |
| Figure 3-10: Agarose gel of amplified qPCR product of the <i>GAPDH</i> | 64 |
| Figure 3-11: Relative normalized expression profiling of the genes during the DDA production process [100] | 67 |
| Figure 3-12: Volumetric productivity and expression levels of <i>CPR</i> over time [100] | 69 |
| Figure 3-13: Streak of <i>C. tropicalis</i> from glycerol stock on YPD agar plates | 71 |
| Figure 3-14: Monitoring of pO ₂ and phosphoric acid in 2 L bioreactor..... | 72 |
| Figure 3-15: Separation of FAs and DCAs of various chain length by various GC/FID methods..... | 74 |
| Figure 3-16: Chromatogram of biotransformation of DAME and oleic acid in shake flask | 75 |
| Figure 3-17: Precipitations of oleic acid observed during the biotransformation..... | 76 |

| | |
|--|-----|
| Figure 3-18: Glucose accumulation observed during the biotransformation phase..... | 78 |
| Figure 3-19: Production of <i>cis</i> -ODA in dependency of pH [107] | 79 |
| Figure 3-20: Monitoring of CO ₂ in exhaust gas as an indicator for cell viability | 81 |
| Figure 3-21: Overview over the various pH shift strategies | 82 |
| Figure 3-22: <i>cis</i> -ODA production in dependency on the pH shift strategy [107]..... | 83 |
| Figure 3-23: Microscopic views at 1,000×magnification of <i>C. tropicalis</i> process at various glucose feeds [107]..... | 86 |
| Figure 3-24: Extracted total lipids from samples exposed to various glucose feed rates [107]..... | 87 |
| Figure 3-25: TLC of extracted lipids from samples exposed to various glucose feeds rates [107]..... | 88 |
| Figure 3-26: Monitoring of gene expression in dependency of glucose feed rates [107] | 89 |
| Figure 3-27: <i>C. tropicalis</i> during DAME biotransformation exposed to various glucose feed rates [107]..... | 90 |
| Figure 3-28: Mass balance of the substrate and product during DAME biotransformation [107]..... | 91 |
| Figure 3-29: <i>cis</i> -ODA product yield in dependency on oleic acid feed rate [107] | 92 |
| Figure 3-30: Purification steps of <i>cis</i> -ODA | 93 |
| Figure 3-31: GC/FID chromatogram of purified <i>cis</i> -ODA | 94 |
| Figure 3-32: Comparison of the GC/MS of <i>cis</i> - and <i>trans</i> -ODA..... | 94 |
| Figure 4-1: Product yield and conversion of oleic acid over the time at different glucose feed rates during the production process [107] | 101 |
| Figure 4-2: Proposed pathway of ω -oxidation and LB formation in dependency on the fatty acids chain-length in <i>C. tropicalis</i> | 105 |
| Figure 4-3: Comparison of CO ₂ in exhaust gas in dependency on DAME feed in comparison to control bioreactor | 107 |

7.3 Abbreviations

| | |
|-----------------|---|
| °C | Celcius |
| µL | microliter |
| ACS | long-chain acyl-CoA synthetase |
| AIR | ribosylaminoimidazole |
| AMP | adenosine monophosphate |
| cDNA | complementary DNA |
| CDW | cell dry weight |
| CFU | colony-forming unit |
| <i>cis</i> -ODA | 1,18- <i>cis</i> -octadec-9-enedioic acid |
| CO ₂ | carbon dioxide |
| CoA | Coenzym A |
| DA | dodecanoic acid |
| DAME | dodecanoic acid methyl ester |
| DCA | dicarboxylic acid |
| DDA | dodecanedioic acid |
| DEPC | diethyl pyrocarbonate |
| DHAP | dihydroxyacetone phosphate |
| DNA | deoxyribonucleic acid |
| dNTP | nucleoside triphosphate |
| dsDNA | double-stranded DNA |
| e.g. | example |
| EDTA | ethylenediaminetetraacetic acid |
| ER | endoplasmic reticulum |

| | |
|---------------|---|
| FA | fatty acid |
| FFA | free fatty acid |
| g | gram |
| GC/FID | Gas chromatography coupled with flame ionization detector |
| GC/MS | gas chromatography coupled with mass spectroscopy |
| Glc | glucose |
| G3P | glycerol-3-phosphate |
| gDNA | genomic DNA |
| h | hour |
| HPLC | high-performance liquid chromatography |
| IRC | inter-run calibrator |
| L | liter |
| LCFA | medium-chain length fatty acid |
| m | meter |
| MCFA | medium-chain length fatty acid |
| mg | milligram |
| min | minute |
| MMLV | moloney murine leukemia miruv |
| MOPS | 3-(N-morpholino)propanesulfonic acid |
| MTBE | methyl-tert-butyl ether |
| NMR | nuclear magnetic resonance |
| NRT | no reverse transcription |
| NTC | no template control |
| OA | oleic acid |

| | |
|-------------------------|--|
| PHA | polyhydroxyalkanoates |
| PL | phospholipid |
| PRPP | phosphoribosyl-pyrophosphate |
| QC RT-PCR | quantitative competitive reverse transcription PCR |
| RNA | ribonucleic acid |
| RT | room temperature |
| S | sterol |
| SE | sterol ester |
| TAG | triacylglycerol |
| T_a | annealing temperature |
| TLC | thin layer chromatography |
| T_m | melting temperature |
| <i>trans</i>-ODA | 1,18- <i>trans</i> -octadec-9-enedioic acid |
| v/v | volume per volume |
| w/v | weight per volume |
| w/w | weight per weight |

7.4 5.8 rRNA analysis of *C. tropicalis* ATCC 20962

5.8 rRNA analysis of beige and reddish colonies on the agar plate with comparison to a *Candida viswanathii* (*Candida tropicalis*) strain ATCC 20962 (GenBank: KU729163.1).

The sequenz identificaiotn was performed using BLAST.

02 Sep 2017

Alignment Results

Alignment: Global DNA alignment against reference molecule
 Parameters: Scoring matrix: Linear (Mismatch 2, OpenGap 4, ExtGap 1)

Reference molecule: beige_FWD, Region 1 to 460
 Number of sequences to align: 3
 Total length of aligned sequences with gaps: 756 bps
 Settings: Similarity significance value cutoff: >= 90%

Summary of Percent Matches:

| | | | | |
|------|---------------------------------------|----------|------------|-----|
| Ref: | beige_FWD | 1 to 460 | (460 bps) | -- |
| 2: | reddish_FWD | 1 to 670 | (670 bps) | 68% |
| 3: | Candida viswanathii strain ATCC 20962 | 1 to 592 | (592 bps) | 39% |

■ Areas of significant similarity (in windows 5 bases in length)



Candida viswanathii strain ATCC 20962 28S large subunit ribosomal RNA gene, partial sequence
 Sequence ID: [KU729163.1](#) Length: 592 Number of Matches: 1

Range 1: 1 to 506 [GenBank](#) [Graphics](#) [Next Match](#) [Previous Match](#)

| Score | Expect | Identities | Gaps | Strand |
|---------------|--|--------------|-----------|-----------|
| 928 bits(502) | 0.0 | 504/506(99%) | 0/506(0%) | Plus/Plus |
| Query 165 | ATATCAATAAGCGGAGGAAAAACCAACACAGGGATTGCCTTAGTAGCGCGAGTGAAGC | 224 | | |
| Sbjct 1 | ATATCAATAAGCGGAGGAAAAAGAAACCAACAGGGATTGCCTTAGTAGCGCGAGTGAAGC | 60 | | |
| Query 225 | GGCAAAAGCTCAAATTTGAAATCTGGCTCTTTCAGAGTCCGAGTTGTAATTTGAAGAAGG | 284 | | |
| Sbjct 61 | GGCAAAAGCTCAAATTTGAAATCTGGCTCTTTCAGAGTCCGAGTTGTAATTTGAAGAAGG | 120 | | |
| Query 285 | TATCTTTGGGCCTGGCTCTTGTCTATGTTTCTTGGAAACAGAAGTCACAGAGGGTGAGAA | 344 | | |
| Sbjct 121 | TATCTTTGGGCCTGGCTCTTGTCTATGTTTCTTGGAAACAGAAGTCACAGAGGGTGAGAA | 180 | | |
| Query 345 | TCCCGTGGCAGTGAAGTACAGCCAGGTCCTGTAAGTTCCCTTCGACGAGTCGAGTTGTTG | 404 | | |
| Sbjct 181 | TCCCGTGGCAGTGAAGTACAGCCAGGTCCTGTAAGTTCCCTTCGACGAGTCGAGTTGTTG | 240 | | |
| Query 405 | GGAAATGCAGCTCTAAGTGGGTGGTAAATCCATCTAAAGCTAAATATTGGCGAGAGACCG | 464 | | |
| Sbjct 241 | GGAAATGCAGCTCTAAGTGGGTGGTAAATCCATCTAAAGCTAAATATTGGCGAGAGACCG | 300 | | |
| Query 465 | ATAGCGAACAGTACAGTGATGGAAGATGAAAAGAACTTTGAAAAGAGAGTGAAAAAGT | 524 | | |
| Sbjct 301 | ATAGCGAACAGTACAGTGATGGAAGATGAAAAGAACTTTGAAAAGAGAGTGAAAAAGT | 360 | | |
| Query 525 | ACGTGAAATTTGTTGAAAGGGAAGGGCTTGAGATCAGACTTGGCAATTTGCAATGTTGCTTC | 584 | | |
| Sbjct 361 | ACGTGAAATTTGTTGAAAGGGAAGGGCTTGAGATCAGACTTGGCAATTTGCAATGTTGCTTC | 420 | | |
| Query 585 | TTGCGGGGCGCCCTTCGCGGTTTGTGCGGGCCAGCATCAGITTTGGCGGTAGGACAATCGC | 644 | | |
| Sbjct 421 | TTGCGGGGCGCCCTTCGCGGTTTGTGCGGGCCAGCATCAGITTTGGCGGTAGGACAATCGC | 480 | | |
| Query 645 | GCGGGAATGTGGCACGGCCTCGGCTG 670 | | | |
| Sbjct 481 | GCGGGAATGTGGCACGGCCTCGGCTG 506 | | | |

02 Sep 2017

Alignment Results

Alignment: Global DNA alignment against reference molecule
 Parameters: Scoring matrix: Linear (Mismatch 2, OpenGap 4, ExtGap 1)

Reference molecule: beige_FWD, Region 1 to 460
 Number of sequences to align: 3
 Total length of aligned sequences with gaps: 756 bps
 Settings: Similarity significance value cutoff: >= 90%

Summary of Percent Matches:

| | | | | | | | |
|------|--|------|-----|---|----------|-----|-----|
| Ref: | beige_FWD | 1 to | 460 | (| 460 bps) | -- | |
| | 2: reddish_FWD | 1 to | 670 | (| 670 bps) | 68% | |
| | 3: Candida viswanathii strain ATCC 20962 | 1 to | 592 | (| 592 bps) | | 39% |

```
beige_FWD      1 ---cgcggtttggtggtgagcaatacgcaggtttggttgaagacgtacgtggagact
reddish_FWD    1 gcccgcggtttggtggtgagcaatacgcaggtttggttgaagacgtacgtggagact
Candida visw   -----
```

```
beige_FWD      58 atattagcgacttaggttctacaaaacgcttgtgcagtcgcccaccacagcttttcta
reddish_FWD    61 atattagcgacttaggttctacaaaacgcttgtgcagtcgcccaccacagcttttcta
Candida visw   -----
```

```
beige_FWD      118 acttttgacctcaaatcaggtaggactaccgctgaacttaagcatatcaataagcggag
reddish_FWD    121 acttttgacctcaaatcaggtaggactaccgctgaacttaagcatatcaataagcggag
Candida visw   1 -----atatcaataagcggag
```

```
beige_FWD      178 gaaagaaaccaacagggattgccttagtagcgggcagtgaaagcggcaaaagctcaaat
reddish_FWD    181 gaaagaaaccaacagggattgccttagtagcgggcagtgaaagcggcaaaagctcaaat
Candida visw   17 gaaagaaaccaacagggattgccttagtagcgggcagtgaaagcggcaaaagctcaaat
```

```
beige_FWD      238 tgaaatctggctctttcagagtcogagttgtaatttgaagaaggtatctttgggcctggc
reddish_FWD    241 tgaaatctggctctttcagagtcogagttgtaatttgaagaaggtatctttgggcctggc
Candida visw   77 tgaaatctggctctttcagagtcogagttgtaatttgaagaaggtatctttgggcctggc
```

```
beige_FWD      298 tcttgtctatgtttcttggaacagaacgtcacagagggtgagaatcccgctgcatgagat
reddish_FWD    301 tcttgtctatgtttcttggaacagaacgtcacagagggtgagaatcccgctgcatgagat
Candida visw   137 tcttgtctatgtttcttggaacagaacgtcacagagggtgagaatcccgctgcatgagat
```

```
beige_FWD      358 gaccaggtccgtgtaaaagttccttcgacgagtcogagttggttgggaatgcagctctaag
reddish_FWD    361 gaccaggtccgtgtaaaagttccttcgacgagtcogagttggttgggaatgcagctctaag
Candida visw   197 gaccaggtccgtgtaaaagttccttcgacgagtcogagttggttgggaatgcagctctaag
```

```
beige_FWD      418 tgggtggtaaattccatctaagctaaatattggcgagagacc-----
reddish_FWD    421 tgggtggtaaattccatctaagctaaatattggcgagagaccgatagcgaacaagtaca
Candida visw   257 tgggtggtaaattccatctaagctaaatattggcgagagaccgatagcgaacaagtaca
```

```
beige_FWD      -----
reddish_FWD    481 gtgatggaaagatgaaaagaactttgaaaagagagtgaaaagtagctgaaattggtgaa
Candida visw   317 gtgatggaaagatgaaaagaactttgaaaagagagtgaaaagtagctgaaattggtgaa
```

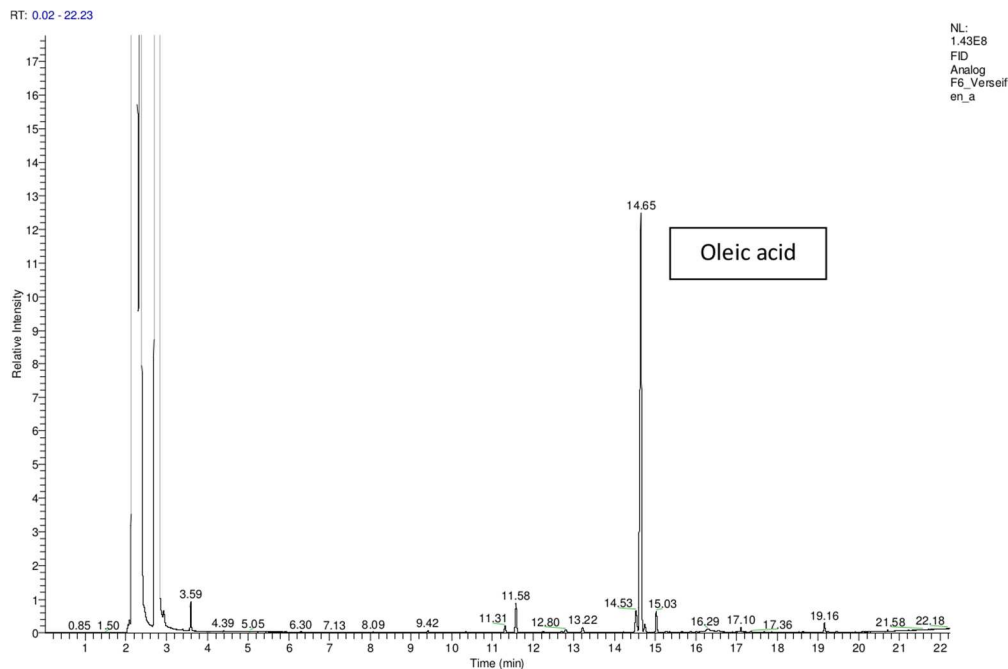
```
beige_FWD      -----
reddish_FWD    541 aggaagggcttgagatcagacttggcattttgcatggtgcttcttcggggggcggcctct
Candida visw   377 aggaagggcttgagatcagacttggcattttgcatggtgcttcttcggggggcggcctct
```

```
beige_FWD      -----
reddish_FWD    601 gcggtttgtcgggccagcatcagtttggcggtaggacaatcgcggggaatgtggcagc
Candida visw   437 gcggtttgtcgggccagcatcagtttggcggyaggacaatcgcggggaatgtggcagc
```

```
beige_FWD      -----
reddish_FWD    661 gcctcggctg-----
Candida visw   497 gcctcggctgtgtgttatagcccgctggatactgccagcctagactgaggactgcggtt
```

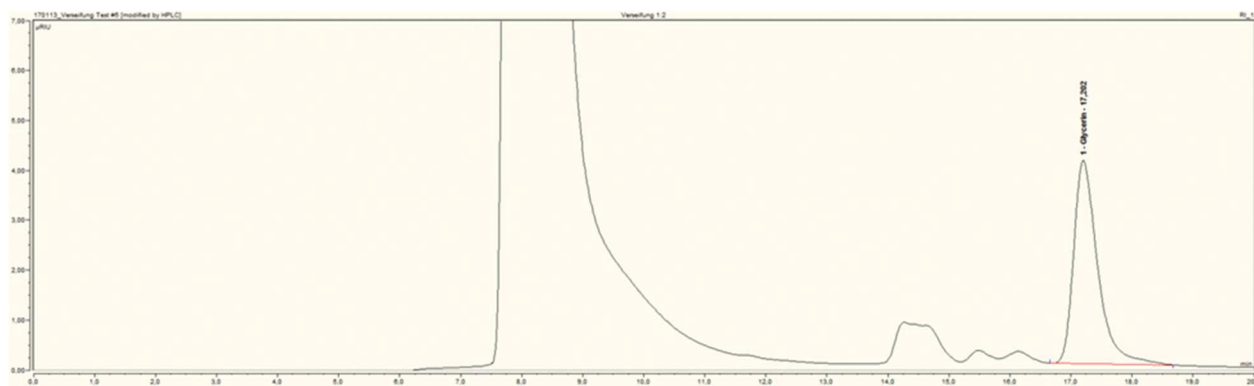
```
beige_FWD      -----
reddish_FWD    -----
Candida visw   557 tatacctaggatggtggcataatgatcttaagtgcg
```

7.5 Analysis of hydrolyzed lipids



GC/FID chromatogram of released fatty acids after hydrolysis of lipids [107]

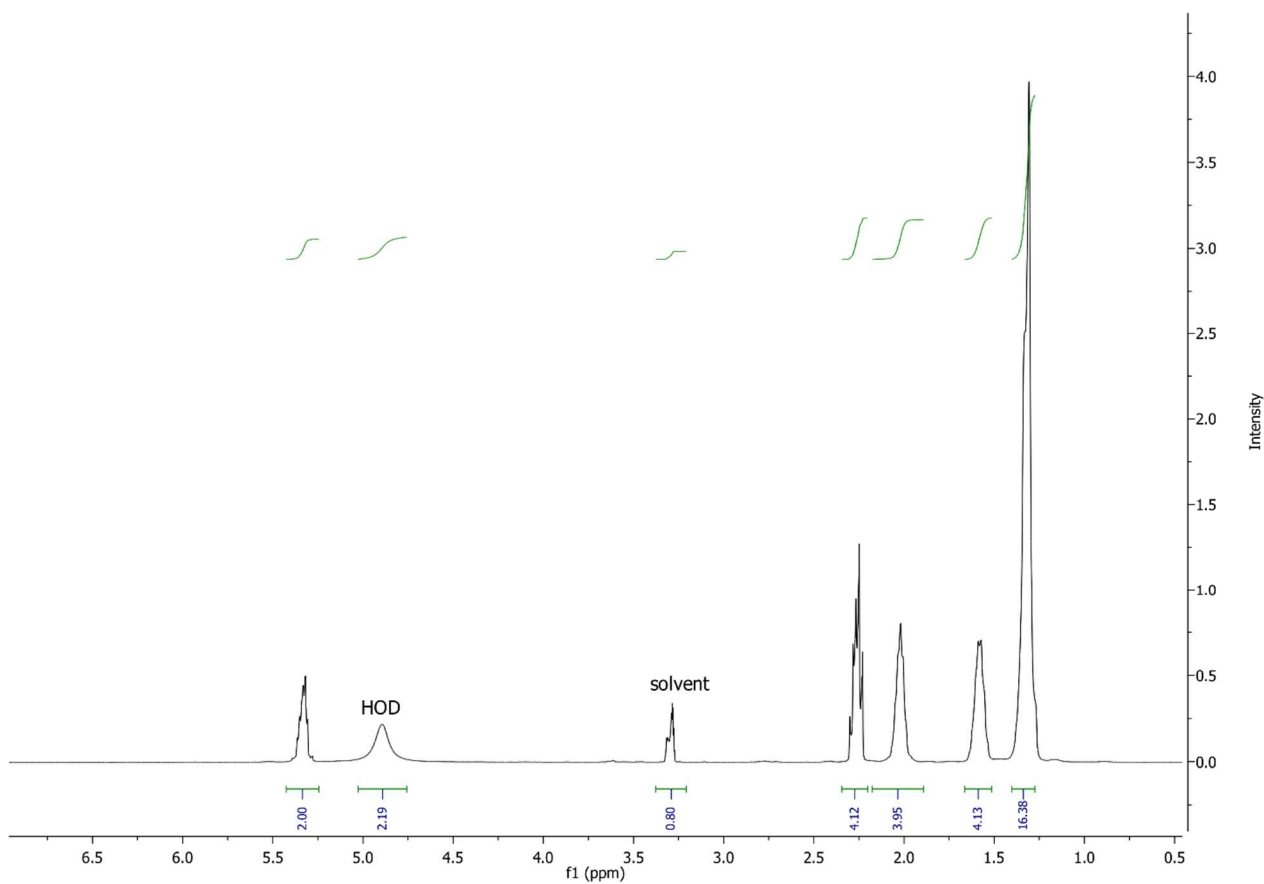
The oleic acid was found to be the most abundant (80% based on the peak area) fatty acid along the released fatty acids after LBs saponification. Retention times: palmitic acid-11.58 min, linoleic acid-14.53 min, oleic acid-14.65 min, stearic acid-15.03 min. The experiment was performed as described in methods.



Detection of glycerol after hydrolysis of LBs by HPLC [107]

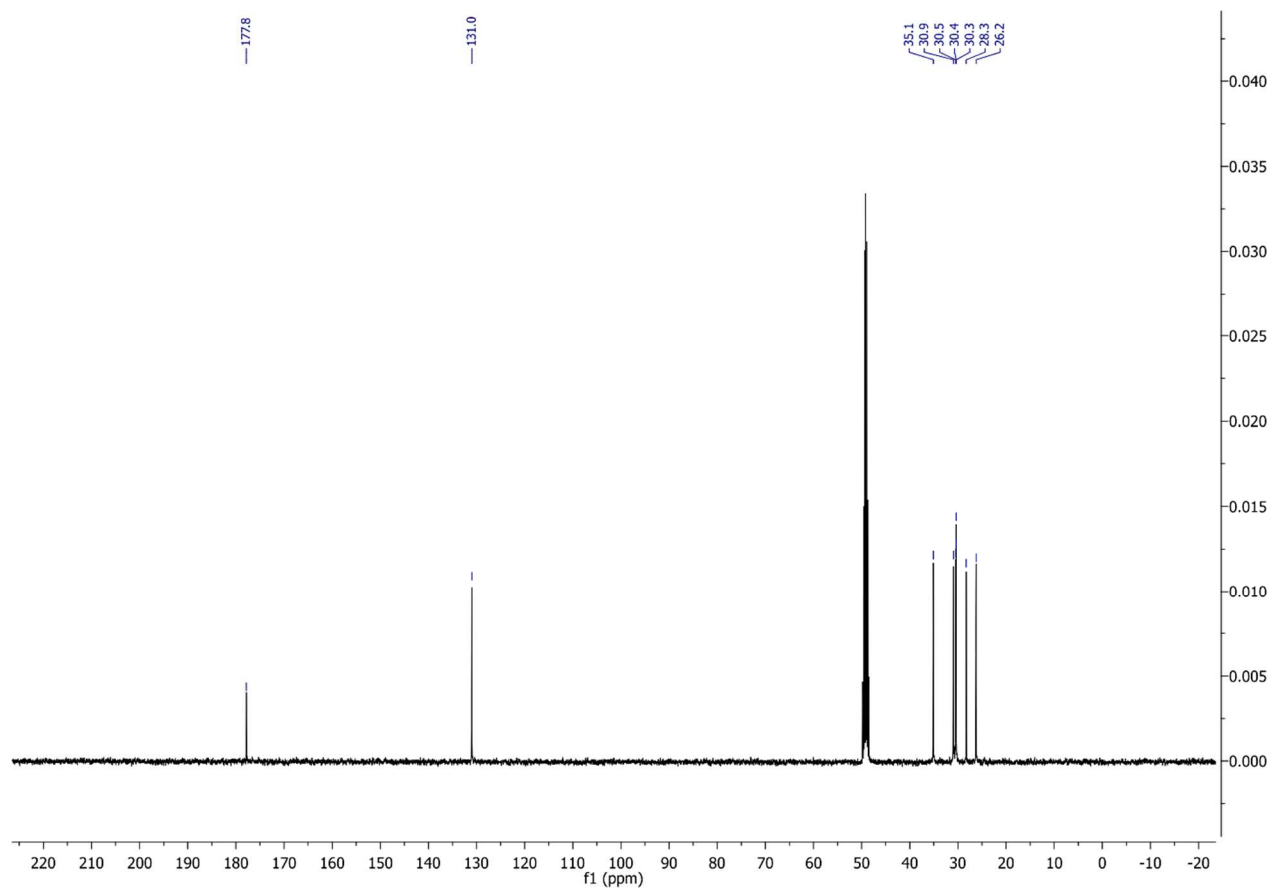
The retention time of glycerol 17.02 min. The experiment was performed as described in methods.

7.6 Nuclear magnetic resonance (NMR) spectroscopy of *cis*-ODA [107]



$^1\text{H-NMR}$ of 1,18-*cis*-Octadec-9-enedioic acid (400 MHz, CD_3OD): δ 5.41 – 5.26 (m, 1H), 2.34 – 2.21 (m, 2H), 2.09 – 1.92 (m, 2H), 1.67 – 1.50 (m, 2H), 1.31 (s, 8H).

Attachments



^{13}C -NMR of 1,18-*cis*-Octadec-9-enedioic acid (100 MHz, CD_3OD): 177.8, 130.9, 35.1, 30.9, 30.5, 30.37, 30.3, 28.3, 26.2.